

**Analysis of senescence-associated secretory phenotype  
induced by different androgen receptor ligands in  
human prostate cancer cells**

**Dissertation**

**in partial fulfillment of the requirements for the degree of  
doctor rerum naturalium (Dr. rer. nat.)**

**submitted to the Faculty Council of the School of Medicine  
at Friedrich Schiller University of Jena**

**by M.Sc. Molecular Medicine Thanakorn Pungsrinont  
born on 20.09.1989 in Bangkok, Thailand**

**Reviewers**

**1. Prof. Dr. rer. nat. Aria Baniahmad**

Institut für Humangenetik, Universitätsklinikum Jena

**2. PD Dr. rer. nat. habil. Jörg Müller**

Institut für Molekulare Zellbiologie, Universitätsklinikum Jena

**3. PD Mag. Dr. rer. nat. habil. Marcus V. Cronauer**

Institut für Pathologie, Universitätsklinikum Bonn

**Date of the public disputation: 06<sup>th</sup> July 2021**

---

**TABLE OF CONTENTS**

<b>LIST OF ABBREVIATIONS .....</b>	<b>v</b>
<b>ZUSAMMENFASSUNG .....</b>	<b>xi</b>
<b>SUMMARY .....</b>	<b>xiii</b>
<b>1 INTRODUCTION.....</b>	<b>1</b>
1.1 Androgen receptor (AR) signaling.....	1
1.2 Prostate cancer (PCa) and hormone therapies.....	3
1.3 AR ligand-induced cellular senescence .....	4
1.4 Senescence-associated secretory phenotype (SASP) and paracrine effects.....	7
1.4.1 SASP affects growth and proliferation .....	8
1.4.2 SASP affects stem/progenitor cells.....	9
1.4.3 SASP affects immune cell responses .....	11
1.5 Senolytic compounds .....	12
<b>2 HYPOTHESES AND OBJECTIVES.....</b>	<b>14</b>
<b>3 MATERIALS AND METHODS .....</b>	<b>15</b>
3.1 Human PCa cell lines and culture .....	15
3.2 Senescence-associated $\beta$ -galactosidase (SA $\beta$ -Gal) staining .....	15
3.3 Collection of conditioned media from senescent PCa cells .....	16
3.4 Analysis of SASP secretome using human cytokine arrays .....	16
3.5 Two-dimensional (2D) monolayer proliferation assays and crystal violet staining .....	17
3.6 Three-dimensional (3D) colony formation assays: Analysis of stemness characteristic of PCa cells .....	19
3.6.1 3D colony formation with AR ligands.....	19
3.6.2 3D colony formation with conditioned media containing SASP secretome .....	20
3.6.3 Analysis of 3D colony formation efficiency of holoclone and meroclone.....	20
3.7 Preparation of peripheral blood mononuclear cells (PBMCs).....	21

---

3.8	Generation of mature dendritic cells and activation of lymphocytes.....	22
3.9	Killing assays of PCa cells by immune cells .....	23
3.10	Flow cytometry .....	23
3.10.1	Analysis of lymphocyte activation.....	24
3.10.2	Annexin V staining for analyzing apoptosis .....	24
3.11	Killing assays of PCa cells by senolytic compounds.....	25
3.12	Protein extraction and Western blotting.....	25
3.12.1	Whole cell lysate (intracellular protein extraction).....	25
3.12.2	Methanol precipitation (secreted protein precipitation).....	26
3.12.3	Western blotting.....	26
3.13	Analysis of PCa phospho-kinome using human phospho-kinase arrays .....	28
3.14	RNA extraction and quantitative reverse transcription-PCR (qRT-PCR) .....	29
3.14.1	RNA extraction and cDNA synthesis .....	29
3.14.2	qRT-PCR.....	29
3.15	Statistical analyses .....	31
<b>4</b>	<b>RESULTS .....</b>	<b>32</b>
4.1	The second-generation AR antagonist Enzalutamide (ENZ) induces cellular senescence in PCa cells leading to inhibition of cell proliferation .....	32
4.2	AR antagonist- and agonist-induced cellular senescent PCa cells exhibit distinct SASP secretomes.....	35
4.3	Bioinformatic gene ontology (GO) analysis suggests paracrine effects of AR ligand-induced SASP on PCa cell proliferation and immune system .....	41
4.4	AR agonist-induced SASP suppresses, whereas antagonist-induced SASP promotes LNCaP cell proliferation .....	45
4.5	AR ligand-induced SASP regulates phospho-kinome of PCa cells.....	47
4.6	AR ligands and conditioned medium containing SASP of AR agonist-treated PCa cells regulate the expression of stemness markers .....	51
4.7	SASP does not affect 3D colony formation of PCa cells.....	53
4.8	AR agonist suppresses 3D colony formation and reduces colony size.....	54
4.9	SASP does not affect lymphocyte-mediated apoptosis.....	56
4.10	SASP suppresses lymphocyte proliferation .....	60



---

4.11	Treatment with AR ligands renders PCa cells resistant to lymphocyte-mediated apoptosis.....	62
4.12	Induction of cellular senescence by AR ligands is associated with enhanced phosphorylation level of the pro-survival/anti-apoptotic factor AKT .....	66
4.13	AR antagonist- and agonist-treated PCa cells are preferentially sensitive to apoptosis induction by AKT and HSP90 inhibitors: Analysis of potential senolytic compounds.....	67
4.14	AR ligands differentially regulate phosphorylation of ribosomal S6 protein, a downstream target of the pro-survival/anti-apoptotic AKT signaling .....	69
<b>5</b>	<b>DISCUSSION .....</b>	<b>72</b>
5.1	AR ligands induce cellular senescence leading to distinct SASP secretomes ..	72
5.2	The SASP of AR ligand-treated PCa cells mediates paracrine effects on neighboring cells .....	74
5.2.1	The SASP of AR ligand-treated cells modulates the phospho-kinome and regulates PCa cell proliferation .....	74
5.2.2	AR agonist, but not the agonist-induced SASP, suppresses PCa stemness .....	77
5.2.3	The SASP of AR ligand-treated cells suppresses lymphocyte proliferation.....	78
5.3	AR ligand-activated pro-survival/anti-apoptotic AKT signaling correlates with resistance of PCa cells against lymphocyte-mediated apoptosis .....	79
5.4	An approach to a new therapeutic strategy: Targeting pro-survival/anti-apoptotic signaling with senolytic compounds after AR ligand-induced cellular senescence .....	81
<b>6</b>	<b>CONCLUSIONS AND FUTURE PERSPECTIVES .....</b>	<b>83</b>
<b>7</b>	<b>REFERENCES.....</b>	<b>85</b>
<b>8</b>	<b>APPENDIX.....</b>	<b>I</b>
8.1	Recipe of cell culture media, self-prepared buffers, solutions, and reaction mixes .....	I
8.2	Supplemental results (Figures and Table).....	IV

8.3	List of figures .....	XIII
8.4	List of tables.....	XIV
8.5	Ehrenwörtliche Erklärung .....	XV
8.6	Acknowledgement .....	XVI

**LIST OF ABBREVIATIONS**

2D	two-dimension
3D	three-dimension
$\alpha$	alpha
A	ampere
ADT	androgen deprivation therapy
AKT	protein kinase B
ALDH1A1	aldehyde dehydrogenase 1 family member A1
AMPK	adenosine monophosphate-activated protein kinase
ANG	angiogenin
ANOVA	analysis of variance
APC	Allophycocyanin
AR	androgen receptor
ARE	androgen response element
$\beta$	beta
BAD	BCL2 associated agonist of cell death
BCL-2	B-cell lymphoma 2
BCL-XL	B-cell lymphoma-extra large
BIC	Bicalutamide, 1 <sup>st</sup> generation AR antagonist
BLC	B lymphocyte chemoattractant
C4-2	castration-resistant human PCa cell line derived from LNCaP cells
CAR-T	chimeric antigen receptor-T lymphocyte
CCL	chemokine ligand
<i>CCND1</i>	a Cyclin D1 encoding gene
CD3, 8	cluster of differentiation 3, 8
<i>CDKN2A</i>	Cyclin-dependent kinase inhibitor 2A, a p16 <sup>INK4a</sup> encoding gene
cDNA	complementary DNA
CFE	colony formation efficiency
CHK-2	checkpoint kinase 2
cm	centimeter
Con. B	conditioned medium derived from BIC-treated PCa cells
Con. D	conditioned medium derived from DMSO-treated PCa cells
Con. E	conditioned medium derived from ENZ-treated PCa cells

Con. R	conditioned medium derived from R1881-treated PCa cells
c-PARP	cleaved poly ADP ribose polymerase
CREB	cAMP response element binding protein
CRPCa	castration-resistant prostate cancer
C-terminal domain	carboxy-terminal domain
CTLA-4	cytotoxic T-lymphocyte-associated protein 4
CXCL or Cxcl	chemokine (C-X-C motif) ligand
DCs	dendritic cells
DEC1	differentiated embryo chondrocyte expressed gene 1
DEPC	diethylpyrocarbonate
DHT	dihydrotestosterone, natural androgen
DMEM	Dulbecco's modified eagle medium
DMF	dimethylformamide
DMSO	dimethyl sulfoxide
DNA	deoxyribonucleic acid
dNTP	deoxynucleoside triphosphate
<i>E2F1</i>	an E2F transcription factor 1 encoding gene
ECL	enhanced chemiluminescence
EDTA	ethylenediaminetetraacetic acid
EGFR	epidermal growth factor receptor
ENZ	Enzalutamide, 2 <sup>nd</sup> generation AR antagonist
ERK	extracellular signal-regulated kinase
EtOH	ethanol
FBS	fetal bovine serum
FITC	fluorescein isothiocyanate
FL-PARP	full length poly ADP ribose polymerase
$\gamma$	gamma
g	gram
GAS1	growth arrest specific 1
GCP-2	granulocyte chemotactin protein-2
GDNF	glial cell-derived neurotrophic factor
GM-CSF	granulocyte-macrophage colony-stimulating factor
GO	gene ontology
gp130	glycoprotein 130

GT	HSP90 inhibitor Ganetespib
h	hour
HEPES	4-(2-hydroxyethyl)-1-piperazineethanesulfonic acid
HKG	housekeeping gene
HLA	human leukocyte antigen
HRP	horseradish peroxidase
HS	human serum
HSP	heat shock protein
IFN- $\gamma$	interferon gamma
IGF-1	insulin-like growth factor-1
IGF-1R	insulin-like growth factor-1 receptor
IGFBP	insulin-like growth factor binding protein
IgG	immunoglobulin G
IL	interleukin
IL-1RA	interleukin 1 receptor antagonist
IL-6R	soluble interleukin 6 receptor
IPA	ingenuity pathway analysis
JNK	c-Jun N-terminal kinases
kDa	kilo Dalton
<i>KITLG</i>	KIT ligand, a SCF encoding gene
KLF4	Kruppel-like factor 4
<i>KLK3</i>	Kallikrein related peptidase 3, a PSA encoding gene
L	liter
LAL	low androgen level
LIN28	Lin-28 homolog, an RNA-binding protein
LNCaP	lymph node cancerous prostate, androgen-sensitive human PCa cell line
LYN	v-yes-1 Yamaguchi sarcoma viral related oncogene homolog
$\mu$	micro
$\mu$ l	microliter
m	milli
m	meter
M	molar
MAPK	mitogen-activated protein kinase
MEFs	mouse embryonic fibroblasts

<i>MET</i>	a MET proto-oncogene encoding gene
MG132	a proteasome inhibitor
MHC	major histocompatibility complex
min	minute
MK	AKT inhibitor MK2206
ml	milliliter
mRNA	messenger RNA
MSK	mitogen and stress activated protein kinase
mTOR	mammalian target of rapamycin
MYC	MYC proto-oncogene, bHLH transcription factor
n	nano
n	number of technical replicates
N	number of independent experiments (biological replicates)
NANOG	homeobox protein NANOG
ND	not detected or below detection level
NETN	NaCl + EDTA + Tris-HCl + NP-40
NK cells	natural killer cells
NKT cells	natural killer T cells
ns	not significant
NT	neurotrophin
N-terminal domain	amino-terminal domain
OCT4	octamer-binding transcription factor 4
OD	optical density
$\pi$	pi
p	pico
p	p-value
p15 <sup>INK4b</sup>	protein encoded by cyclin-dependent kinase inhibitor 2B gene
p16 <sup>INK4a</sup>	protein encoded by cyclin-dependent kinase inhibitor 2A gene
p21 <sup>Cip1/Waf1</sup>	protein encoded by cyclin-dependent kinase inhibitor 1A gene
p53	tumor suppressor protein p53
PAGE	polyacrylamide gel electrophoresis
p-AKT	phosphorylated AKT
PARP	Poly ADP-ribose polymerase
PBMC	peripheral blood mononuclear cell

---

PBS	phosphate buffered saline
p-BAD	phosphorylated BAD
PCa	prostate cancer
<i>PCNA</i>	a proliferating cell nuclear antigen encoding gene
PD-1	programmed cell death protein 1
PD-L1	programmed death-ligand 1
PFA	paraformaldehyde
PI3K	phosphoinositide 3-kinase
PIGF or PGF	placental growth factor
PKC	protein kinase C
<i>POU5F1</i>	POU class 5 homeobox 1, an OCT4 encoding gene
pRB	retinoblastoma protein
p-S6	phosphorylated S6
PSA	prostate-specific antigen
PTEN	phosphatase and tensin homolog
PVDF	polyvinylidene fluoride
qRT-PCR	quantitative reverse transcription polymerase chain reaction
R1881	methyltrienolone, synthetic androgen
RAF1	rapidly accelerated fibrosarcoma kinase 1
RANTES	regulated upon activation normal T cell expressed and secreted
RAS	rat sarcoma protein
RNA	ribonucleic acid
rpm	rounds per minute
RPMI	Roswell Park Memorial Institute
RSK	ribosomal S6 kinase
S	Serine
S6	ribosomal protein S6
S6 <sup>P-/-</sup>	unphosphorylatable S6
SA $\beta$ -Gal	senescence-associated $\beta$ -galactosidase
SAL	supraphysiological androgen levels
SASP	senescence-associated secretory phenotype
SCF	stem cell factor protein
SD	standard deviation
SDS	sodium dodecyl sulfate

sec	second
SEM	standard error of the mean
SOX2	SRY (sex determining region Y)-box transcription factor 2
SRC	sarcoma tyrosine kinase
STAT	signal transducer and activator of transcription
T	Threonine
<i>TBP</i>	a TATA-box binding protein encoding gene
TBS-T	tris-buffered saline and Tween 20 (Polysorbate 20)
T cells	T-lymphocytes
TECK	thymus expressed chemokine
TGF $\beta$	transforming growth factor beta
TIMP	tissue inhibitor of metalloproteinase
TNF $\alpha$	tumor necrosis factor alpha
TNF R	tumor necrosis factor receptor
TPO	Thromboprotein
TRAIL	TNF-related apoptosis-inducing ligand
V	volt
VEGF	vascular endothelial growth factor
x	times (concentration)
XCR1	X-C motif chemokine receptor 1
x g	times gravity
X-Gal	5-bromo-4-chloro-3-indolyl-beta-D-galacto-pyranoside
Y	Tyrosine



## ZUSAMMENFASSUNG

Der Androgenrezeptor (AR) spielt eine maßgebliche Rolle in der medikamentösen Therapie des Prostatakarzinoms (PCa). Sowohl supraphysiologische Androgen Level (SAL) als auch einige AR-Antagonisten inhibieren die Proliferation von PCa Zellen durch die Induktion zellulärer Seneszenz. Hierbei kommt es zu einem permanenten Zellzyklusarrest. Hier zeigte sich, dass Enzalutamid (ENZ), ein klinisch verwendetes Anti-Androgen der zweiten Generation, auch zur Seneszenzinduktion führt. Eine solche Induktion der Seneszenz scheint zunächst eine potenzielle Therapiestrategie für das PCa zu eröffnen. Jedoch ist bekannt, dass seneszente Zellen im Rahmen des Senescence-Associated Secretory Phenotype (SASP) Zytokine und Chemokine sezernieren. Der SASP ist möglicherweise in der Lage, das Tumormikromileu zu modulieren und Effekte parakrin auf umgebende Zellen zu vermitteln. Die Effekte des SASPs sind jedoch abhängig von der Bilanz aus sezernierten tumorfördernden und tumorhemmenden Faktoren. Diese Faktoren variieren je nach dem, welcher Stimulus zur Induktion der Seneszenz führte. Bislang wurde die Komposition und funktionelle Auswirkung des SASP-Sekretoms der mit AR-Liganden-behandelten PCa Zellen noch nicht untersucht.

In dieser Dissertation wurden humane PCa Zelllinien mit AR-Liganden behandelt, um zelluläre Seneszenz zu induzieren. Hiernach wurde die Komposition des SASP-Sekretoms dieses konditionierten Kulturmediums analysiert. Die Ergebnisse der Analyse zeigten, dass das SASP-Sekretom von SAL-behandelten Zellen sich von dem ENZ-behandelter Zellen unterscheidet. Die funktionelle Auswirkung des SASPs wurde durch die Kultivierung von PCa und Immunzellen in konditioniertem Kulturmedium untersucht. Interessanterweise unterdrückt der SASP von SAL-behandelten Zellen die Proliferation von PCa Zellen, während der SASP der mit Antagonisten-behandelten Zellen diese anregt. Weiterhin reduziert SAL die PCa Stammzeleigenschaften. Diese neuen Erkenntnisse legen die Folgerung nahe, dass SAL in der Behandlung des PCas einen Vorteil gegenüber Antagonisten hat. Jedoch zeigten weitere Untersuchungen eine Unterdrückung der Lymphozyten Proliferation durch das SASP von sowohl SAL- als auch ENZ-behandelten Zellen. Darüber hinaus zeigten AR-Liganden-behandelte PCa Zellen eine Resistenz zur Lymphozyten-vermittelten Apoptose. Diese immunsuppressiven Effekte könnten zu langfristigen Nachteilen in der Therapie des PCas führen. Daher wurden potenzielle Senolytika zur Eliminierung dieser AR-Liganden-induzierten

zellulär seneszenten Zellen untersucht. Aktiviertes AKT konnte in dieser Arbeit als zugrunde liegender Mechanismus hinter der apoptotischen Resistenz von SAL- und von ENZ-behandelten Zellen identifiziert werden. Dieser Mechanismus unterschied sich jedoch in den AKT-Downstream-Signalen. Diese unterschiedliche Regulation der AKT-Downstream-Signale führte zu einer auffälligen unterschiedlichen Sensibilität gegenüber spezifischer Senolytika; ENZ-behandelte Zellen hierbei zu AKT Inhibitoren und SAL-behandelte Zellen zu HSP90 Inhibitoren. Diese neuen Einsichten deuten darauf hin, dass eine Behandlung mit Senolytika bei AR-Liganden-induzierten zellulären Seneszenz eine nützliche therapeutische Strategie beim PCa sein könnte. Hierbei muss jedoch die Wahl angemessener Senolytika für jeden spezifischen AR-Liganden bedacht werden.

Zusammengefasst werden in dieser Arbeit erstmalig SASP-vermittelte unerwünschte Nebenwirkungen einer AR-Liganden-induzierten zellulären Seneszenz beleuchtet. In dieser Dissertation wird hiermit auch die potenzielle Strategie der Eliminierung AR-Liganden-behandelter Zellen mittels Senolytika aufgezeigt.

## SUMMARY

The androgen receptor (AR) represents a major drug target in prostate cancer (PCa) therapy. Both supraphysiological androgen level (SAL) and some AR antagonists inhibit PCa cell proliferation via induction of cellular senescence, an irreversible cell cycle arrest. Here, it is shown that the clinically used second-generation AR antagonist Enzalutamide (ENZ) also induces cellular senescence. An induction of cellular senescence seems to be a potential strategy for PCa therapy. Unfortunately, senescent cells are known to secrete cytokines and chemokines termed as senescence-associated secretory phenotype (SASP). The SASP may modulate the tumor microenvironment and mediate paracrine effect to neighboring cells. However, the effect of SASP depends on the balance between secreted tumor promoting and suppressing factors. These factors can vary when different senescence-inducing stimuli are used. So far, the composition and functional effect of SASP secretome of AR ligand-treated PCa cells have not yet been analyzed.

In this thesis, human PCa cell lines were treated with AR ligands to induce cellular senescence. Thereafter, conditioned media were collected and analyzed for the composition of SASP secretomes. The results show that the SASP secretome of SAL-treated cells differs from that of ENZ-treated cells. Functional effects of SASP were examined by culturing PCa and immune cells with conditioned media. Interestingly, the SASP of SAL-treated cells suppresses, but the SASP of antagonist-treated cells promotes PCa cell proliferation. SAL also reduces PCa stemness. These novel findings suggest that SAL may provide more advantage than antagonists to inhibit PCa. However, further results show that the SASP of either SAL- or ENZ-treated cells suppresses lymphocyte proliferation. Moreover, AR ligand-treated PCa cells are resistant to lymphocyte-mediated apoptosis. Such immune-suppressive effects may provide long-term disadvantages for PCa therapy. Therefore, potential senolytic compounds to eliminate AR ligand-induced cellular senescent cells were also analyzed. This study identifies activated AKT as an underlying mechanism for apoptotic resistance of both SAL- and ENZ-treated cells, but through distinct AKT downstream signals. The different regulation of the AKT downstream signal by AR ligands strikingly leads to a distinct apoptotic sensitivity towards specific senolytic compounds; ENZ-treated cells towards AKT inhibitor and SAL-treated cells towards HSP90 inhibitor. These novel findings suggest that treatment with

senolytic compounds after AR ligand-induced cellular senescence might be a very useful therapeutic strategy in PCa therapy, but a suitable senolytic compound for a particular AR ligand should be considered.

Taken together, this is the first study highlighting undesired side-effects mediated by AR ligand-induced cellular senescence via SASP. Thus, this thesis also demonstrates a potential strategy to eliminate AR ligand-treated cells by using senolytic compounds.

## 1 INTRODUCTION

### 1.1 Androgen receptor (AR) signaling

Androgen receptor (AR) is a nuclear transcription factor and a member of the steroid hormone receptor superfamily (Gelman 2002). The protein structure of AR contains four distinct domains: (1) a large amino (N)-terminal transactivation domain, which is responsible for the receptor-mediated transactivation; (2) a central DNA-binding domain, which consists of two zinc fingers that form the DNA-binding structure for recognizing and binding to the androgen response element (ARE) on the promoter and enhancer of target genes; (3) a hinge region that possesses a ligand-dependent nuclear localization signal to mediate nuclear localization; and (4) a carboxy (C)-terminal ligand-binding domain, which is responsible for the binding of AR ligands (Gelman 2002, Claessens *et al.* 2001, Cutress *et al.* 2008, McEwan 2004). N- and C-terminal transactivation domains consist of transcriptional activation function-1 and -2, respectively. Both activation function-1 and -2 are responsible for the recruitment of co-regulators and transcription complexes to AR in order to regulate the transcription of target genes (Bevan *et al.* 1999, Heery *et al.* 1997).

Although AR is known as a nuclear transcription factor, the AR signaling and function can be classified into two manners: (1) genomic action and (2) non-genomic action (Liao *et al.* 2013, Leung and Sadar 2017). In general, the AR localizes in the cytoplasm without ligand binding (Figure 1). It forms a complex with heat shock proteins (HSPs) and other chaperones, which disable AR from entering into the nucleus (Hessenkemper and Baniahmad 2012). Upon binding of androgens (AR agonists) to the receptor, the activated AR then dissociates from HSPs (including HSP90), dimerizes, translocates into the nucleus, and binds to AREs. The binding of the activated AR to ARE recruits co-regulators leading to transactivation or trans-repression of target gene transcription. Such process is considered as genomic signaling of AR, which is thought to occur over several hours (Liao *et al.* 2013).

However, it is known that AR signaling pathway can also occur in a non-genomic manner (Figure 1). This non-genomic signaling of AR does not require nuclear translocation and DNA binding. Moreover, it was shown that such signaling occurs rapidly within minutes (Peterziel *et al.* 1999). Instead of translocating into the nucleus after binding of androgens, the activated

AR in the cytoplasm can interact with or function through several signaling molecules including PI3K/AKT, SRC, RAS/RAF1, PKC, MAPK/ERK (Gatson *et al.* 2006, Baron *et al.* 2004, Migliaccio *et al.* 2000, Peterziel *et al.* 1999). Activation of these signaling cascades along with the regulation of AR target genes lead to cell proliferation and survival.

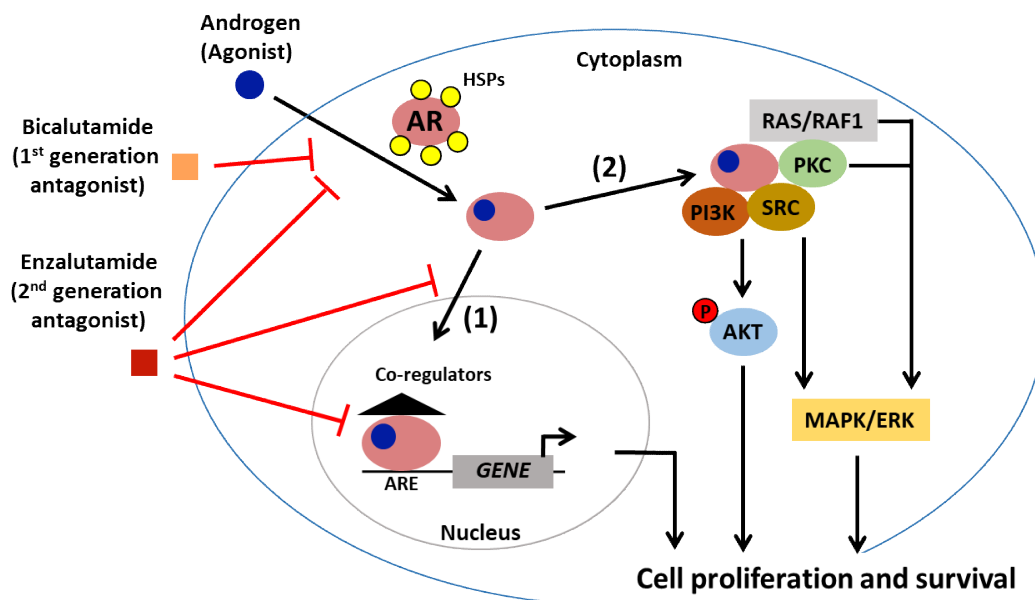


**Figure 1. Genomic and non-genomic signaling of AR control cell proliferation and survival.** In the cytoplasm, the androgen receptor (AR) forms a complex with heat shock proteins (HSPs). Activation of the AR is triggered by binding of androgen (AR agonist) to the receptor. The activated AR dissociates from HSPs, and subsequently mediates either (1) genomic or (2) non-genomic AR signaling. (1) The activated AR translocates into the nucleus, where it binds to the androgen response element (ARE) at the promoter of the target genes. Upon binding to ARE, it recruits co-regulators to regulate the gene transcription. Many AR target genes are involved in cell proliferation/survival regulation. (2) Instead of translocating into the nucleus, the activated AR interacts with and functions through several signaling molecules important for cell proliferation and survival in the cytoplasm, e.g., Src, PI3K/AKT, PKC, RAS/RAF1, MAPK/ERK. It is suggested that both genomic and non-genomic actions of AR control cell proliferation and survival. Activation of AR by androgen can be blocked by Bicalutamide (1<sup>st</sup> generation AR antagonist) or Enzalutamide (2<sup>nd</sup> generation AR antagonist). Both antagonists competitively inhibit androgen binding to AR. Unlike Bicalutamide, Enzalutamide inhibits AR nuclear translocation, DNA binding, and co-regulators recruitment. (Modified from Liao *et al.* 2013, Rodriguez-Vida *et al.* 2015).

Notably, in the absence of androgens, several growth factors and cytokines can also activate AR through multiple signaling pathways including PI3K/AKT or RAS/RAF/MAPK/ERK (Ueda *et al.* 2002, Traish and Morgentaler 2009, Edline and Hsieh 2014) (not shown in Figure 1). The activated AR by signal transduction factors eventually translocates into the

nucleus, binds to ARE, and regulates target genes transcription, thus, considering as a ligand-independent genomic AR signaling.

## **1.2 Prostate cancer (PCa) and hormone therapies**

For decades, prostate cancer (PCa) is the most diagnosed cancer and the second leading cause of cancer mortality of men in many Western countries (Jemal *et al.* 2007, Siegel *et al.* 2020). Evidences show that androgens play a critical role for the growth of both normal and cancerous prostate through the AR (Ntais *et al.* 2003, Andriole *et al.* 2004, Lonergan and Tindall 2011). Thus, AR represents a major drug target in the treatment of PCa.

The idea of PCa treatment originated from Huggins and Hodges's clinical observation in 1941 suggested that PCa growth can be controlled by reducing the levels of androgens through castration (Huggins and Hodges 1941). This finding brought up the current treatment option of androgen deprivation therapy (ADT) as a standard therapeutic strategy for PCa. Although it is initially effective, yet, the tumor in many patients gradually develops later on to a stage of castration-resistant PCa (CRPCa) (Harris *et al.* 2009). However, the tumor still relies on AR signaling at this stage with adaptive AR signaling activation pathways (Decker *et al.* 2012, Nelson 2012). Hence, inhibition of AR signaling by AR antagonists is still applicable.

The AR antagonists Bicalutamide (BIC) and Enzalutamide (ENZ) are clinically used and applied in order to block AR actions in PCa (Wellington and Keam 2006, Rodriguez-Vida *et al.* 2015). BIC is a first-generation AR antagonist. Mechanistically, BIC competes with androgen for binding to cytosolic AR (Figure 1). The conformational change of AR after binding with BIC is distinct from agonist (Osguthorpe and Hagler 2011). It leads to blockade of co-activator binding sites and thus interferes with normal AR target gene expression. However, antagonistic actions of BIC might not be totally secured. Evidences show that BIC could still stimulate AR nuclear translocation and DNA binding (Masiello *et al.* 2002). Moreover, the switching role from antagonist to agonist of the BIC has also been reported (Culig *et al.* 1999, Bohl *et al.* 2005). In contrast to BIC, ENZ as a second-generation AR antagonist exhibits improved antagonistic activities. It competitively inhibits androgen binding to AR with five- to eightfold greater affinity than BIC (Tran *et al.* 2009, Rodriguez-Vida *et al.*

2015). Also, ENZ inhibits AR nuclear translocation, DNA binding, and co-activator recruitment (Figure 1).

Unfortunately, despite the initial response to AR antagonist treatment including reduction level of the diagnostic marker prostate-specific antigen (PSA) and regression of tumor growth, a resistance or adaptive response eventually occurs and results in re-growth of the tumor (Decker *et al.* 2012, Perner *et al.* 2015, Lakshmana and Baniahmad 2019). For example, upregulation of glucocorticoid receptor has been detected during AR antagonist treatment (Puhr *et al.* 2018). The activation of glucocorticoid receptor signaling has been proposed as one of the underlying adaptive mechanisms for cells to bypass AR blockade. Interestingly, the outcomes of either BIC or ENZ treatment have been associated with increased PCa stem/progenitor cells (Wen *et al.* 2016), which might as well be the reason for tumor re-growth.

Interestingly, it seems that the level of androgen plays an important role in PCa growth. The treatment with AR agonist at supraphysiological androgen level (SAL) is also applied to CRPCa patients in clinical trials as an alternative approach to AR antagonists (Teply *et al.* 2018, Denmeade 2018). Such therapeutic strategy is called bipolar androgen therapy, since it creates rapid cycling between extremely high and low levels of androgen in the blood during a treatment cycle. This seems to contradict with the original idea of Huggins and Hodges's observation. Nevertheless, evidences suggest a concentration dependent response of PCa proliferation toward androgens (Sonnenschein *et al.* 1989, Roediger *et al.* 2014). Sonnenschein *et al.* (1989) and Roediger *et al.* (2014) showed that SAL inhibits PCa cell proliferation, while lower androgen levels enhance proliferation. This indicates an opposite effect of different androgen concentrations used in androgen-sensitive PCa cell line.

### **1.3 AR ligand-induced cellular senescence**

Cellular senescence is defined as a permanent cell cycle arrest and has initially been proposed as one of the cancer inhibition strategies (Campisi 2001, Campisi and d'Adda di Fagagna 2007). Interestingly, it has been described that cellular senescence can be induced by AR signaling in PCa. On one hand, treatment with SAL using the natural androgen dihydrotestosterone (DHT) or the synthetic androgen methyltrienolone (R1881) induces cellular senescence in PCa cells



and *ex vivo* in PCa patient samples (Mirochnik *et al.* 2012, Roediger *et al.* 2014). On the other hand, an induction of cellular senescence has been shown in PCa cells that were treated with first-generation AR antagonist BIC (Burton *et al.* 2013, Esmaili *et al.* 2016a) or other AR antagonist-like compounds including atraric acid, halogen-substituted anthranilic acid esters, and aminosteroids (Hessenkemper *et al.* 2014, Roell *et al.* 2019, Fousteris *et al.* 2010). Thus, cellular senescence might be one of the underlying mechanisms for AR ligand-mediated PCa growth inhibition. Of note, an induction of cellular senescence by second-generation AR antagonist ENZ has not yet been reported.

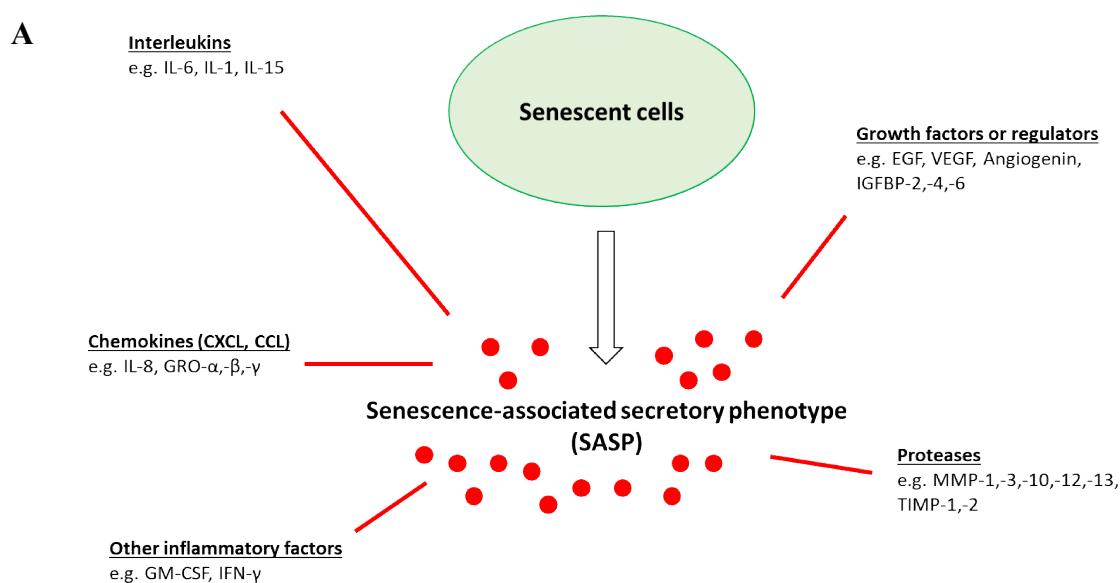
In general, cellular senescence can be triggered by different stimuli including telomere shortening, DNA damage, chromatin perturbation, chemotherapeutic agent treatment, radiation exposure, activation of oncogenes, oxidative stress, and other stress inducers (Campisi and d'Adda di Fagagna 2007). Mechanistically, these stimuli often lead to activation of p53-p21<sup>Cip1/Waf1</sup> and/or p16<sup>INK4a</sup>-pRB tumor suppressor pathways. These pathways may crosstalk with each other but can also independently cause cell cycle arrest and maintain the senescent state. Although most senescent cells exhibit activation of these pathways, senescence induction being independent of p53-p21<sup>Cip1/Waf1</sup> or p16<sup>INK4a</sup>-pRB has also been reported (Kotollosi *et al.* 2020).

Several markers are used to characterize senescent cells. A specific marker to identify senescent cells is the senescence-associated  $\beta$ -galactosidase (SA  $\beta$ -Gal) activity (Campisi and d'Adda di Fagagna 2007, Dimri *et al.* 1995, Lee *et al.* 2006). The elevated SA  $\beta$ -Gal reflects an increased lysosomal biogenesis that commonly occurs in senescent cells. Moreover, since both cyclin-dependent kinase inhibitors p21<sup>Cip1/Waf1</sup> and p16<sup>INK4a</sup> are often upregulated in senescent cells, detection of these two factors at mRNA and protein are applied as markers for cellular senescence (Krishnamurthy *et al.* 2004) along with the detection of SA  $\beta$ -Gal activity. Other proteins may also be used to identify senescent cells such as DEC1 and p15<sup>INK4b</sup> (Collado *et al.* 2005, Collado and Serrano 2006, Kotollosi *et al.* 2020). In addition, detection of senescence-associated heterochromatic foci (Narita *et al.* 2003) and senescence-associated DNA-damage foci (Takai *et al.* 2003) may also be used as markers for some senescent cells.

In PCa, AR ligand-induced cellular senescence is detected by SA  $\beta$ -Gal activity and the p16<sup>INK4a</sup>-pRB pathway, while p53-p21<sup>Cip1/Waf1</sup> pathway is only affected weakly. In line with

this, an upregulated p16<sup>INK4a</sup> was detected in BIC- and atraric acid-induced cellular senescence (Esmaceli *et al.* 2016a, Hessenkemper *et al.* 2014), whereas detection of senescence-associated heterochromatic foci, upregulated p16<sup>INK4a</sup>, and hypophosphorylated pRB were observed in DHT- or R1881-treated cells at SAL (Roediger *et al.* 2014). Interestingly, it was shown that both SAL-induced and antagonist-induced cellular senescence are mediated through the SRC-AKT pathway (Hessenkemper *et al.* 2014, Roediger *et al.* 2014, Kokal *et al.* 2020).

Growth arrest is the hallmark of cellular senescence, yet, senescent cells remain metabolically active and often become resistance to cell-death signals (Campisi and d'Adda di Fagagna 2007, Hampel *et al.* 2004, Salminen *et al.* 2011). Senescent cells acquire widespread alteration in gene expression and intracellular signaling. These features lead to enhanced secretion of cytokines, chemokines, growth factors, and proteinases known as the senescence-associated secretory phenotype (SASP) (Coppé *et al.* 2010) (Figure 2A). SASP represents a major debating topic for the consequences of cellular senescence induction, because it can mediate paracrine effects on neighboring non-senescent tumor cells and may act as a tumor promoter (Gonzalez-Meljem *et al.* 2018, Coppé *et al.* 2008, 2010). Interestingly, although induction of cellular senescence in PCa by AR ligands has been well described, the paracrine effects of SASP are rarely investigated.



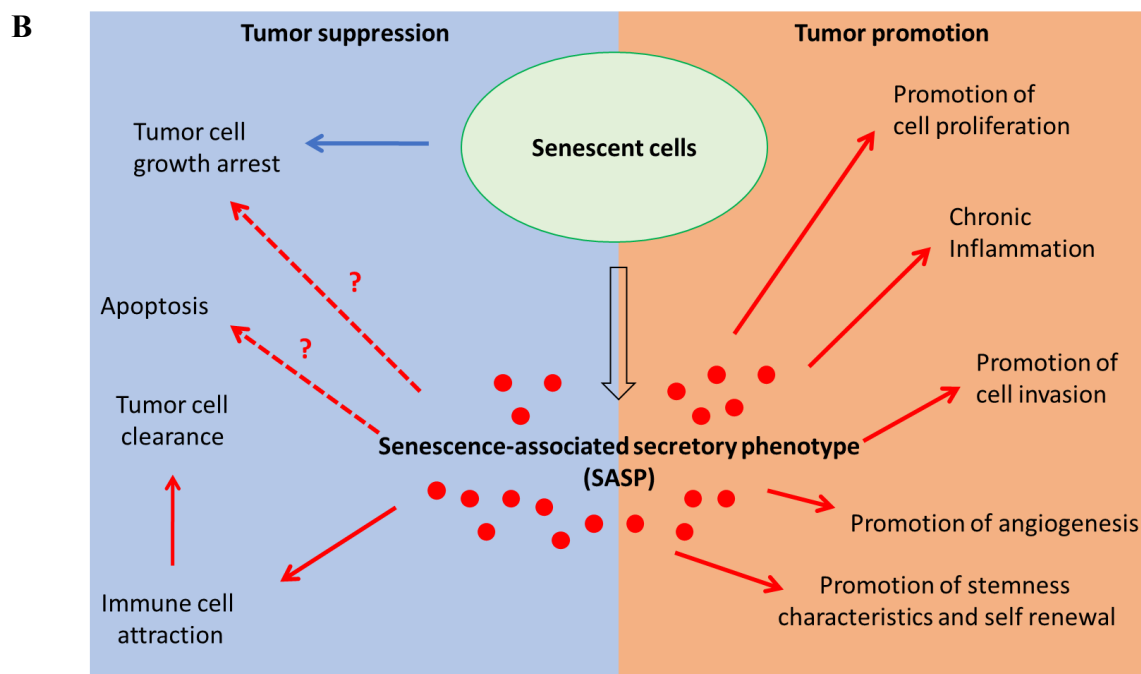


**Figure 2. Senescent cells are accompanied by SASP factors.** (A) One of the major features of senescent cells is the senescence-associated secretory phenotype (SASP). SASP factors are comprised of but not limited to secreted interleukins, chemokines, growth factors or regulators, proteases, and other inflammatory factors. (B) The benefit of cellular senescence induction remains controversial. On the one hand for tumor suppression aspect, senescent cells are already growth arrested, and some SASP factors are thought to attract immune cells to the site for tumor clearance. SASP may also trigger apoptosis or growth arrest. On the other hand, SASP factors including proteases, growth, and angiogenesis factors can mediate paracrine effects on neighboring non-senescent tumor cells, resulting in promotion of proliferation, invasion, angiogenesis, and stemness for tumor promotion aspect. (Modified from Coppé *et al.* 2010, Lecot *et al.* 2016).

#### 1.4 Senescence-associated secretory phenotype (SASP) and paracrine effects

Senescent cells are accompanied by SASP. SASP factors can mediate autocrine and paracrine effects. The autocrine effect is not in focus as much as the paracrine effects, because the senescent cells are already growth arrested. In contrast, paracrine effects from SASP are controversially discussed whether it promotes or suppresses tumor growth (Figure 2B). SASP gene expression and secretion profiles are cell type specific and may differ when cells are exposed to different senescence-inducing stimuli (Basisty *et al.* 2020, Coppé *et al.* 2010, Rao and Jackson 2016). Hence, the effects on neighboring non-senescent tumor cells by SASP then rely on the balance between secreted tumor-promoting and -suppressive factors. This may depend as well on how senescence is induced, such as by AR agonist or antagonist, since AR is a transcription factor but also interacts with multiple signaling cascades.

### 1.4.1 SASP affects growth and proliferation

One of the major concerns for the effects of SASP is whether it promotes growth and proliferation of the tumor. In fact, SASP contains many secreted growth factors that are potent stimulators of cell proliferation. It is well described that the SASP from senescent fibroblasts can promote tumor growth and cancer cell proliferation (Saleh *et al.* 2018, Coppé *et al.* 2010, Liu and Hornsby 2007, Krtolica *et al.* 2001). Similar outcome has been observed when neoplastic prostate epithelium was treated with SASP from senescent prostate fibroblasts (Bavik *et al.* 2006). Interestingly, regardless of how senescence is induced (by oncogene overactivity, oxidative stress, DNA damage, or replicative exhaustion), these fibroblasts exhibit tumor promoting capability by secreting a subset of growth promoting factors (Saleh *et al.* 2018, Bavik *et al.* 2006, Krtolica *et al.* 2001).

Unfortunately, this may occur as well in case of conventional cancer therapies such as chemotherapy or radiation. Such therapies can enhance growth factors in the tumor microenvironment via senescence induction and thus resulting in a pro-tumorigenic response (Toste *et al.* 2016, Ohuchida *et al.* 2004). Notably, irradiation in PCa patients is associated with a significantly increased release of exosomes (Lehmann *et al.* 2008). Moreover, ADT, a standard therapeutic option for PCa, was shown to induce SASP in PCa epithelial cells (Pernicová *et al.* 2011). However, neither the paracrine effect of ADT-induced SASP nor irradiation-induced exosomes on non-senescent PCa cells were reported.

Not all SASP factors from senescent cells promote growth and cell proliferation. Although limited, evidences exist describing SASP-mediated inhibition of cell proliferation, such as through growth arrest or apoptosis induction. It has been shown that the conditioned medium derived from senescent breast cancer cells can induce a senescent growth arrest in naive breast cancer cells (Di *et al.* 2008). Consistently, the induction of SA  $\beta$ -Gal activity, cell size, and p21<sup>Cip1/Waf1</sup> protein level were observed in naive breast cancer cells by culturing with conditioned medium. Another case showed that conditioned medium derived from senescent primary human foreskin fibroblasts can activate MYC and sensitize the immortalized pre-transformed cells to TRAIL-induced apoptosis (Vjetrovic *et al.* 2014). In case of prostate cells, impaired growth of immortalized prostate cells by SASP from mesenchymal stromal

cells was observed (Alessio *et al.* 2019). However, Alessio *et al.* (2019) further showed that the same SASP mediates no effect on metastatic PCa cells.

Taken together, the paracrine effect of SASP on cell growth and proliferation has been described in both directions as promoter and suppressor depending on cell type and tissue context. Hence, the question remains open for the effect of AR ligand-induced SASP.

#### **1.4.2 SASP affects stem/progenitor cells**

Stem cells are characterized by two unique capabilities, self-renewal and differentiation. Once differentiated, cells usually lose the self-renewal ability. In general, one can obtain pluripotent stem cells from the inner cell mass of early stage blastocysts (Kashyap *et al.* 2009, Thomson *et al.* 1998). However, studies showed that pluripotent stem cells can be induced from differentiated adult cell types by epigenetic reprogramming (Kashyap *et al.* 2009, Yu *et al.* 2007, Aoi *et al.* 2008, Takahashi *et al.* 2007). The highest efficiency of induced pluripotency is achieved by a combination of four transcription factors of either Yamanaka's factors or Thomson's factors introduced into the differentiated cells (Figure 3). Yamanaka's factors include OCT4, SOX2, KLF4, and MYC. Thomson's factors include OCT4, SOX2, NANOG, and LIN28. These factors are also considered as stem cell markers. Interestingly, OCT4 and SOX2 appear to be critically required, whereas in some cases, other factors are dispensable (Nakagawa *et al.* 2008, Huangfu *et al.* 2008). Nevertheless, a combination of all six factors, OCT4, SOX2, NANOG, MYC, KLF4, and LIN28, has been shown to enhance pluripotency with reduced time of reprogramming (Liao *et al.* 2008). Since stem cells can be induced from differentiated cells (perhaps by mutations, dedifferentiation, or epigenetic reprogramming), cancer stem cells may also be derived in a similar manner from stem cells, progenitor cells, differentiated cells, or cancer cells (Figure 3).

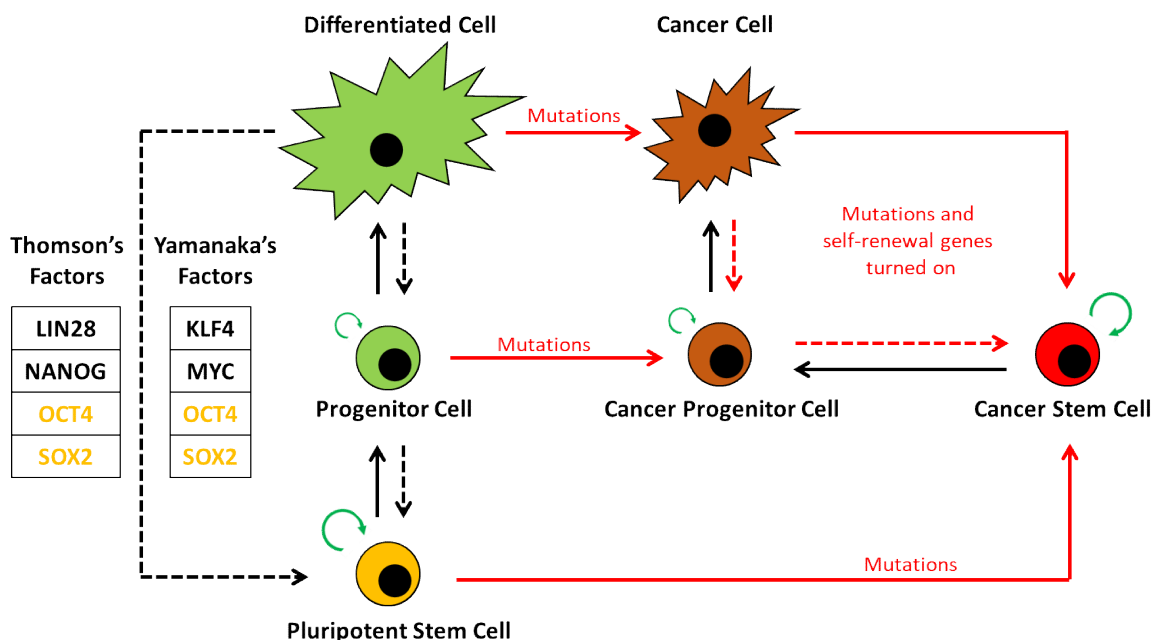


**Figure 3. Overview of the origin of the cancer stem cells.** Cancer stem cells can be derived from stem cells, progenitor cells, differentiated cells, or cancer cells via mutations and/or when self-renewal genes turned on (red arrow). Pluripotent stem cells exhibit the ability to self-renew (green arrow) and to differentiate (solid black arrow) into several cell lineages, whereas differentiated cells lose the self-renewal ability. However, pluripotency can be achieved by dedifferentiation (dash arrow) or epigenetic reprogramming of differentiated cells through introduction of either Thomson's factors or Yamanaka's factors. Among these factors, OCT4 and SOX2 seem to be critically required. (Modified from Kashyap *et al.* 2009, Khan *et al.* 2019, Sin and Lim 2017).

SASP is also associated with an induction of a cancer stem cell-like phenotype (Saleh *et al.* 2018, Cahu *et al.* 2012). The high expression of some key SASP factors is strongly correlated with stem cell features in tumor cells and has been shown to play an important role in the self-renewal and proliferation of cancer stem cells (Ma *et al.* 2015, Yang *et al.* 2014, Levina *et al.* 2010). *KITLG* encodes SCF (stem cell factor) protein, one of the major secreted factors of SASP, is an example. Levina *et al.* (2010) showed that while chemotherapy of non-small cell lung cancer cells can promote lung cancer stemness, blocking SCF-c-kit signaling is sufficient to inhibit cancer stem cell proliferation and survival. Hence, this study suggests a role of the SCF in cancer stem cells, which could be as well a target for improving antitumor efficacy of chemotherapy in human lung cancer (Levina *et al.* 2010). Consistently, it has been reported that chemotherapy-induced senescence could change stem-cell-related properties of malignant cells and promotes cancer stemness (Milanovic *et al.* 2018). Milanovic *et al.* (2018) revealed that this senescence-associated stemness unexpectedly exerts highly aggressive growth

potential by escaping from cell-cycle blockade. These findings suggest implications toward cancer therapy strategies.

One of the hypothesized explanations for relapse of many cancer types in patients after certain therapeutic treatment is the cancer stem/progenitor cells, which survive or are resistant to such therapies. Interestingly, it has been suggested that epithelial stem/progenitor cells are critical for regulation and maintenance of the prostatic gland and also play an important role in PCa development (Choi *et al.* 2012, Klarmann *et al.* 2009). Among other possibilities, PCa stem/progenitor cells might survive ADT and contribute to re-growth of PCa and CRPCa (Wen *et al.* 2016, Klarmann *et al.* 2009, Li and Tang 2011). Moreover, Wen *et al.* (2016) reported that treatment with AR antagonist either BIC or ENZ also leads to an increased PCa stem/progenitor population. This suggests an unwanted side-effect by these current clinically used AR antagonists. Note that an underlying mechanism behind an enrichment of PCa stem/progenitor population might be the AR antagonist-induced SASP.

### **1.4.3 SASP affects immune cell responses**

Immune cell attraction leading to tumor clearance is probably the main proposed tumor suppressive characteristic of SASP (Figure 2B). Secreted factors as component of SASP can attract immune cells, such as natural killer (NK) cells, T cells, and natural killer T (NKT) cells, to the tissue microenvironment (Velarde *et al.* 2013, Rao and Jackson 2016). These cells can recognize a number of SASP cytokines through their diverse cell surface receptors (Saleh *et al.* 2018, Morvan and Lanier 2016, Bernardini *et al.* 2014, Bromley *et al.* 2008) and mediate cytolytic activity on senescent cells and neighboring tumor cells (Xue *et al.* 2007, Kang *et al.* 2011). However, how immune cells would respond to SASP is depending on secreted factors from senescent cells and the tumor microenvironment.

In the last decade, immunotherapies have become more popular in the clinic-oriented research field as option for fighting against cancer. In fact, many cancer immunotherapeutic strategies have been approved for melanoma, lung cancer, kidney cancer, urothelial cancer, breast cancer, and PCa (Boettcher *et al.* 2019, Hodi *et al.* 2010, Tang *et al.* 2018, Kantoff *et al.* 2010). An idea of cancer immunotherapy is to boost up the cytotoxic potential of the human immune system against malignancies. Immunotherapeutic options include vaccine therapies (DNA-, cell-, peptide, or viral vector-based vaccines) and usage of immune checkpoint

inhibitors (Boettcher *et al.* 2019). Interestingly, there are currently many ongoing clinical trials for PCa, but only Sipuleucel-T (cell-based vaccine) has been approved so far since 2010. In line with this, metastatic PCa does not show satisfying response towards checkpoint blockade of PD-1/PD-L1 and CTLA-4 (Boettcher *et al.* 2019, Kwon *et al.* 2014). It seems that PCa exhibits some mechanisms of immunosuppression to limit the effectiveness of therapy. Several tumor-intrinsic mechanisms of resistance to immune response are including but not limited to: (1) insufficient tumor antigen, (2) loss of MHC/HLA expression, (3) loss of PTEN, (4) disruption of IFN- $\gamma$  signaling, (5) regulation by oncogenic signaling, (6) tumor dedifferentiation and stemness, and (7) immune-suppressive tumor microenvironment (Kalbasi and Ribas 2020, Vitkin *et al.* 2019).

Indeed, it is possible that the immune-suppressive tumor microenvironment might be the consequence of secreted SASP factors after conventional therapies. Surprisingly, while SASP is generally acknowledged for being immune attractant, SASP-suppressed immune response has mostly been described in case of mouse prostate tumor, human PCa cell line, and human PCa cells-derived xenograft mouse model (Saleh *et al.* 2018, Toso *et al.* 2014, Di Mitri *et al.* 2014, Simova *et al.* 2016, Kloss *et al.* 2018). Secreted Cxcl2, IL-1RA, and TGF  $\beta$  are examples of SASP factors that have been suggested as immune-suppressive cytokines (Rao and Jackson 2016, Toso *et al.* 2014, Di Mitri *et al.* 2014, Kloss *et al.* 2018). In case of AR ligand-induced senescent PCa cells, AR ligands may regulate the expression of tumor antigens, stemness, signaling cascades, and secretion of SASP factors, in which all together could lead to immune response modulation.

## **1.5 Senolytic compounds**

Senescent cells appear to have the capability of resisting cell death by upregulating pro-survival/anti-apoptotic networks (Saleh *et al.* 2018, Salminen *et al.* 2011, Hampel *et al.* 2004). Interestingly, SASP is also suggested to be involved in this apoptotic-resistant feature (Özcan *et al.* 2016). To overcome this feature of senescence, senolytic agents have been developed and are currently in focus. Senolytic compounds are small molecule compounds that selectively kill senescent cells by targeting activated pro-survival/anti-apoptotic pathways (Wong *et al.* 2018). Most targeted factors and pathways are PI3K/AKT survival pathway,



BCL-2/BCL-XL anti-apoptotic pathway, p53/p21 pathway, HSP90, cell surface glycoproteins, and tyrosine kinase receptors, etc. (Wong *et al.* 2018, Saleh *et al.* 2018).

Interestingly, different senescence inducing stimuli might cause distinct activation of pro-survival/anti-apoptotic pathways (Wong *et al.* 2018, Hernandez-Segura *et al.* 2017). Indeed, this can perhaps be applied to cells that were induced by AR ligand to undergo cellular senescence. In line with this, AR interaction with some survival signaling cascades is well described (Gatson *et al.* 2006, Baron *et al.* 2004, Migliaccio *et al.* 2000, Peterziel *et al.* 1999). Evidence indicates some factors in senescent PCa as potential drug target for senolytic agent. Roediger *et al.* (2014) showed that SAL-induced cellular senescence exhibits activated pro-survival AKT pathway as indicated by enhanced levels of phospho-AKT (p-AKT), suggesting that AKT might serve as a potential target in this condition. Another interesting target factor for senolysis is HSP90, because both AR and AKT are HSP90 clients (Hessenkemper and Baniahmad 2012, He *et al.* 2013, Centenera *et al.* 2015, Zhang *et al.* 2005). It should be kept in mind that AR agonist- and antagonist-treated cells might exhibit different upregulated pro-survival/anti-apoptotic signaling, which preferentially sensitize cells to specific senolytic compounds.

Since the benefit of senescence induction is controversial and limited information is known for AR ligand-induced SASP, targeting and eliminating senescent cells using senolytic compounds could be a necessary approach along with conventional PCa therapy.

## 2 HYPOTHESES AND OBJECTIVES

The AR signaling represents a major drug target for PCa therapy. An induction of cellular senescence (irreversible cell cycle arrest) has been described in PCa cells after treating with SAL, first-generation AR antagonist BIC, and other AR antagonist-like compounds (Roediger *et al.* 2014, Esmaeili *et al.* 2016a, Hessenkemper *et al.* 2014, Roell *et al.* 2019, Foustieris *et al.* 2010). However, cellular senescence induction by ENZ, a clinically used and a second-generation AR antagonist, has not yet been reported. It is hypothesized that ENZ also induces cellular senescence in PCa cells. In this thesis, human PCa cell lines were treated with AR ligands to induce cellular senescence. Cells were also treated with ENZ to examine the capability of ENZ on cellular senescence induction.

Although AR ligand-induced cellular senescence seems to be a potential strategy to inhibit PCa cell proliferation, the benefit of senescence induction remains controversial. This is because senescent cells exhibit SASP that can affect tumor microenvironment and neighboring cells. The effect of SASP depends on the balance between secreted tumor promoting and suppressing factors. So far, the composition and the effect of SASP secretome of AR ligand-treated PCa cells have not been analyzed. Actions of AR in both genomic and non-genomic manner lead to the hypothesis that agonist- and antagonist-induced cellular senescent PCa cells exhibit distinct SASP secretomes. It is further hypothesized that the distinct SASP between SAL- and antagonist-treated cells differentially mediates paracrine effects on PCa and immune cells. Thus, this thesis aims to detect factors in the secretory profile of AR ligand-induced cellular senescent PCa cells and compare the SASP secretome between control-, agonist-, and antagonist-treated cells. Further, functional effects of AR ligand-induced SASP on PCa cell proliferation, PCa stemness, immune cell proliferation, and immune clearance of PCa cells were analyzed.

This thesis also aims to analyze senolytic activities of potential senolytic compounds in PCa cells that were senescence-induced by AR ligands. Senescent cells are known to be apoptotic-resistant by activating pro-survival/anti-apoptotic pathways, which can be targeted by senolytic compound (Salminen *et al.* 2011, Wong *et al.* 2018). An apoptotic-resistant feature together with the possibility that AR ligand-induced SASP may act as tumor promoter will indeed provide disadvantages in PCa therapy. Therefore, using senolytic compounds to eliminate AR ligand-induced cellular senescent PCa cells may be a useful strategy to avoid side-effects of SASP.

### 3 MATERIALS AND METHODS

(Compositions of all media, buffers and staining solutions are listed in chapter 8 Appendix)

#### 3.1 Human PCa cell lines and culture

The androgen-dependent human PCa cell line LNCaP-tet (LNCaP) (Protopopov *et al.* 2002) was cultured in RPMI medium 1640 (Gibco, Life Technologies) supplemented with 5% fetal bovine serum (FBS) (Gibco, Life Technologies). The CRPCa cell line C4-2 is derived from the LNCaP cell line (Wu *et al.* 1994). C4-2 cells were cultured in DMEM medium (Gibco, Life Technologies) supplemented with 5% FBS.

LNCaP and C4-2 were cultivated on 10 cm culture dishes (Greiner Bio-One) in an incubator with 5% CO<sub>2</sub> (HERACELL 240i) at 37°C. They were sub-cultured when the cell density reached the confluency of 80%. Briefly, the old medium was removed and cells were washed once with 2 ml of 1x PBS buffer. Then, 1 ml of 1x trypsin/EDTA solution was added to the cells and incubated for 2 min at 37°C. Trypsin was then inactivated by adding fresh FBS-containing medium specific for the particular cell line. After detaching, cells were resuspended and an aliquot of the cell suspension was transferred to a new culture dish. The ratio for sub-culturing LNCaP and C4-2 cells was 1:3 for every 3 days.

#### 3.2 Senescence-associated $\beta$ -galactosidase (SA $\beta$ -Gal) staining

Cellular senescence assays were performed using 6-well culture plates (Greiner Bio-One). LNCaP or C4-2 cells were seeded at  $3.5 \times 10^4$  cells per well. After 48 h of incubation, cellular senescence was induced by treating cells with 1 nM R1881 (Perkin Elmer), 1  $\mu$ M BIC (Sigma-Aldrich), or 1  $\mu$ M ENZ (Selleckchem) for 72 h. Cells were treated with 0.1% DMSO as solvent control.

To detect the cellular senescence marker, SA  $\beta$ -Gal staining was performed as described by Dimri *et al.* (1995). Briefly, cells were washed once with 1x PBS and fixed for 5 min with 1 ml per well of 1% glutaraldehyde fixing solution. Fixed cells were washed again with 1x PBS and stained with 1.5 ml per well freshly prepared SA  $\beta$ -Gal staining solution. Cells were incubated for 24 to 48 h in a CO<sub>2</sub>-free incubator (HERATHERM) at 37°C.

The staining solution composed of 5-bromo-4-chloro-3-indolyl  $\beta$ -D-galactoside (X-Gal), which is a galactopyranoside. This galactopyranoside will be cleaved by active  $\beta$ -galactosidase and generates an insoluble bluish-greenish product (Dimri *et al.* 1995). The stained cells were counted using the light microscope Axiovert 135 (Zeiss). Two fields per well were selected randomly and at least 200 cells per field were counted. Three independent experiments were performed, and the mean percentage of stained cells was calculated.

### **3.3 Collection of conditioned media from senescent PCa cells**

In order to analyze the SASP of AR ligand-induced cellular senescent PCa cells, first cellular senescence was induced in LNCaP or C4-2 cells. Thereafter, the supernatant defined as conditioned medium containing SASP of senescent cells was collected for further investigation.

LNCaP or C4-2 cells were seeded at  $5 \times 10^5$  cells per 10 cm culture dish. After 48 h of incubation, cellular senescence was induced by treating cells with AR ligands for 72 h as earlier described. To collect conditioned medium from these senescent cells, cells were washed twice with 2 ml of 1x PBS (each time) to remove hormones/AR ligands. Subsequently, 9 ml of fresh medium without FBS (0% FBS medium) was added and further incubated for 48 h. The conditioned medium was collected and filtered with 0.2  $\mu$ m filter (Sarstedt) to remove cell debris. Collected conditioned medium from R1881- (Con. R), BIC- (Con. B), ENZ- (Con. E), or DMSO-treated cells (Con. D) were immediately used for each experiment and stored at 4°C for refreshing/retreatment in some long-term experiments.

### **3.4 Analysis of SASP secretome using human cytokine arrays**

Detection of SASP secretome from senescent PCa cells was performed with Human Cytokine Antibody Array C1000 kit (RayBiotech) according to manufacturer's protocol. For each condition/treatment, two antibody arrays were used to detect in total 120 cytokines (60 cytokines per array). All incubation and washing steps were performed at room temperature on Polymax 2040 shaker and mixer platform (Heidolph) at 30 rpm.

Briefly, each antibody array was placed into a well of the incubation tray provided by the kit. The arrays were incubated with Blocking Buffer for 30 min at room temperature. After

removing Blocking Buffer, each membrane was incubated for 5 h at room temperature with 1.5 ml undiluted conditioned medium Con. R, Con. E, or Con. D. Conditioned media were removed, and each membrane was washed three times with 2 ml of 1x Wash Buffer I (5 min incubation each time). After that, each membrane was washed with 1x Wash Buffer II in the same manner as Wash Buffer I. After Wash Buffer II was removed, each membrane was incubated for 2 h with 1 ml of the Biotinylated Antibody Cocktail. Wash steps with Wash Buffer I and II were repeated. Then, each membrane was further incubated for 2 h with 2 ml of 1x HRP-Streptavidin and followed by washing steps with Wash Buffer I and II. Next, membranes were transferred to plastic sheet on a flat surface and incubated for 2 min (without rocking/shaking) at room temperature with 500  $\mu$ l of Detection Buffer mixture (1:1 ratio Detection Buffer C + Detection Buffer D) per membrane. Detection of the signals was performed by ImageQuant<sup>TM</sup> LAS 4000 (GE Healthcare) and quantification of the signals was performed with LabImage 1D software (Kapelan Bio-Imaging).

Quantified signal of 120 cytokines was normalized to the signal of positive control spots (provided by the manufacturer) of particular membrane. The normalized signals detected from Con. R- and Con. E-treated membranes were calculated in relative to the normalized signals from Con. D-treated membrane.

To analyze the consequent biological processes, molecular functions, and pathways associated with these secreted cytokines, bioinformatic gene ontology (GO) analysis and ingenuity pathway analysis (IPA) were kindly performed by Marzieh Ehsani (Baniahmad's group). To compare the secretome with transcriptome regulation, the data of cytokine arrays were analyzed with the RNA sequencing data. RNA sequencing was kindly performed by Kimia Mirzakhani (Baniahmad's group).

### **3.5 Two-dimensional (2D) monolayer proliferation assays and crystal violet staining**

Experiments were performed with PCa cells that were cultured as 2D monolayer model (Figure 4A). LNCaP or C4-2 cells were seeded at  $1.3 \times 10^4$  cells per well in 6-well culture plates and incubated for 24 h. To analyze the effect of AR ligands, cells were treated for 9 days with AR ligands. The medium and AR ligands were refreshed every 3 days. To examine the effect of AR ligand-induced SASP, cells were treated with conditioned medium

Con. R, Con. B, Con. E, or Con. D for 8 days. Conditioned media were refreshed every 2 days. Note that conditioned medium was diluted at 1:1 ratio with 10% FBS-containing medium (specific for each cell line) before treatment.

The effect on cell proliferation was analyzed by crystal violet staining as previously described (Esmacili *et al.* 2016a, 2016b). Briefly, the cells were washed once with 1x PBS and fixed with 1% glutaraldehyde fixing solution for 10 min. Fixed cells were washed again with 1x PBS and stained with freshly prepared 0.1% crystal violet solution for 30 min. The unbound dye was removed by washing several times with deionized H<sub>2</sub>O, and the stained cells were dried overnight. Cells were completely destained using Sørensen's solution and the crystal violet absorbance was measured at OD 590 nm with SPECORD<sup>®</sup> 50 PLUS UV/Vis spectrophotometer (Analytik Jena).

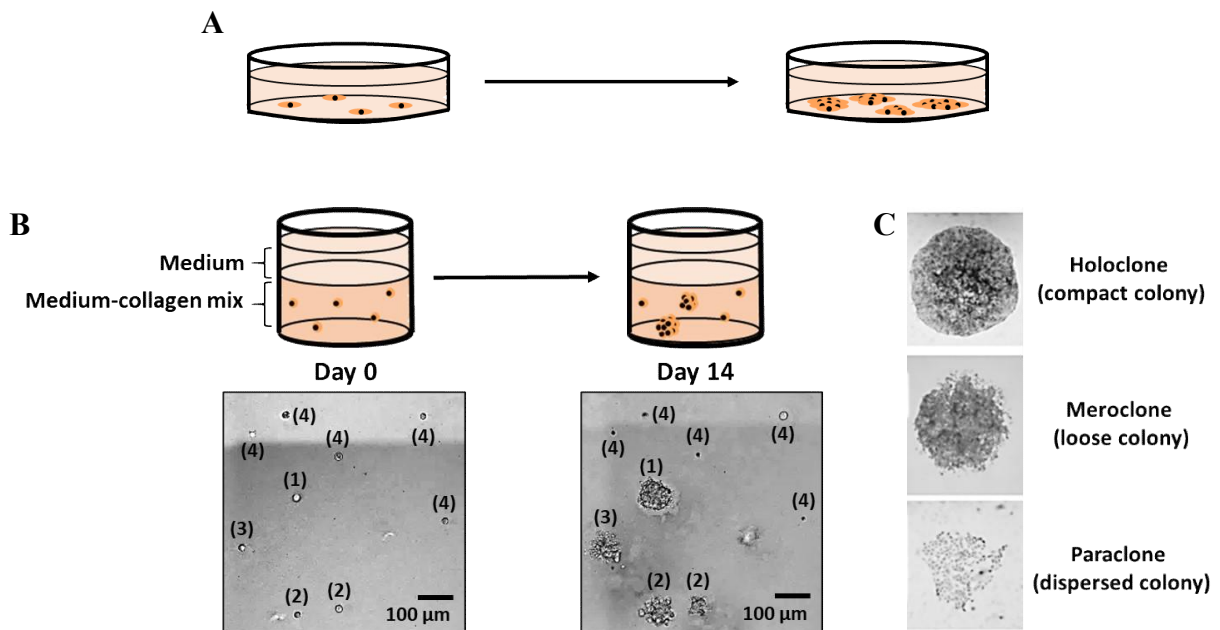


**Figure 4. Illustration figures for 2D monolayer proliferation and 3D colony formation assays.** (A) After sub-culturing or seeding, cells adhere on the bottom surface of the petri dish and proliferate as monolayer (2D). (B) 3D colony formation assays aim to analyze the colony formation capability of single cells. Suspension of cells is seeded in medium-collagen mix and thus, position of individual cell is fixed. After 14 days of incubation, picture taken on day 14 is compared with the picture taken on day 0 of the same field. Hence, (1) holoclone, (2) meroclone, (3) paraclone, or (4) cells which are not able to form colony can be identified and calculated for colony formation efficiency (%). (C) Representative pictures (from Beaver *et al.* 2014) illustrate the difference in morphology between holoclone, meroclone, and paraclone.

### **3.6 Three-dimensional (3D) colony formation assays: Analysis of stemness characteristic of PCa cells**

Stem cells are characterized by their self-renewal ability. The link between stem cell capacity and colony forming ability in 2D monolayer was established by Barrandon and Green (1987). However, three-dimensional (3D) cancer cell culture was later established due to the fact that it is more relevant to the *in vivo* situation. Hence, this study conducted 3D colony formation assays by adapting the protocols from Bahmad *et al* (2018) to examine the effects of AR ligands and AR ligand-induced SASP on stemness characteristic of PCa cells.

Using medium-collagen mix, the assay allows each single cell to grow freely in 3D as suspension culture, however, the position of each cell is fixed, making it easy to analyze which single cell is forming holoclone, meroclone, or paraclone (Figure 4B and C). The definition of each clonal type is based on morphology and proliferation/renewal capacity. The cancer holoclones are rounded tightly packed cells that can be passaged indefinitely (Beaver *et al.* 2014). Paraclones are irregular in composition and loosely packed cells, which incapable of further proliferation or self-renewal (Beaver *et al.* 2014). Meroclones have intermediate morphology and phenotype between holoclones and paraclones. Note that it has been reported that both holoclone- and meroclone-derived from PCa cell lines contain a population of stem cells (Beaver *et al.* 2014).

#### **3.6.1 3D colony formation with AR ligands**

To examine the effects of AR ligands, two experimental setups were proceeded. In experimental setup #1, LNCaP cells were trypsinized from 10 cm culture dishes. The trypsin was neutralized by adding 4 ml of 0.5% FBS RPMI medium and cells were centrifuged at 200 x g for 5 min at room temperature. The supernatant was removed and the cells were singled by gently resuspending with 0% FBS RPMI medium. Next, the cell suspension in 0% FBS RPMI medium was mixed in a 1:1 ratio with collagen I, rat tail (Gibco, Life Technologies) to reach cell density of 2,000 cells per 100  $\mu$ l. Seeding of LNCaP cells was performed by adding 100  $\mu$ l mix (2,000 cells) into each well of 96-flat bottom-well culture plate (Greiner Bio-One). The medium-collagen mix was allowed to solidify in a 5% CO<sub>2</sub> incubator at 37°C for 1 h. Thereafter, 200  $\mu$ l of fresh 5% FBS RPMI medium with appropriate concentration of AR ligand was added per well. The cells were treated with AR ligands for

14 days. For each well, the treatment was refreshed every 2 days by replacing 100  $\mu$ l fresh 5% FBS RPMI medium with appropriate concentration of AR ligand.

In experimental setup #2, LNCaP cells were seeded at  $2.5 \times 10^5$  cells per 10 cm culture dish. The cells were treated with AR ligands for 6 days. Next, trypsinization and seeding of AR ligand-treated cells into 96-well culture plate were performed as experimental setup #1. After solidification of medium-collagen mix, 200  $\mu$ l of fresh 5% FBS RPMI medium without AR ligand was added per well and the cells were cultured for 14 days. The treatment was refreshed every 2 days by exchanging 100  $\mu$ l fresh 5% FBS RPMI medium without AR ligand.

### **3.6.2 3D colony formation with conditioned media containing SASP secretome**

To examine the paracrine effects of AR ligand-induced SASP on stemness characteristic of LNCaP cells, trypsinization and seeding of LNCaP cells into 96-well culture plate were performed as experimental setup #1. For treatment, the conditioned medium collected from AR ligand-induced cellular senescent LNCaP cells was diluted 1:1 ratio with 10% FBS medium and then 200  $\mu$ l of the diluted medium was added to each well. The treatment was refreshed every 2 days by replacing 100  $\mu$ l freshly diluted medium per well. Cells were treated with conditioned media for 14 days.

### **3.6.3 Analysis of colony formation efficiency of holoclone and meroclone**

To analyze the colony formation efficiency (CFE) of holoclone and meroclone, pictures of four random fields per well were taken by AxioCam MRm R3 camera mounted with the brightfield microscope CellObserver Z1 (Zeiss). The resulting images were processed by ZEN Blue software (Zeiss). Colony sizes at day 14 were measured by Fiji ImageJ software. The colony diameter is defined as  $2 \cdot (A/\pi)^{1/2}$ , where A is the area of colony computed by the software. Based on preliminary data, colonies that exhibit diameter less than 40  $\mu$ m were neither considered as holoclones nor meroclones. Holoclones and meroclones were distinguished by the morphology of the colony (Barrandon and Green 1987, Beaver *et al.* 2014) (Figure 4C). For precise calculation of CFE, pictures of the same field were taken after seeding (day 0) and on day 14 (Figure 4B). This enables us to consider specifically whether how many single cells on day 0 formed colony on day 14. Note that, if the colony on day 14



was formed from a clump of cells since day 0, it will be excluded from calculation. The formula of CFE was calculated according to the following:

$$\text{CFE (\%)} = 100\% \times \left( \frac{\text{Total number of holoclone or meroclone formed on day 14}}{\text{Total number of single cell counted on day 0}} \right)$$

### 3.7 Preparation of peripheral blood mononuclear cells (PBMCs)

Preparation of peripheral blood mononuclear cells (PBMCs) was adapted from Junking *et al.* (2017). For each experiment, 36 ml of blood sample from healthy male donor was collected in S-Monovette<sup>®</sup> EDTA K<sub>3</sub> tubes (Sarstedt). The blood sample was gently mixed 1:1 ratio with 2% FBS in 1x PBS buffer. Next, each 30 ml of PBS-blood mixture was gently added to the top of 15 ml Lymphoprep<sup>™</sup> solution (STEMCELL Technologies) per one reaction tube. Of note, the reaction tube should be tilted and the PBS-blood mixture should be allowed to slowly flow down from the wall of the tube to the Lymphoprep<sup>™</sup> solution by gravity. Separation phase of PBMCs was achieved through gradient centrifugation at 800 x g for 20 min at room temperature without brake function. PBMCs from two reaction tubes were transferred into the same new reaction tube and subsequently mixed with 30 ml red blood cell lysis buffer. After 5 min incubation, centrifugation was performed at 450 x g for 10 min. Supernatant was then removed and the PBMCs pellet was washed by resuspending with 30 ml of pure RPMI medium 1640 followed by centrifugation at 450 x g for 10 min. Supernatant was again discarded and the PBMCs pellet was resuspended with 10 ml serum free AIM-V medium (Gibco, Life Technologies). Cell suspension was distributed for 2 ml per well into 6-well culture plate and incubated for 2 h in a 5% CO<sub>2</sub> incubator at 37°C.

After 2 h of incubation, non-adherent cells were gently collected from each well into a reaction tube. Centrifugation at 1,000 rpm for 5 min at room temperature was performed. Supernatant was discarded and the cell pellet was resuspended with 1 ml freshly prepared lymphocyte freezing solution. The non-adherent cells were cryopreserved as a source of lymphocytes. After removing non-adherent cells, adherent cells were further cultured as a source of dendritic cells.

### 3.8 Generation of mature dendritic cells and activation of lymphocytes

The protocol for generating dendritic cells and activating lymphocytes were adapted from Junking *et al.* (2017). Briefly, the monocytes (adherent PBMCs) were first cultured in serum free AIM-V medium supplemented with 50 ng/ml GM-CSF (ImmunoTools) and 25 ng/ml IL-4 (ImmunoTools) for 5 days in order to differentiate them into immature dendritic cells. The medium and cytokines were refreshed every day. The immature dendritic cells were further cultured in serum free AIM-V medium supplemented with 50 ng/ml TNF- $\alpha$  (ImmunoTools) and 50 ng/ml IFN- $\gamma$  (ImmunoTools) for 2 days in order to differentiate cells into mature dendritic cells. These mature dendritic cells were used for activation of lymphocytes. Successful differentiation was confirmed by cell morphology under light microscope Axiovert 135.

To activate the lymphocytes, the frozen non-adherent PBMCs were thawed up and co-cultured with mature dendritic cells for 3 days in AIM-V medium supplemented with 5% human serum (HS) (Sigma-Aldrich). After that, the activated non-adherent PBMCs (lymphocytes) were transferred into new 6-well culture plate. Clonal expansion of activated lymphocytes was performed by culturing the cells for 10 days in serum free AIM-V medium supplemented with 20 ng/ml IL-2 (ImmunoTools), 10 ng/ml IL-7 (ImmunoTools), and 20 ng/ml IL-15 (ImmunoTools). Medium and cytokines were refreshed every 2 days. Successful activation and expansion of lymphocytes were confirmed by flow cytometry.

To examine the paracrine effects of AR ligand-induced SASP on lymphocyte activation and expansion, the procedures were performed as mentioned above. However, during the activation process, conditioned medium of AR ligand-treated LNCaP or C4-2 cells was diluted at 1:1 ratio with 10% human serum (HS)-containing RPMI or DMEM medium (depending on the source of conditioned medium). Moreover, during the clonal expansion process, conditioned medium was diluted at 1:1 ratio with 4% HS RPMI or DMEM medium and applied with or without addition of IL-2, -7, and -15. As control for both steps, 0% FBS medium was used instead of conditioned medium. Treated lymphocytes were analyzed by flow cytometry and by the size of lymphocyte cluster formation during expansion period. To analyze the size of lymphocyte clusters, pictures of five random fields per well were taken by Fujifilm X-T20 mirrorless digital camera mounted with the light microscope. Cluster was

detected and the cluster's size (area) was measured by countPHICS software (Brzozowska *et al.* 2019).

### 3.9 Killing assays of PCa cells by immune cells

To address the cytolytic activity of immune effector cells, co-culturing of activated lymphocytes (effectors) and PCa cells (targets) was performed. The incubation time as well as the ratio between effectors and targets were optimized based on preliminary experiments. Effectors were co-cultured with targets at 5:1 ratio. To detect the protein levels of cleaved PARP (c-PARP) as apoptotic marker by Western blotting, protein extraction was performed after co-cultured for 1.5 h. To analyze the percentage of apoptotic target cells, Annexin V staining was performed after co-cultured for 3 h and subsequently detected by flow cytometry. To analyze the target cells viability, crystal violet staining was performed after 6 h of co-culturing.

PCa cells as targets were seeded at  $1.5 \times 10^5$  cells per 10 cm culture dish for c-PARP analysis, at  $4 \times 10^4$  cells per 35 mm culture dish (VWR) for Annexin V analysis, and at  $4 \times 10^4$  cells per well of 6-well culture plate for crystal violet staining. After 48 h of incubation, cells were either treated for 72 h with AR ligands (in 5% FBS medium) or for 96 h with conditioned media derived from AR ligand-induced cellular senescent cells. Note that conditioned medium was diluted at 1:1 ratio with 10% FBS medium prior treatment. Since different treatments might lead to unequal cell number, one set of targets per treatment was trypsinized and counted in Neubauer chamber. The number of effectors required for each treatment was calculated and added to the other set of targets at 5:1 ratio. AIM-V medium supplemented with 5% HS was used during co-culturing (killing) process of AR ligand-treated PCa cells. Conditioned medium was diluted at 1:1 ratio with 10% HS medium and used during killing process of conditioned media-treated PCa cells.

### 3.10 Flow cytometry

Flow cytometry was performed and analyzed with BD Accuri C6 Plus flow cytometer and software (BD Biosciences) according to manufacturer's protocols.

### 3.10.1 Analysis of lymphocyte activation

To analyze the surface proteins CD3 and CD8 of lymphocytes, non-adherent PBMCs and activated lymphocytes were collected by centrifugation for 5 min at 450 x g. After removing the supernatant, cells were washed twice by resuspending with cold 1x PBS supplemented with 2% FBS and followed by 450 x g centrifugation for 5 min at 4°C each time. Note that cells were equally distributed into different pre-cooled light protected reaction tubes before second wash. Next, the supernatant was removed and cell pellet in each reaction tube was resuspended with 50 µl of corresponding antibodies staining solution (Table 1). Mouse IgG1 antibody was used as isotype control. Incubation for 30 min with antibodies was performed at 4°C in the dark. Again, cells were washed twice with cold 2% FBS in 1x PBS buffer and followed by centrifugation (450 x g, 5 min at 4°C) each time. Supernatant was discarded. The pellet was resuspended and fixed with cold 1% PFA fixing solution and immediately processed for detection with flow cytometer.

**Table 1. List of antibodies used for flow cytometry**

Antibody	Conjugated fluorophores	Source	Isotype	Company, Ref. no.	Dilution	Diluent
<b>Human CD3</b>	FITC	Mouse	IgG1	Immuno Tools, 21620033	1:50	2% FBS in 1x PBS
<b>Human CD8</b>	APC	Mouse	IgG1	Immuno Tools, 21810086	1:50	2% FBS in 1x PBS
<b>Mouse IgG1</b>	FITC	Mouse	IgG1	Immuno Tools, 21275513	1:50	2% FBS in 1x PBS
<b>Mouse IgG1</b>	APC	Mouse	IgG1	Immuno Tools, 21275516	1:50	2% FBS in 1x PBS
<b>Annexin V</b>	APC	Chicken	-	Immuno Tools, 31490016	1.5:100	1x Annexin binding buffer

### 3.10.2 Annexin V staining for analyzing apoptosis

To analyze the percentage of apoptotic target cells after co-cultured with lymphocytes, Annexin V staining was performed. For each treatment/condition (two 35 mm culture dishes), supernatant containing lymphocytes and detached target cells were collected into 15 ml reaction tube. Remaining attached target cells were washed once with 1x PBS (1 ml per dish) and the supernatant was collected to the same reaction tube. Trypsinization of attached target cells (0.5 ml per dish) was performed with 2 min incubation at 37°C. Trypsin was inactivated by adding fresh 5% FBS medium (1 ml per dish). The trypsinized cells were collected into the

reaction tube. Centrifugation was performed at 450 x g for 5 min. After removing the supernatant, cell pellet was resuspended with cold 1x Annexin binding buffer and equally distributed into different pre-cooled light protected reaction tubes (98.5  $\mu$ l each). 1.5  $\mu$ l of Annexin V was added to corresponding reaction tubes. After 15 min incubation (4°C in dark condition), the Annexin V staining was immediately detected with flow cytometry. Mouse IgG1 APC conjugated was used as fluorophore control.

### **3.11 Killing assays of PCa cells by senolytic compounds**

To analyze the senolytic activity of senolytic agents in senescent PCa cells, the AKT inhibitor MK2206 (MK) and the HSP90 inhibitor Ganetespib (GT) were used. LNCaP cells were seeded at  $5 \times 10^5$  cells per 10 cm culture dish for MK experiments and at  $1.2 \times 10^5$  cells per 10 cm culture dish for GT experiments. Cellular senescence was first induced by treating cells with AR ligands for 72 h. Thereafter, the medium and ligands were removed, and cells were further treated with 1  $\mu$ M MK (Selleckchem), 25 nM GT (Selleckchem), or 0.1% DMSO as solvent control. Protein extraction and Western blotting were performed to detect the apoptotic marker.

### **3.12 Protein extraction and Western blotting**

#### **3.12.1 Whole cell lysate (intracellular protein extraction)**

To extract intracellular protein, whole cell lysate preparation was adapted from Esmaili *et al.* (2016a, 2016b). Briefly, cells were washed once with 1x PBS, then scraped in cold 1x PBS, and transferred to 1.5 ml reaction tube. The tube was centrifuged (2,500 rpm, 5 min, at 4°C) to collect the cells. The cell pellet was resuspended in NETN buffer (5-fold volume of the pellet) supplemented with phosphatase inhibitors and incubated in ice for 10 min. The mixture was then frozen in liquid nitrogen for 1 min and thawed up in 37°C water bath for 3 cycles. Centrifugation (15,000 rpm, 15 min, at 4°C) was performed to precipitate the cell debris. The supernatant was collected into a new cooled tube as whole cell protein extract. Quantification of protein concentration was performed with NanoDrop ND-1000 Spectrophotometer (Peachlab). The extracted protein was long-term stored at -80°C.

### 3.12.2 Methanol precipitation (secreted protein precipitation)

To concentrate secreted proteins, methanol precipitation of conditioned medium was performed. A total of 8 ml conditioned medium was distributed into two pre-cooled reaction tubes (4 ml each). Subsequently, 36 ml of cold methanol (VWR) was added to each falcon and followed by 15 sec strong mixing. The mixture was incubated at 4°C for 20 min to precipitate the secreted protein. The precipitated protein was collected through centrifugation (4,700 rpm, 20 min, at 4°C). Pellets of both tubes were resuspended with the same 100 µl cold 90% methanol until homogeneous. The mixture was collected into a new cooled 1.5 ml reaction tube and followed by centrifugation (15,000 rpm, 15 min, at 4°C). After removing the supernatant, the pellet was resuspended with 50 µl of Milli-Q H<sub>2</sub>O and long-term stored at -80°C as precipitated secreted protein. Quantification of protein concentration was performed by preparing sample with Pierce™ BCA™ Protein-Assay kit (Thermo Scientific) and measured with the NanoDrop ND-1000 Spectrophotometer.

### 3.12.3 Western blotting

Western blotting was performed to analyze either intracellular or secreted protein levels. Proteins were separated by SDS-PAGE, using 1 ml stacking gel (5% acrylamide) and 5 ml separating gel (10-15% acrylamide depending on the size of the target protein). For intracellular protein sample, each 35 µg of protein was diluted in NETN buffer and mixed with 3 µl of 5x SDS to reach in total 15 µl. For secreted protein sample, each 50 µg of protein was diluted in Milli-Q H<sub>2</sub>O and mixed with 6 µl of 5x SDS to reach in total of 30 µl mix. The mixture was boiled at 99°C for 10 min, and loaded into a well of polyacrylamide gel. Gel electrophoresis was performed with Mini-PROTEAN® Tetra Vertical Electrophoresis Cell (Bio-Rad), 1x running buffer was used, and the voltage was set to 80 V. Once, the PageRuler™ Prestained Protein Ladder bands (Thermo Scientific) were distinctively separated, the voltage was changed to 150 V.

The proteins were transferred onto Amersham Hybond P 0.2 PVDF Western blotting membrane (GE Healthcare) by wet-tank-blotting system (bsb11-biotech service blu). Briefly, the membrane was activated in methanol for 10 sec. The wet-blot sandwich was made up by one sponge on cathode side, four blotting papers (Whatmann), the membrane, the gel, four blotting papers, and one sponge on the anode side. Note that, sponges and blotting papers were

prior soaked with 1x blotting buffer. After putting the sandwich into the blotting chamber, the 1x blotting buffer supplemented with either 10 or 20% methanol (depending on the size of the target protein) was filled to cover the sandwich. The wet-tank-blotting system was set to run at 200 mA for 2 h. After blotting, the membrane was blocked with 10% skim milk (Biomol) for 1 h at room temperature, and followed by three times washing with 1x TBS-T buffer (5 min each time).

For target protein detection, the membrane was incubated for 16 h at 4°C with specific primary antibody (Table 2) against protein of interest. The membrane was again washed three times with 1x TBS-T buffer (5 min each time), and further incubated at room temperature with secondary antibody (Table 2) against particular primary antibody for 1 h. Later, three times washing step was repeated and the membrane was incubated for 2 min with Amersham™ ECL™ Western Blotting Detection Reagents (GE Healthcare). The signals were detected by ImageQuant™ LAS 4000 machine. LabImage 1D software was used for quantification of protein expression, and the expression of protein was normalized to the expression of  $\beta$ -Actin (loading control).

**Table 2. List of antibodies against human proteins used for Western blotting**

Target	1 <sup>st</sup> /2 <sup>nd</sup> Antibody	Source	Company, Ref. no.	Dilution with 1x TBS-T	Protein size (kDa)
ALDH1A1	1 <sup>st</sup>	Rabbit	Invitrogen, PA5-34901	1:1,000	55
ANG	1 <sup>st</sup>	Rabbit	Bosterbio, A00146	1:2,000	14
AKT	1 <sup>st</sup>	Rabbit	Cell Signaling, 4685	1:2,000	60
AR	1 <sup>st</sup>	Mouse	Biogenex, 256M	1:2,000	110
MYC	1 <sup>st</sup>	Rabbit	Cell Signaling, 5605	1:1,000	57-65
Mouse IgG HRP*	2 <sup>nd</sup>	Horse	Cell Signaling, 7076	1:10,000	-
OCT4	1 <sup>st</sup>	Rabbit	Cell Signaling, 2750	1:1,000	45
p-AKT (S473)	1 <sup>st</sup>	Rabbit	Cell Signaling, 4058	1:5,000	60
PARP	1 <sup>st</sup>	Mouse	Cell Signaling, 9546	1:2,000	Uncleaved: 116 Cleaved: 89
PSA	1 <sup>st</sup>	Rabbit	Cell Signaling, 2475	1:1,000	29
p-S6 (S235/236)	1 <sup>st</sup>	Rabbit	Cell Signaling, 2211	1:5,000	32
p16 <sup>INK4a</sup>	1 <sup>st</sup>	Mouse	Santa Cruz, sc-81613	1:500	16-25
p21 <sup>Cip1/Waf1</sup>	1 <sup>st</sup>	Mouse	Cell Signaling, 2946	1:2,000	21
Rabbit IgG HRP*	2 <sup>nd</sup>	Goat	Cell Signaling, 7074	1:10,000	-

<b>SOX2</b>	1 <sup>st</sup>	Rabbit	ABclonal, A6171	1:1,000	35-40
<b>S6</b>	1 <sup>st</sup>	Rabbit	Cell Signaling, 2217	1:5,000	32
<b>TIMP2</b>	1 <sup>st</sup>	Rabbit	ABclonal, A1558	1:1,000	24
<b>β-Actin</b>	1 <sup>st</sup>	Mouse	Abcam, ab6276	1:10,000	42

(\*). Secondary antibodies are conjugated to horseradish peroxidase (HRP).

### 3.13 Analysis of PCa phospho-kinome using human phospho-kinase arrays

To analyze and compare the phosphorylation profiles of kinases and their protein substrates between conditioned media-treated LNCaP cells, Human Phospho-Kinase Array kit (R&D Systems) was applied according to the manufacturer's protocol. For each condition/treatment, there are two antibody arrays recognizing in total 43 kinase phosphorylation sites and 2 other proteins. All incubation and wash steps were performed at 20 rpm on Polymax 2040 shaker and mixer platform.

LNCaP cells were seeded at  $2.5 \times 10^5$  cells per 10 cm culture dish. After 24 h, cells were treated for 6 days with Con. R, Con. B, Con. E, or Con. D as control. Cell lysate was performed with Lysis Buffer 6 as described in manufacturer's protocol. Quantification of protein concentration was performed with Pierce<sup>TM</sup> BCA<sup>TM</sup> Protein-Assay kit and measured with NanoDrop ND-1000 Spectrophotometer.

Each antibody array was placed into a well of the incubation tray provided by the kit. The arrays were incubated with blocking buffer (Array Buffer 1) for 1 h at room temperature. While the membranes were blocking, the samples were prepared by diluting 600 µg cell lysate (maximum 500 µl) to a final volume of 3 ml with Array Buffer 1. After removing blocking buffer, each membrane was incubated for 16 h at 4°C with 1.5 ml of the prepared samples (300 µg per membrane). The samples were removed, and each membrane was washed three times with 1x Wash Buffer (10 min incubation at room temperature each time). After Wash Buffer was removed, each membrane was incubated for 2 h at room temperature with 1 ml of the diluted Detection Antibody Cocktail. The washing step was repeated. Then, each membrane was incubated for 30 min at room temperature with 1 ml of diluted HRP-Streptavidin and followed by washing step with Wash Buffer. Next, membranes were transferred to plastic sheet on a flat surface and incubated for 1 min (no rocking/shaking) at room temperature with 500 µl of prepared Chemi Reagent Mix (1:1 ratio Chemi Reagent 1 +



Chemi Reagent 2) per membrane. Detection of the signals was performed by ImageQuant™ LAS 4000 and quantification of the signals was performed with LabImage 1D software. The quantified signals were normalized to the signal of positive control spots (provided by the manufacturer) of particular membrane. The normalized signals detected from Con. R-, Con. B-, or Con. E-treated samples were calculated in relative to the signals from Con. D-treated sample. To analyze the pathways associated with SASP factors, bioinformatic ingenuity pathway analysis (IPA) was kindly performed by Marzieh Ehsani (AG Baniahmad).

### **3.14 RNA extraction and quantitative reverse transcription-PCR (qRT-PCR)**

(Composition of reaction mixes are listed in chapter 8 Appendix)

#### **3.14.1 RNA extraction and cDNA synthesis**

RNA extraction was performed using peqGOLD TriFast™ kit (Peqlab). Briefly, cells were washed once with 1x PBS, incubated with 1 ml TriFast reagent per 10 cm culture dish for 5-10 min (cells were lysed), followed by pipetting 10 times up and down, and transferred to a reaction tube. For each tube, 0.2 ml chloroform was added, the tubes were shaken for 15 sec, and incubated for 10 min. RNA, DNA, and protein were separated into three layers after centrifugation (12,000 x g, 5 min). RNA phase was transferred into new cooled tube, 250 µl of 99.8% isopropanol was added per tube, mixed, and followed by 20 min incubation at 4°C. Purified RNA extract was precipitated by centrifugation (12,000 x g, 20 min, at 4°C), and washed twice with 1 ml of 75% EtOH (centrifuge at 12,000 x g, 10 min, at 4°C each wash). Supernatant was removed and RNA pellet was air dried. Dried RNA pellet was resolved in 15 µl DEPC-treated H<sub>2</sub>O (Roth). Concentration of RNA was measured by NanoDrop ND-1000 Spectrophotometer. Quality of RNA was confirmed by agarose gel electrophoresis. Extracted RNA (2 µg) was synthesized into cDNA using High Capacity cDNA Reverse Transcription kit (Applied Biosystems). The final cDNA product was diluted 1:1 by DEPC-treated H<sub>2</sub>O. Extracted RNA was long-term stored at -80°C, while cDNA was stored at -20°C.

#### **3.14.2 qRT-PCR**

To analyze the transcription levels of target genes, qRT-PCR was performed with cDNA using SsoAdvanced Universal SYBR® Green Supermix (Bio-Rad), gene specific primers (Table 3), and Bio-Rad CFX96™ Real Time PCR detection system (Bio-Rad). qRT-PCR results were

analyzed via  $\Delta\Delta C_t$  method (Pfaffl 2001) with CFX manager software (Bio-Rad) or via the following formula:

$$\text{Ratio} = \frac{(E_{\text{target}})^{-C_{t\text{treatment}}}}{(E_{\text{HKG}})^{-C_{t\text{treatment}}}} \div \frac{(E_{\text{target}})^{-C_{t\text{control}}}}{(E_{\text{HKG}})^{-C_{t\text{control}}}}$$

$$\text{where } E = 1 + \left( \frac{\% \text{ primer efficiency}}{100} \right)$$

The ratio (relative normalized expression) value represents the expression level of target gene by particular treatment, normalized to housekeeping gene (HKG), and relative to control treatment. E is defined as qPCR amplification efficiency of particular target or HKG. Ct value is defined as PCR cycles that the PCR product of a particular target or HKG is amplified across the threshold (background level).

**Table 3. List of human primers used for qRT-PCR analysis**

Gene	Primer	Sequence 5' → 3'	Annealing Temperature
<i>β-Actin</i>	fwd	CACCACACCTTCTACAATGAGC	60°C
	rev	CACAGCCTGGATAGCAACG	
<i>ANG</i>	fwd	CACACTTCCTGACCCAGCACTA	60°C
	rev	TTCTCTGTGAGGGTTTCCATTC	
<i>CDKN2A</i> (p16 <sup>INK4a</sup> )	fwd	CTTGCCTGGAAAGATACCG	55°C
	rev	CCCTCCTCTTTCTTCCTCC	
<i>CCND1</i> (Cyclin D1)	fwd	TCAACCTAAGTTCGGTTCGGATG	60°C
	rev	GTCAGCCTCCACACTCTTGC	
<i>MYC</i>	fwd	GCTGCTTAGACGCTGGATTT	60°C
	rev	GAGTCGTAGTCGAGGTCATAGTT	
<i>E2F1</i>	fwd	GCAGAGCAGATGGTTATGG	60°C
	rev	GATCTGAAAGTTCTCCGAAGAG	
<i>KLK3 (PSA)</i>	fwd	GAGGCTGGGAGTGCAGAGAAG	60°C
	rev	TTGTTCTGATGCAGTGGGC	
<i>MET</i>	fwd	GGTCAATTCAGCGAAGTCCT	55°C
	rev	TGGAGACACTGGATGGGAGT	
<i>NANOG</i>	fwd	CCTATGCCTGTGATTTGTGG	65°C
	rev	AAGTGGGTTGTTTGCCTTTG	
<i>PCNA</i>	fwd	TTTTCTGTCACCAAATTTGTACCTC	55°C
	rev	CTGCATTTAGAGTCAAGACCCTTT	

<b><i>POU5F1</i></b> <b>(OCT4)</b>	fwd	GGGTTCTATTTGGGAAGGTA	60°C
	rev	GTTGCCTCTCACTCGGTTCT	
<b><i>KITLG</i></b> <b>(SCF)</b>	fwd	TGTTGGATAAGCGAGATGGT	60°C
	rev	GGGTTCTGGGCTCTTGAATG	
<b><i>TBP</i></b>	fwd	GCGTGTGAAGATAACCCAAGG	55°C
	rev	CGCTGGAACTCGTCTCACT	
<b><i>CCL25</i></b> <b>(TECK)</b>	fwd	GCCTGCTGCGATATTCTACC	55°C
	rev	TGGAAGGTCTGCGTGTTGT	
<b><i>TIMP2</i></b>	fwd	CCAAGCAGGAGTTTCTCGAC	55°C
	rev	GACCCATGGGATGAGTGTTT	

### 3.15 Statistical analyses

For statistical analyses, two-tailed unpaired t-test, one-way ANOVA, and *post hoc* tests (Dunnett's and Bonferroni's multiple comparisons test) were performed with GraphPad Prism 8.0 software. In this thesis, t-test was conducted to compare the means between two groups (comparing each treatment to control treatment). One-way ANOVA was performed to compare the means of all treatments to each other. *Post hoc* test (either Dunnett's or Bonferroni's multiple comparisons test) was required after ANOVA to specify whether which pair among analyzed groups is statistically significant difference (McHugh 2011, Mishra *et al.* 2019).

Mean, standard deviation (SD), and standard error of mean (SEM) were calculated from number of biological replicates/independent experiments (N) or technical replicates (n). A 95% confidence interval ( $p\text{-value} (p)\leq 0.05$ ) was considered as statistically significant (\*). A 99% confidence interval ( $p\leq 0.01$ ) and a 99.9% confidence interval ( $p\leq 0.001$ ) were indicated by two (\*\*) and three stars (\*\*\*), respectively.

## 4 RESULTS

### 4.1 The second-generation of AR antagonist Enzalutamide (ENZ) induces cellular senescence in PCa cells leading to inhibition of cell proliferation

Enzalutamide (ENZ) is a second-generation of AR antagonist, which is currently used for treating PCa patients (Rodriguez-Vida *et al.* 2015). Our group has previously reported that AR agonist at SAL, first-generation AR antagonist Bicalutamide (BIC), and other AR antagonist-like compounds induce cellular senescence in PCa cells (Roediger *et al.* 2014, Esmaeili *et al.* 2016a, Hessenkemper *et al.* 2014, Roell *et al.* 2019, Fousteris *et al.* 2010). However, senescence induction by ENZ has never been reported. Thus, the hypothesis was that ENZ can also induce cellular senescence in PCa cells. To analyze whether ENZ can induce cellular senescence, androgen-sensitive LNCaP and castration-resistant C4-2 human PCa cell lines were used.

Each cell line was treated with AR ligands for 72 h to induce cellular senescence. The senescent cells were detected by SA  $\beta$ -Gal staining as a specific senescence marker (Dimri *et al.* 1995) (Figure 5A). Confirming previous studies, SAL induces cellular senescence in both cell lines after treating with either the synthetic AR agonist R1881 (Figure 5A and B) or the natural androgen DHT (data not shown). An induction of cellular senescence by antagonists was also observed with either BIC or ENZ (Figure 5A and B). This is the first report showing that a clinically used AR antagonist ENZ induces cellular senescence in human PCa cells (Pungsrinont *et al.* 2020). In line with this, ENZ upregulates both transcription and protein levels of *CDKN2A/p16<sup>INK4a</sup>*, another molecular marker and a key regulator of senescence (Figure 5C and D).

To examine whether AR ligands also trigger apoptosis, the apoptotic marker cleaved PARP (c-PARP) was analyzed. In comparison to the loaded c-PARP positive control, no c-PARP was detected after AR ligand treatment (Figure 5E). Hence, the data suggest that AR ligands do not induce apoptosis in LNCaP and C4-2 cells.

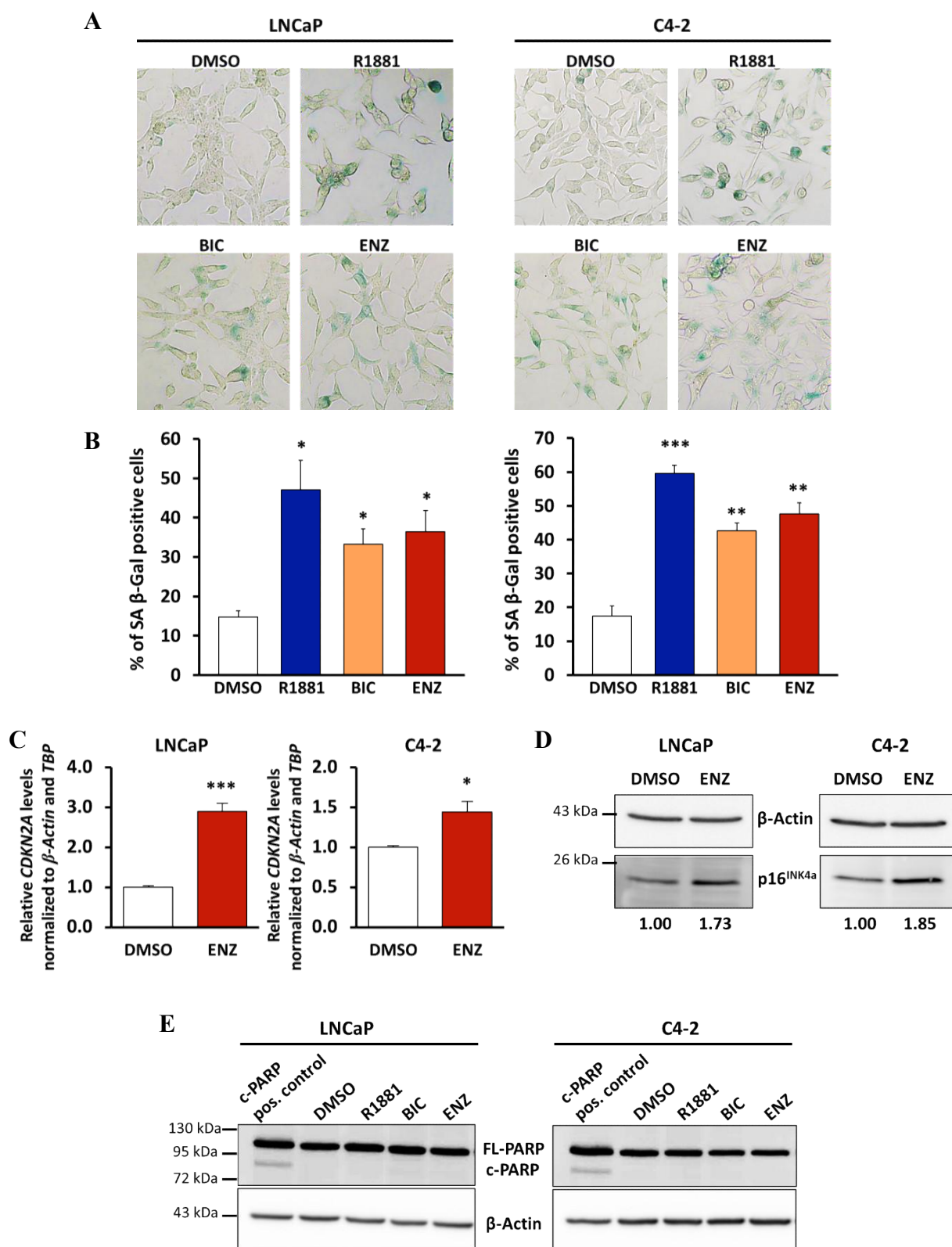
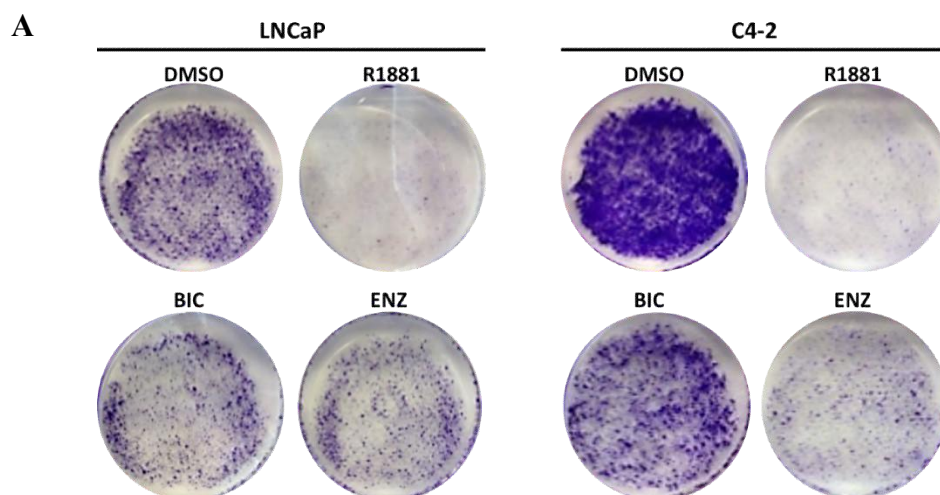


**Figure 5. AR ligands induce cellular senescence and not apoptosis. (A and B)** LNCaP and C4-2 cells were treated with R1881 (1 nM), BIC (1  $\mu$ M), ENZ (1  $\mu$ M), or DMSO (0.1%) as solvent control

for 72 h. SA  $\beta$ -Gal staining was performed and stained cells were counted. **(A)** Representative pictures of cells after SA  $\beta$ -Gal staining were taken under light microscope. **(B)** Percentage (%) of SA  $\beta$ -Gal positive stained cells. Bar graphs are shown as mean + SEM from three independent experiments (N = 3). **(C and D)** Cells were treated with ENZ (1  $\mu$ M) or DMSO (0.1%). **(C)** mRNA level of *CDKN2A* encoding p16<sup>INK4a</sup> was analyzed by qRT-PCR after 48 h of treatment. *CDKN2A* expression was normalized to the expression of housekeeping genes  *$\beta$ -Actin* and *TBP*. The mRNA expression of DMSO-treated cells was set arbitrarily as 1. Bar graphs are shown as mean + SEM from three independent experiments (N = 3). **(D)** Protein level of p16<sup>INK4a</sup> was detected after 72 h of treatment by Western blotting and normalized to  $\beta$ -Actin. Numbers indicate normalized p16<sup>INK4a</sup> band intensities relative to DMSO control. **(E)** Detection of full length PARP (FL-PARP) and cleaved PARP (c-PARP) after 72 h of treatment was conducted by Western blotting.  $\beta$ -Actin served as loading control. Protein extracted from apoptotic LNCaP cells treated with 1  $\mu$ M AKT inhibitor (MK2206) was loaded as positive control for c-PARP. Statistical analyses in (B) and (C) were performed by using two-tailed unpaired t-test comparing each treatment to DMSO treatment. \*,  $p \leq 0.05$ ; \*\*,  $p \leq 0.01$ ; \*\*\*,  $p \leq 0.001$ .

This study also analyzed the cell proliferation of ENZ-treated PCa cells along with other ligand-treated cells. Proliferation assays were analyzed by crystal violet staining, which reflected the cell number of each treatment. As expected, a remarked suppression of cell proliferation by AR ligands including ENZ was observed in both LNCaP and C4-2 cell lines (Figure 6A and B). Moreover, mRNA expressions of key factors that control cell proliferation were analyzed. *MYC* mRNA level was significantly suppressed by all ligands (Supplemental Figure S1). Apart from *MYC*, SAL prominently suppressed *CCND1*, *E2F1*, and *PCNA* mRNA levels, whereas antagonists significantly suppressed *E2F1* level. These results are being in line with the observed inhibition of cell proliferation.

Taken together, the results show that AR ligands do not induce apoptosis, but induce cellular senescence and suppress expression of some key factors that mediate cell proliferation. Thus, it leads to inhibition of PCa cell proliferation.



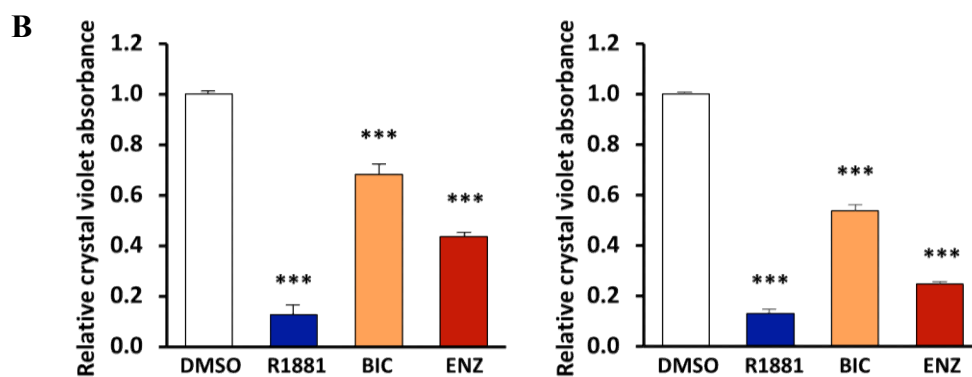


**Figure 6. AR ligands suppress PCa cell proliferation.** LNCaP or C4-2 cells were treated with R1881 (1 nM), BIC (1  $\mu$ M), ENZ (1  $\mu$ M), or DMSO (0.1%) as solvent control for 9 days. Crystal violet staining was performed on day 0 (1<sup>st</sup> day of treatment) and day 9. **(A)** Representative crystal violet staining pictures of cells after 9 days of treatment. **(B)** Crystal violet absorbance (OD 590 nm) on day 9 was normalized to the value of day 0 and presented as relative to DMSO treatment. Bar graphs are shown as mean + SEM from total of six technical replicates (n = 6) of three independent experiments. Statistical analysis was performed by using two-tailed unpaired t-test comparing each treatment to DMSO treatment. \*\*\*,  $p \leq 0.001$ .

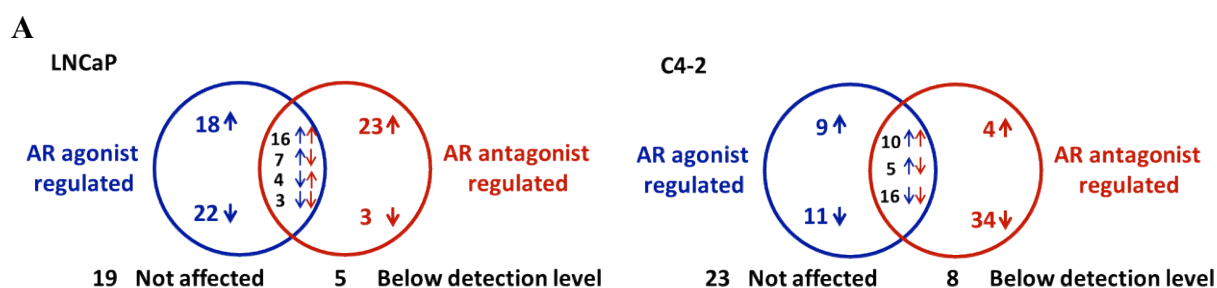
#### 4.2 AR antagonist- and agonist-induced cellular senescent PCa cells exhibit distinct SASP secretomes

Senescent cells are known to secrete cytokines and chemokines termed as SASP, which can affect tumor microenvironment and neighboring cells (Coppé *et al.* 2010, Lecot *et al.* 2016). The effect of SASP depends on the balance between secreted tumor promoting and suppressing factors. However, the composition of SASP secretome of AR ligand-treated PCa cells has not yet been studied. Notably, AR is a transcription factor and some SASP genes are AR responsive genes (Jin *et al.* 2013). Thus, the hypothesis was that expression levels of SASP factors in PCa cells are different among AR ligand-treated cells and may lead to distinct SASP secretomes.

To analyze and compare the cytokine secretion profiles of AR ligand-induced cellular senescence, conditioned media from DMSO- (Con. D), R1881- (Con. R), and ENZ-treated (Con. E) PCa cells were collected and loaded on human cytokine antibody arrays. The antibody arrays can detect in total 120 different cytokines. The results from cytokine arrays reveal that AR agonist and antagonist induce a different secreted level of cytokines from both LNCaP and C4-2 cells (Figure 7; Supplemental Figure S2). The data of 120 cytokines were summarized in

Venn's diagrams (Figure 7A). Among the detected cytokines, secreted levels of 96 cytokines from LNCaP cells and 89 cytokines from C4-2 cells were altered by AR ligands.

The secretory profile was first compared between agonist- and antagonist-treated cells. The data show that, on one hand, secreted level of some cytokines was changed in the same direction (enhanced or suppressed) by both agonist and antagonist (Figure 7B), representing an overlapping secretome of SAL- and ENZ-induced cellular senescent cells. On the other hand, secreted level of some cytokines was altered in an opposite direction between the two ligands (Figure 7C). Moreover, secretion of some cytokines was only affected by either agonist or antagonist alone (Figure 7D). These data indicate that AR ligand-treated PCa cells exhibit distinct secretory profiles.



**B**

LNCaP		C4-2	
Enhanced by R1881 and ENZ	Suppressed by R1881 and ENZ	Enhanced by R1881 and ENZ	Suppressed by R1881 and ENZ
Eotaxin-3 ( <i>CCL26</i> )	Amphiregulin ( <i>AREG</i> )	BMP-6	CCL27
gp130 ( <i>IL6ST</i> )	Axl	CCL23	CXCL-11
IGF-1	IGFBP-2	CCL28	EGFR
IGFBP-1		CNTF	ICAM-1
IGFBP-4		EGF	IL-1 R1
IL-15		Eotaxin-1 ( <i>CCL11</i> )	MIF
IL-16		IFN- $\gamma$ ( <i>IFNG</i> )	MSP ( <i>MST1</i> )
IL-7		IL-12 p70 ( <i>IL12A</i> )	NT-3 ( <i>NTF3</i> )
Leptin ( <i>LEP</i> )		IL-17A	SCF ( <i>KITLG</i> )
MCP-3 ( <i>CCL7</i> )		IL-8 ( <i>CXCL8</i> )	TECK ( <i>CCL25</i> )
MCP-4 ( <i>CCL13</i> )			TIMP-1
PARC ( <i>CCL18</i> )			TIMP-2
PDGF-BB ( <i>PDGFB</i> )			TPO ( <i>THPO</i> )
RANTES ( <i>CCL5</i> )			TRAIL R3 ( <i>TNFRSF10C</i> )
SCF ( <i>KITLG</i> )			TRAIL R4 ( <i>TNFRSF10D</i> )
TGF $\beta$ 1 ( <i>TGFB1</i> )			VEGF-A

**C**

LNCaP		C4-2
Enhanced by R1881 but suppressed by ENZ	Suppressed by R1881 but enhanced by ENZ	Enhanced by R1881 but suppressed by ENZ
Angiogenin ( <i>ANG</i> )	CXCL-11	Angiogenin ( <i>ANG</i> )
BDNF	IL-5	CCL2
BLC ( <i>CXCL13</i> )	Lymphotoxin ( <i>XCL1</i> )	gp130 ( <i>IL6ST</i> )
GCP-2 ( <i>CXCL6</i> )	TIMP-2	IL-6R
GDNF		MCP-3 ( <i>CCL7</i> )
IL-2		
IL-6R		



LNCaP		C4-2	
R1881	ENZ	R1881	ENZ
<b>Enhanced secretion:</b>	<b>Enhanced secretion:</b>	<b>Enhanced secretion:</b>	<b>Enhanced secretion:</b>
BMP-6	Eotaxin-1 ( <i>CCL11</i> )	Adiponectin ( <i>ADIPOQ</i> )	CCL1
CCL1	GRO $\alpha$ ( <i>CXCL1</i> )	Axl	Eotaxin-2 ( <i>CCL24</i> )
CCL2	IL-1 R4 ( <i>IL1RL1</i> )	BDNF	Eotaxin-3 ( <i>CCL26</i> )
CCL23	IL-12 p70 ( <i>IL12A</i> )	$\beta$ -NGF ( <i>NGF</i> )	HGF
CCL8	IL-17A	bFGF ( <i>FGF2</i> )	
EGF	IL-2 R $\alpha$ ( <i>IL12RA</i> )	BLC ( <i>CXCL13</i> )	<b>Suppressed secretion:</b>
FGF-7	IL-4	GRO $\alpha$ ( <i>CXCL1</i> )	Angiopoietin-2 ( <i>ANGPT2</i> )
FLT-3 ligand ( <i>FLT3LG</i> )	IL-8 ( <i>CXCL8</i> )	IGFBP-4	CCL8
Fractalkine ( <i>CX3CL1</i> )	MIP-1 $\alpha$ ( <i>CCL3</i> )	IL-16	FLT-3 ligand ( <i>FLT3LG</i> )
GM-CSF ( <i>CSF2</i> )	MIP-1 $\beta$ ( <i>CCL4</i> )		IGF-1
IFN- $\gamma$ ( <i>IFNG</i> )	MSP ( <i>MST1</i> )	<b>Suppressed secretion:</b>	IGFBP-2
IL-1 $\alpha$ ( <i>IL1A</i> )	NAP-2 ( <i>PPBP</i> )	Amphiregulin ( <i>AREG</i> )	IL-1 $\alpha$ ( <i>IL1A</i> )
IL-3	NT-3 ( <i>NTF3</i> )	BTC	IL-1 $\beta$ ( <i>IL1B</i> )
MIG ( <i>CXCL9</i> )	OSM	Dtk ( <i>TYRO3</i> )	IL-11
SDF-1 $\alpha$ ( <i>CXCL12</i> )	PIGF ( <i>PGF</i> )	ENA-78 ( <i>CXCL5</i> )	IL-15
TARC ( <i>CCL17</i> )	TECK ( <i>CCL25</i> )	Fas	IL-3
TGF $\beta$ 3 ( <i>TGFB3</i> )	TIMP-1	FGF-9	Leptin ( <i>LEP</i> )
TNFSF14	TNF R1 ( <i>TNFRSF1A</i> )	GITR ligand ( <i>TNFSF18</i> )	M-CSF ( <i>CSF1</i> )
	TNF R2 ( <i>TNFRSF1B</i> )	ICAM-3	MDC ( <i>CCL22</i> )
<b>Suppressed secretion:</b>	TPO ( <i>THPO</i> )	IGFBP-3	MIG ( <i>CXCL9</i> )
Adiponectin ( <i>ADIPOQ</i> )	TRAIL R3 ( <i>TNFRSF10C</i> )	Lymphotactin ( <i>XL1</i> )	MIP-1 $\beta$ ( <i>CCL4</i> )
AgRP	uPAR ( <i>PLAUR</i> )	PARC ( <i>CCL18</i> )	MIP-3 $\alpha$ ( <i>CCL20</i> )
Angiopoietin-2 ( <i>ANGPT2</i> )	VEGF-A		MIP-3 $\beta$ ( <i>CCL19</i> )
$\beta$ -NGF ( <i>NGF</i> )			NAP-2 ( <i>PPBP</i> )
bFGF ( <i>FGF2</i> )	<b>Suppressed secretion:</b>		NT-4 ( <i>NTF4</i> )
ENA-78 ( <i>CXCL5</i> )	BMP-4		OPG ( <i>TNFRSF11B</i> )
Fas	IL-1 $\beta$ ( <i>IL1B</i> )		OSM
FGF-9	TNF $\alpha$ ( <i>TNF</i> )		PIGF ( <i>PGF</i> )
GITR ( <i>TNFRSF18</i> )			RANTES ( <i>CCL5</i> )
GRO $\alpha/\beta/\gamma$ ( <i>CXCL1/2/3</i> )			SDF-1 $\alpha$ ( <i>CXCL12</i> )
ICAM-1			TARC ( <i>CCL17</i> )
ICAM-3			TGF $\beta$ 1 ( <i>TGFB1</i> )
IGF-1R			TGF $\beta$ 3 ( <i>TGFB3</i> )
IGFBP-3			TNF $\alpha$ ( <i>TNF</i> )
IGFBP-6			TNF $\beta$ ( <i>LTA</i> )
IL-1 R1			TNF R1 ( <i>TNFRSF1A</i> )
IL-11			TNF R2 ( <i>TNFRSF1B</i> )
IL-12 p40 ( <i>IL12B</i> )			TNFSF14
MIF			uPAR ( <i>PLAUR</i> )
MIP-3 $\beta$ ( <i>CCL19</i> )			VEGF-D
NT-4 ( <i>NTF4</i> )			
TRAIL R4 ( <i>TNFRSF10D</i> )			

**Figure 7. AR ligand-induced cellular senescent PCa cells possess distinct sets of secreted cytokines.** Cellular senescence was induced in LNCaP or C4-2 cells by treating with either AR agonist at SAL (1 nM R1881) or antagonist (1  $\mu$ M ENZ) for 72 h. Cells were also treated with DMSO as a solvent control. Thereafter, cells were washed twice with 1x PBS and further incubated with 0% FBS medium for 48 h. The conditioned medium was collected and loaded on human cytokine arrays to detect the secretion of 120 cytokines as shown in Supplemental Figure S2. Note that a regulated cytokine secretion is defined when the secretion level was altered by at least 20% compared to control-treated sample. (A) Venn's diagrams summarize the total number of secreted cytokines regulated by AR ligands. The data are derived from two independent experiments. (B) Lists of secreted cytokines that were regulated in the same direction by both R1881 and ENZ. (C) Lists of secreted cytokines which were oppositely regulated between R1881 and ENZ. (D) Lists of secreted cytokines that were only regulated by either R1881 or ENZ. Enhanced and suppressed secretion in (B-D) is relative to control (DMSO)-treated cells.

Next, the secretory profile was compared between LNCaP and C4-2 cells treated with the same ligand. On one hand, secreted level of some cytokines was similarly altered by both cell lines. This includes the secretion of Angiogenin (ANG), which was enhanced by SAL and suppressed by ENZ (Figure 7C). On the other hand, the secreted level of some cytokines was oppositely altered by the two cell lines treated with the same ligand. This includes the secretion of SCF, TECK, and TIMP-2. SCF secretion by LNCaP cells was enhanced, while the secretion by C4-2 cells was suppressed by either SAL or ENZ (Figure 7B). ENZ enhanced the secretion of TECK and TIMP-2 in LNCaP cells (Figure 7C and D), but suppressed the secretion in C4-2 cells (Figure 7B). Note that TIMP-2 secretion was suppressed by SAL in both cell lines. Thus, the results indicate that cytokine secretion of senescent PCa cells is both AR ligand and cell line dependent.

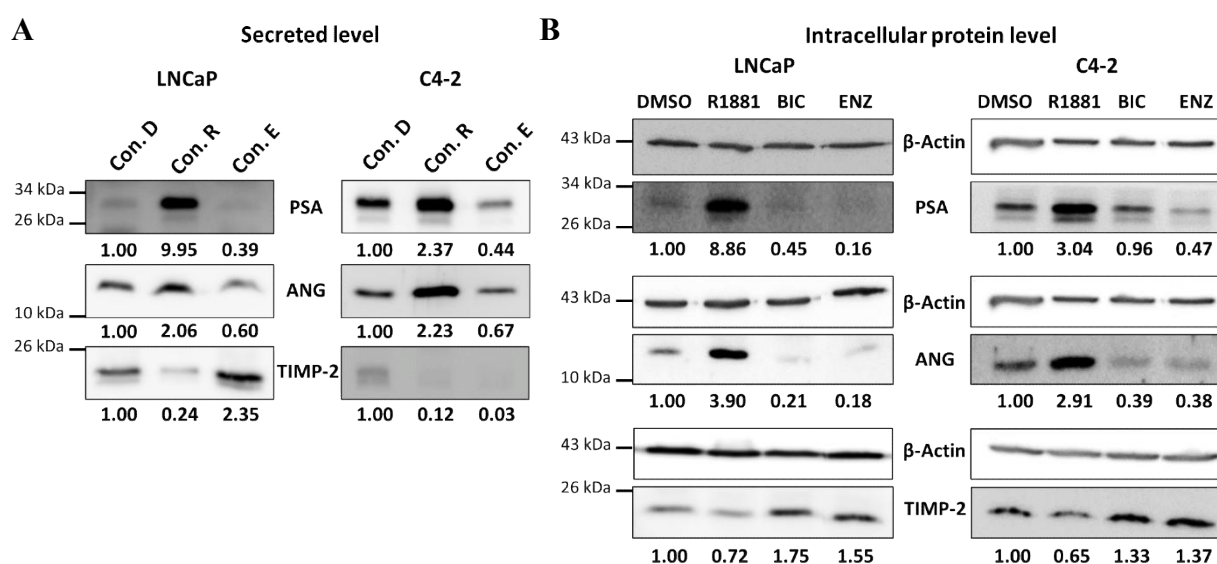
To confirm the results from cytokine arrays, secreted proteins of AR ligand-treated PCa cells were concentrated by performing methanol precipitation of conditioned media and subsequently analyzed by Western blotting. Con. D, Con. R, and Con. E refer to conditioned media derived from DMSO-, R1881-, and ENZ-treated cells, respectively. ANG and TIMP-2 were chosen as representative targets due to a strong detected signal on cytokine arrays (Supplemental Figure S2). Secreted PSA, a protein which is encoded by the AR target gene *KLK3*, was also analyzed and served as a control. As expected, PSA secretion was enhanced by AR agonist and suppressed by antagonist in both cell lines (Figure 8A). ANG secretion was also enhanced by agonist and suppressed by antagonist. TIMP-2 secretion was suppressed by agonist in both cell lines. Moreover, the results show an enhanced TIMP-2 secretion by antagonist-treated LNCaP cells, but suppressed secretion by C4-2 cells. These results confirm the data of cytokine arrays.

It was hypothesized that the cytokine secretion may be reflected at transcription level because AR is a transcription factor. To address this, intracellular protein and mRNA levels were analyzed. As control, expected effects by AR ligands on PSA/*KLK3* level were observed in both cell lines at all three levels (secreted, intracellular protein, and mRNA levels) (Figure 8A-C). This indicates that the differences in PSA secretion correlate with transcriptional regulation. Supporting the hypothesis, AR ligand-mediated changes of ANG level were similarly observed at secreted and intracellular levels of both cell lines. Moreover,

*TIMP2/TIMP-2* suppression by agonist and induction by antagonist were detected in LNCaP cells at mRNA, intracellular protein, and secreted levels.

However, the secreted level of TIMP-2 by antagonist-treated C4-2 cells neither correlated to intracellular protein nor to mRNA levels (Figure 8A-C). Similarly, secreted TECK level did not correlate with the mRNA expression of antagonist-treated C4-2 cells (Figure 7B; Figure 8C). An uncorrelation between secreted and transcription levels was also observed for *SCF/KITLG* in LNCaP, but not in C4-2 cells (Figure 7B; Figure 8C). Notably, the levels of approximately 30% of cytokines in both cell lines are similarly influenced (enhanced, suppressed, or not affected) by SAL at mRNA and secreted levels (Figure 8D). Hence, the data indicate that secretion of some SASP factors is associated with regulated transcriptional level, whereas secretion of other factors is independent of transcription.

Taken together, the data show that AR ligand-induced cellular senescent PCa cells possess distinct SASP secretomes. The results suggest that secretion of some SASP factors is both AR ligand and cell line dependent. Although secreted levels of some cytokines are associated with AR ligand-controlled transcription, some are not and may be regulated at a non-genomic level by AR ligands. In line with this, it is known that the AR also interacts with multiple signaling cascades in the cytoplasm. It seems that other unknown mechanisms and cellular pathways are involved for the cytokine secretion.



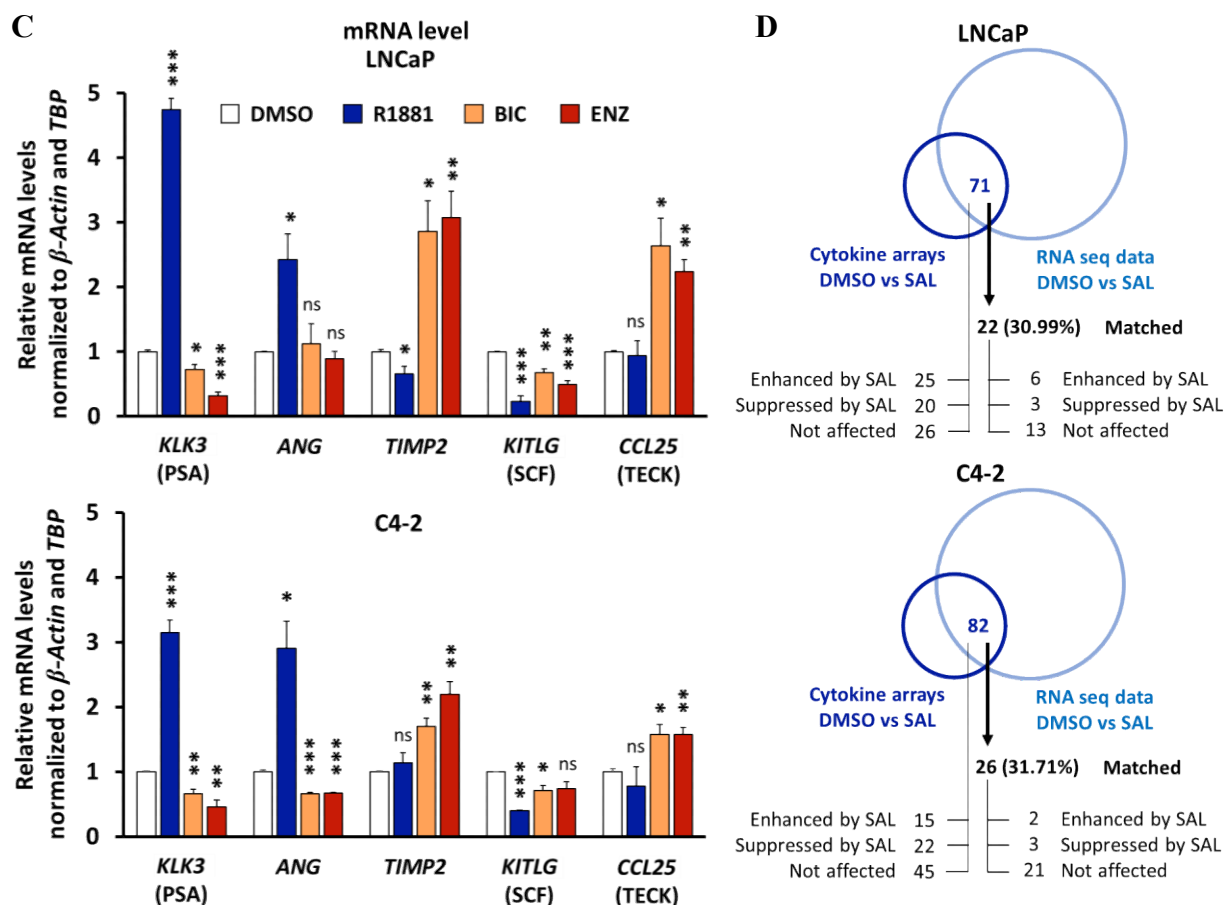


**Figure 8. Secreted level of some SASP factors by AR ligands is independent of transcription regulation.** (A) Western blot analysis of secreted proteins by LNCaP and C4-2 cells. Secreted proteins of AR ligand-induced cellular senescent cells were precipitated from conditioned medium by methanol. Equal amount was loaded on SDS-PAGE. Angiogenin (ANG) and TIMP-2 are representative targets selected to confirm the results of cytokine arrays. Secreted PSA served as a control. Con. D, Con. R, and Con. E are conditioned media derived from control (DMSO)-, R1881-, and ENZ-treated cells, respectively. Numbers indicate band intensities relative to Con. D sample. (B) PSA, ANG, and TIMP-2 intracellular protein levels were detected by Western blotting and normalized to  $\beta$ -Actin. Protein extraction was performed after 72 h treatment of 1 nM R1881, 1  $\mu$ M BIC, 1  $\mu$ M ENZ, or 0.1% DMSO as solvent control. Numbers indicate normalized band intensities relative to DMSO control. (C) mRNA levels of *KLK3*, *ANG*, *TIMP2*, *KITLG*, and *CCL25* were analyzed by qRT-PCR. RNA extraction was conducted after 48 h treatment with the same concentration as (B). Bar graphs are shown as mean + SEM from three independent experiments (N = 3).  $\beta$ -Actin and TBP served as housekeeping genes. Statistical analysis was performed by using two-tailed unpaired t-test comparing each treatment to DMSO treatment. \*,  $p \leq 0.05$ ; \*\*,  $p \leq 0.01$ ; \*\*\*,  $p \leq 0.001$ ; ns, not significant. (D) Schematic figures summarize the overlapping data from cytokine arrays (small circle) and RNA sequencing (big circle) upon 1 nM R1881 (SAL) treatment versus DMSO as solvent control. Out of 120 targets from cytokine arrays, the regulation of 71 and 82 cytokines is available in RNA sequencing data of LNCaP and C4-2, respectively. The levels of 22 from 71 targets (30.99%) for LNCaP and 26 from 82 targets (31.71%) for C4-2 were similarly altered at both RNA and secreted levels. Threshold for alteration of secreted level was set at  $\pm 20\%$ , and of RNA at the value of  $\log_2$  fold change  $\pm 1$ .

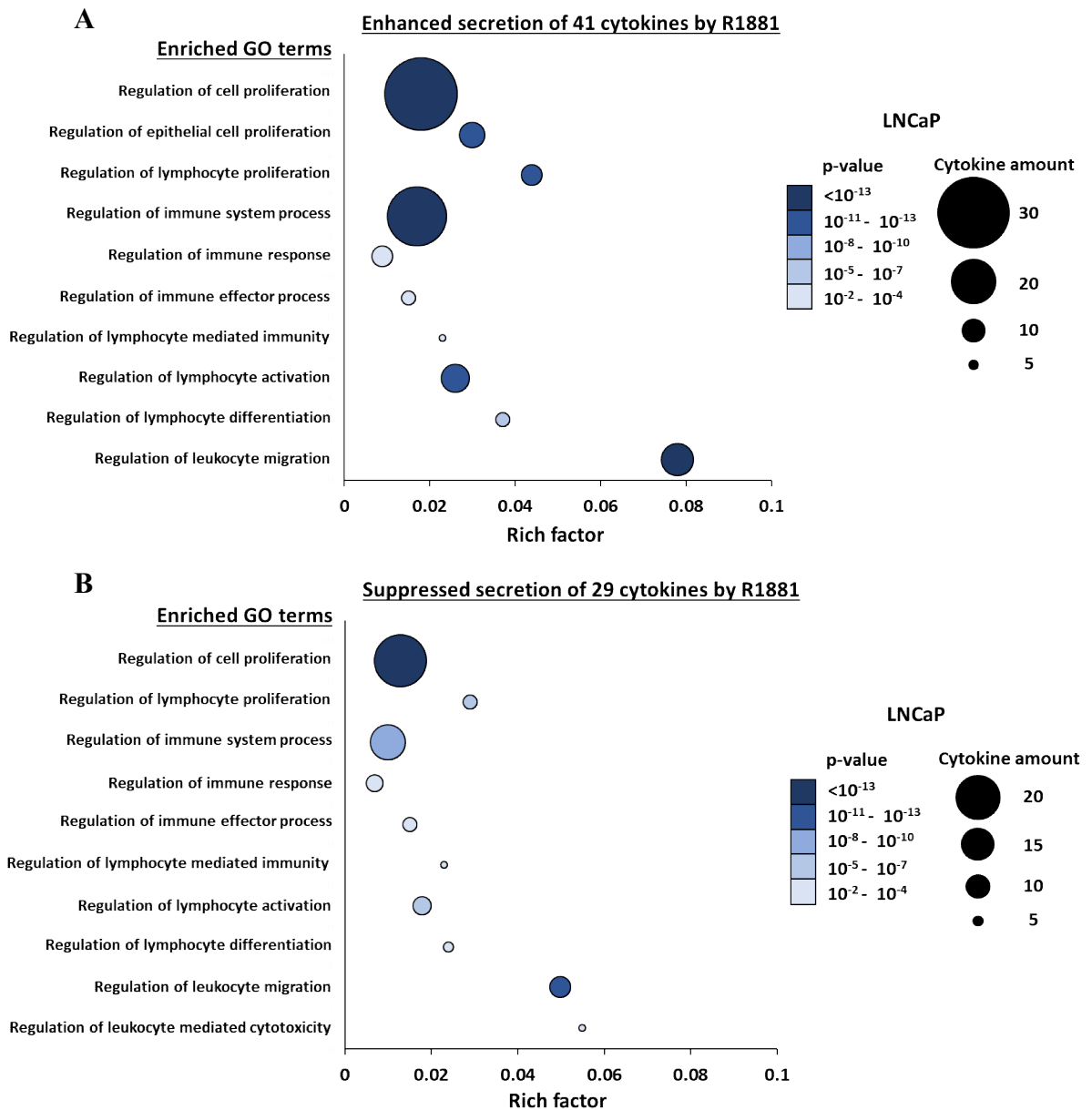
### **4.3 Bioinformatic gene ontology (GO) analysis suggests paracrine effects of AR ligand-induced SASP on PCa cell proliferation and immune system**

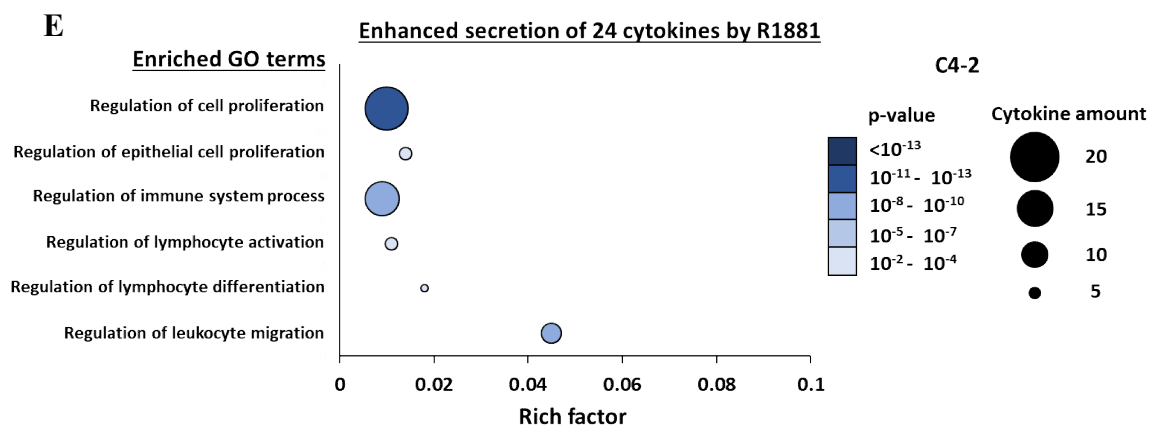
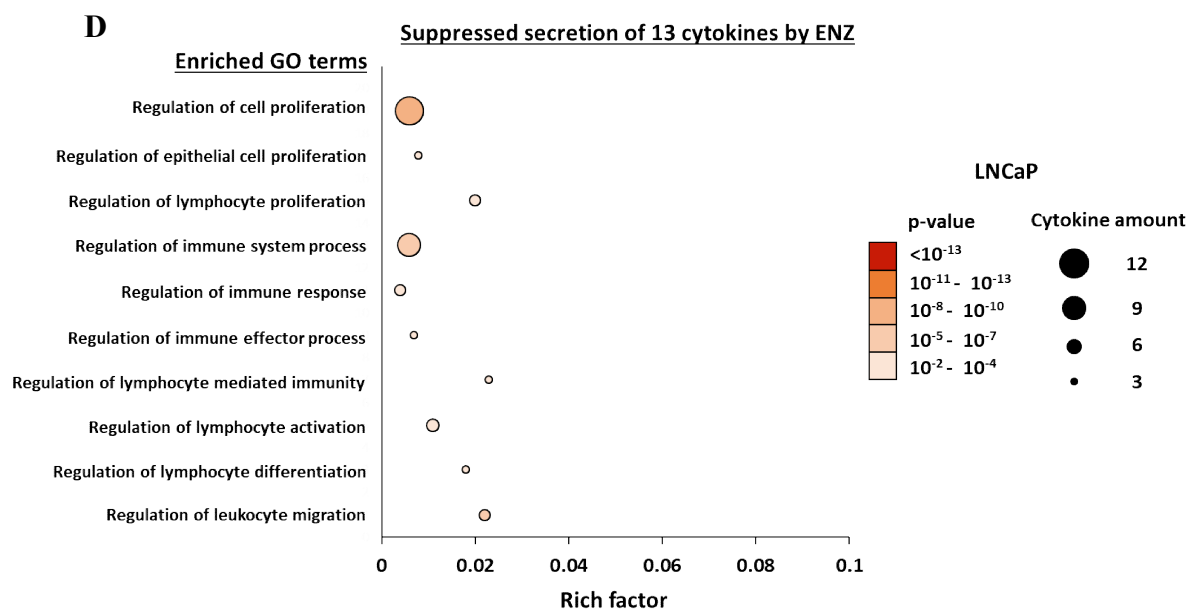
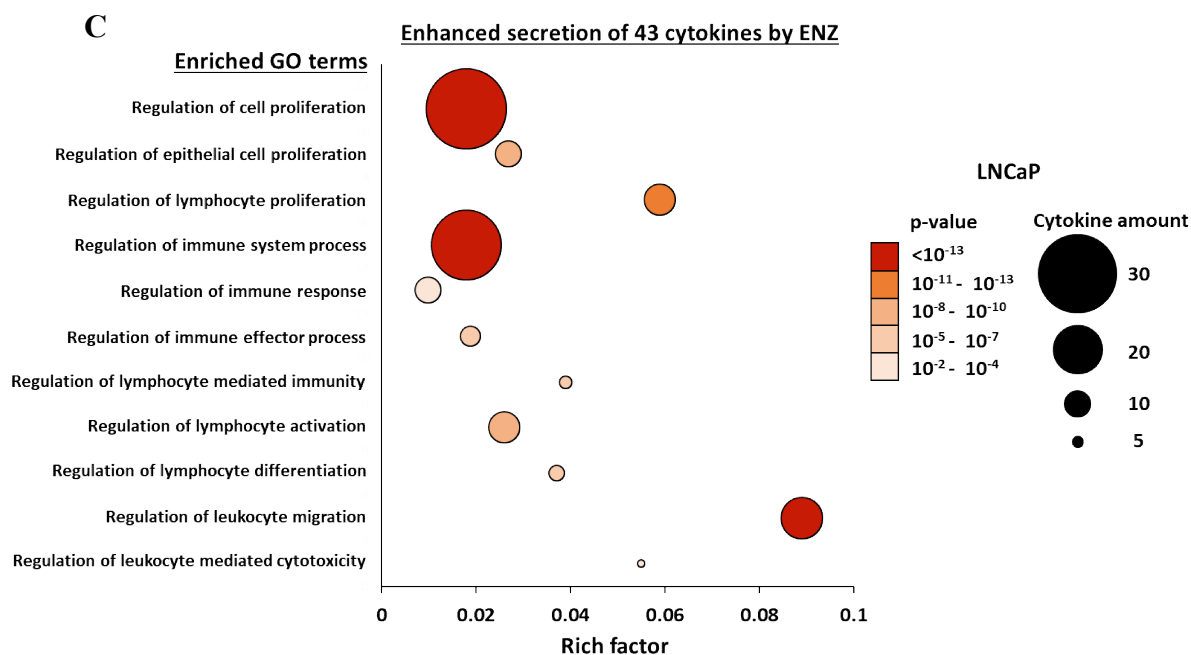
Major concern regarding an induction of senescence is the paracrine effect on neighboring non-senescent cells via SASP. The effect relies on the balance between secreted tumor-promoting and -suppressive factors. In this study, effects of SASP on PCa cell proliferation and immune cells are in focus. To address this, bioinformatic gene ontology (GO) was used to analyze whether the secreted cytokines may influence cell proliferation and immune system. For each cell line, cytokines were categorized into four sets based on their regulated secretion detected by cytokine arrays. The four sets include secreted cytokines, which are (1) enhanced by R1881, (2) suppressed by R1881, (3) enhanced by ENZ, or (4) suppressed by ENZ. Each set was analyzed for GO. An outcome was obtained and presented as “enriched GO terms” (Figure 9; Table 4).

The data reveal that all sets of cytokines secreted by both cell lines were significantly enriched in the GO term “regulation of cell proliferation” (Figure 9; Table 4). This GO term was enriched by the majority of cytokines secreted by LNCaP (Supplemental Table S1) and C4-2 cells (data not shown). Thus, it suggests that the secreted cytokines may regulate the proliferation of other cells. Biological process including GO terms “regulation of the immune system process” and “regulation of leukocyte migration” were also significantly enriched by secreted cytokines from all conditions (Figure 9; Table 4). Thus, the data suggest possible effect of the secreted cytokines towards regulation of immune system as well. Interestingly, it seems that the cytokines secreted by LNCaP cells may have more impact to the immune system than cytokines secreted by C4-2 cells. In line with this, most of GO terms regarding immune system were significantly enriched by all sets of cytokines secreted from treated LNCaP cells (Table 4). This includes regulation of immune response, immune effector process, lymphocyte proliferation, lymphocyte mediated immunity, lymphocyte activation, and lymphocyte differentiation.

Taken together, GO analysis indicated that distinct sets of cytokines secreted by AR ligand-induced cellular senescent PCa cells may mediate paracrine effect on cell proliferation and immune system. The analysis pointed to cytokines in each set that are associated with regulation of those biological processes. However, GO analysis software did not provide the

information on up- or downregulation. Therefore, it is unclear whether these sets of secreted cytokines will promote or suppress the process. Further experiments are required to examine the effect of AR ligand-induced SASP.





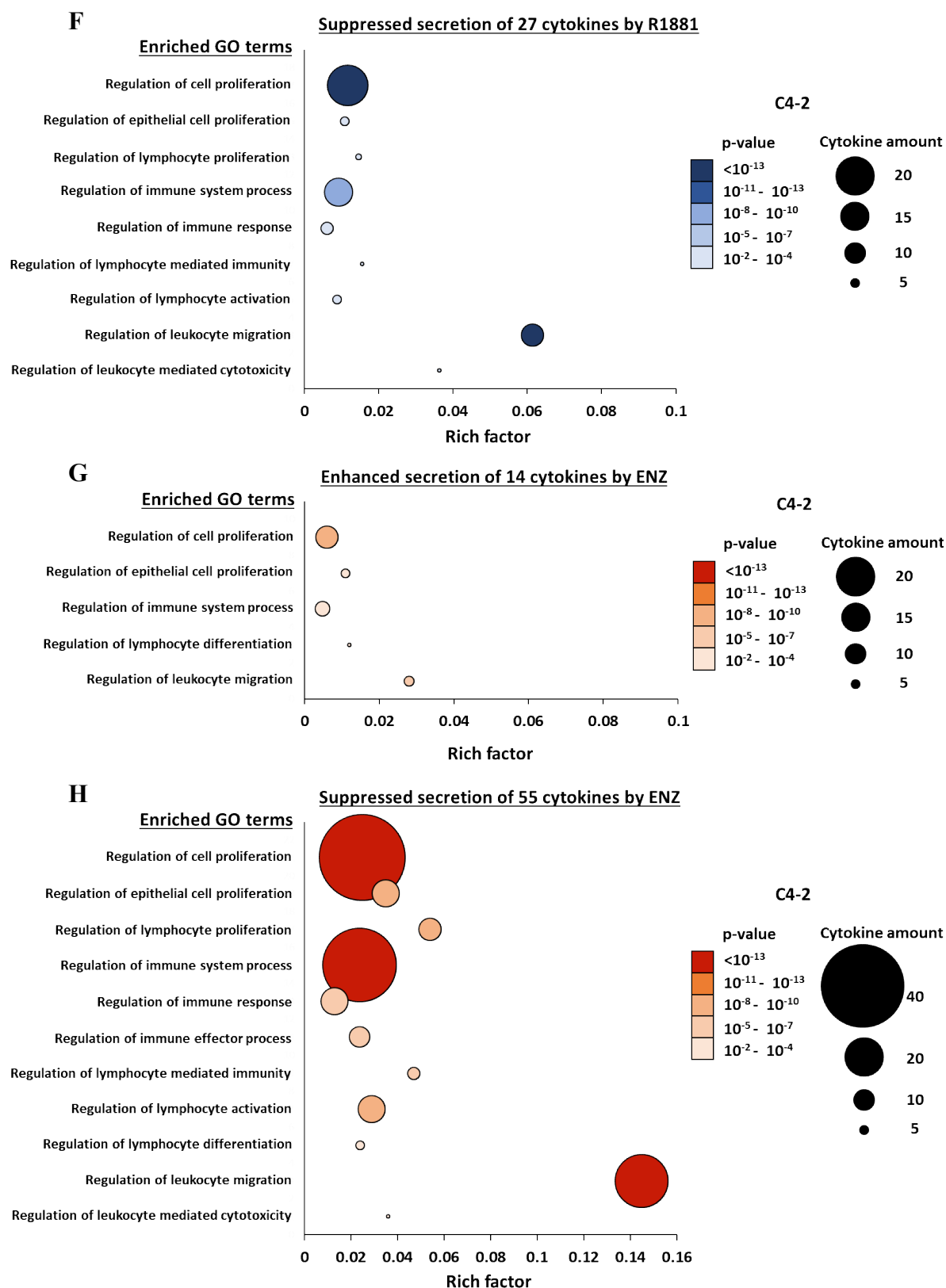


**Figure 9. Cytokines secreted by AR ligand-treated PCa cells significantly enriched in GO terms regarding cell proliferation and immune system. Each set of regulated cytokine secretion from AR**



ligand-induced cellular senescent (A-D) LNCaP or (E-H) C4-2 cells was analyzed with gProfile R package (v0.6.8) to predict whether the secreted cytokines can influence cell proliferation and immune system. Significant enriched GO terms by secreted cytokines from (A, B, E, and F) R1881 (SAL)- or (C, D, G, and H) ENZ-treated cells are shown. The p-value for each GO term is indicated by the shade of colors. The number of cytokines enriched in particular GO term is demonstrated by the size of circle. Rich factor for particular GO term = cytokine amount ÷ total number of genes in database involved in particular biological process.

**Table 4. Summary of significant enriched GO terms regarding cell proliferation and immune system by secreted cytokines of AR ligand-treated PCa cells**

Enriched GO Terms		LNCaP				C4-2			
		R1881		ENZ		R1881		ENZ	
		Enhanced cytokine secretion	Suppressed cytokine secretion	Enhanced cytokine secretion	Suppressed cytokine secretion	Enhanced cytokine secretion	Suppressed cytokine secretion	Enhanced cytokine secretion	Suppressed cytokine secretion
Cell proliferation	Regulation of cell proliferation	*	*	*	*	*	*	*	*
	Regulation of epithelial cell proliferation	*		*	*	*	*	*	*
	Regulation of lymphocyte proliferation	*	*	*	*		*		*
Immune system	Regulation of immune system process	*	*	*	*	*	*	*	*
	Regulation of immune response	*	*	*	*		*		*
	Regulation of immune effector process	*	*	*	*				*
	Regulation of lymphocyte mediated immunity	*	*	*	*		*		*
	Regulation of lymphocyte activation	*	*	*	*	*	*		*
	Regulation of lymphocyte differentiation	*	*	*	*	*		*	*
	Regulation of leukocyte migration	*	*	*	*	*	*	*	*
	Regulation of leukocyte mediated cytotoxicity		*	*			*		*

\* indicates significant enriched GO term by particular set of secreted cytokines.

#### 4.4 AR agonist-induced SASP suppresses, whereas antagonist-induced SASP promotes LNCaP cell proliferation

The results from GO analysis indicate that cytokines secreted by AR ligand-treated PCa cells may affect the regulation of cell proliferation. Since distinct secretory profiles were detected among AR ligand-treated cells, it was hypothesized that the paracrine effect of SASP from agonist-treated cells is different to the effect of SASP from antagonist-treated cells. To analyze this hypothesis, PCa cell proliferation assays with conditioned media were conducted. LNCaP cells were treated with conditioned media collected from AR ligand-treated LNCaP, whereas C4-2 cells were treated with conditioned media of AR ligand-treated C4-2. Con. D, Con. R, Con. B, and Con. E refer to conditioned media derived from DMSO-, R1881-, BIC-, and ENZ-treated cells, respectively.

Earlier results showed that AR ligands regulate PCa cell proliferation. Therefore, it is necessary to confirm that no AR ligand remains in the conditioned media that may affect cell proliferation. For that purpose, qRT-PCR was performed to detect the expression of the AR target *KLK3* (PSA). As control, *KLK3* mRNA level was significantly induced by androgen treatment and inhibited by AR antagonists in both cell lines (Supplemental Figure S3). In contrast, treatment with conditioned media did not affect *KLK3* mRNA level. These data suggest that the conditioned media do not have enough ligands to regulate AR activity.

Interestingly, the results show that LNCaP cell proliferation, but not C4-2 cells, was affected by conditioned media (Figure 10A and B). In line with this, Con. R treatment significantly suppressed the proliferation of LNCaP cells. Furthermore, either Con. B or Con. E surprisingly promoted LNCaP cell proliferation. These novel findings hint to the possible undesired side-effect of AR antagonist treatment and suggest a tumor suppressive role of Con. R. Thus, the effect of conditioned media from agonist-treated cells is opposite to the effect of conditioned medium from antagonist-treated cells.

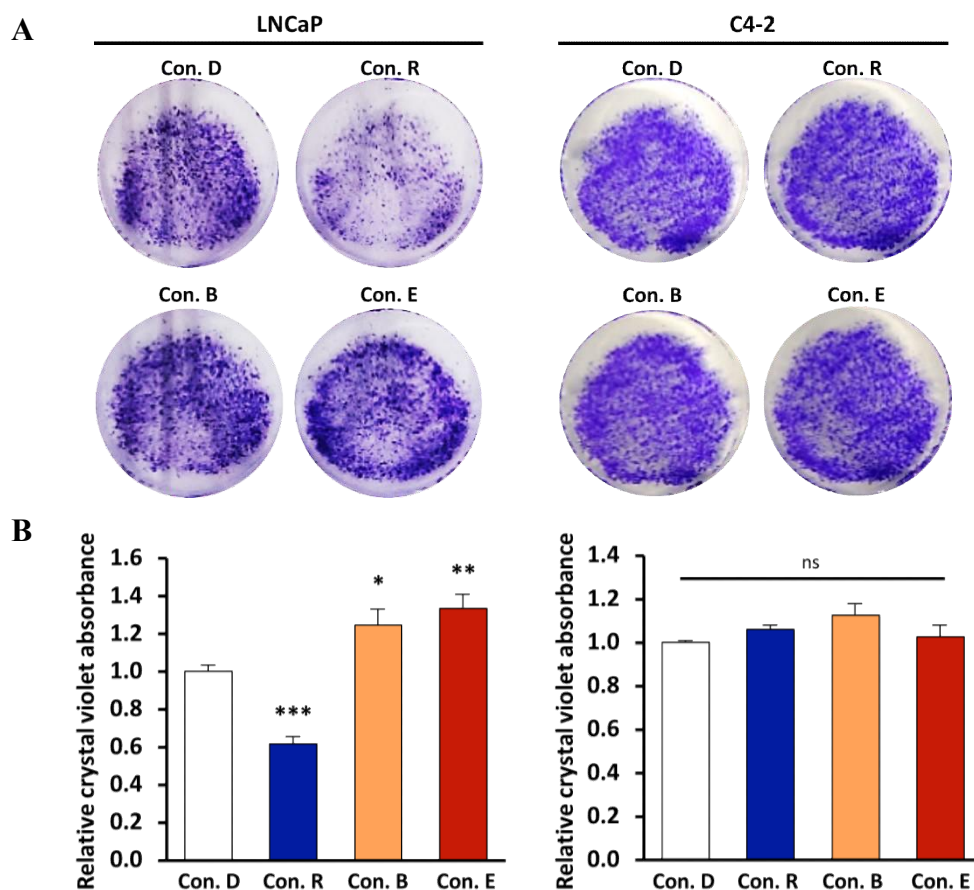


**Figure 10. Conditioned media from AR ligand-induced cellular senescence mediate paracrine effect on LNCaP cell proliferation.** Similar experiments were performed as Figure 6 except that the LNCaP and C4-2 cells were treated with Con. R, Con. B, Con. E, or Con. D as control for 8 days. **(A)** Representative crystal violet staining pictures of cells after 8 days of treatment. **(B)** Crystal violet absorbance (OD 590 nm) on day 8 was normalized to the value of day 0 and presented as relative to Con. D treatment. Bar graphs are shown as mean + SEM from total of six technical replicates (n = 6) of three independent experiments. Statistical analysis was performed by using one-way ANOVA followed by Dunnett's multiple comparisons test. \*,  $p \leq 0.05$ ; \*\*,  $p \leq 0.01$ ; \*\*\*,  $p \leq 0.001$ ; ns, not significant.

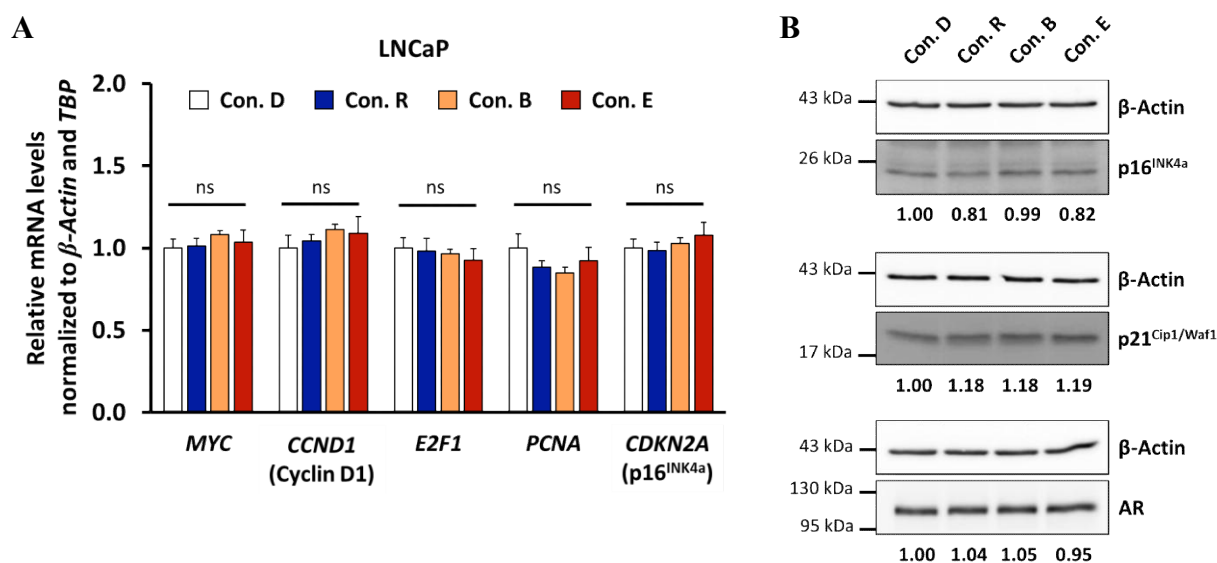
The results of GO analysis were further analyzed to pinpoint towards possible cytokines associated with the observed effect of LNCaP proliferation. Since LNCaP cell proliferation was oppositely regulated by Con. R and Con. E, it may be explained by distinct secretory profiles between agonist- and antagonist-treated cells. Hence, the cytokines that the secretion level was similarly affected by both agonist and antagonist are unlikely to be underlying factors. In fact, the secreted level of cytokine that inhibit cell proliferation is expected to be enhanced in Con. R but suppressed in Con. E, and *vice versa* for the secreted level of cytokine that promote cell proliferation. Here, according to the list of secreted cytokines that enriched in the GO term "regulation of cell proliferation" (Supplemental Table S1), secreted levels of 10 cytokines were oppositely altered (enhanced or suppressed) between R1881 and ENZ treatment. They are ANG, BLC, GCP-2, GDNF, IL-2, soluble IL-6R, CXCL-11, IL-5, TIMP-2, and lymphotactin. The secretion of the first six cytokines was enhanced by R1881 and suppressed by ENZ. In contrast, the secretion of the last four cytokines was suppressed by R1881 and enhanced by ENZ. Therefore, the data suggest that regulation of LNCaP cell proliferation by conditioned media might be mediated by but not limited to these secreted cytokines. Secreted cytokines affected by either R1881 or ENZ alone should not be excluded.

#### 4.5 AR ligand-induced SASP regulates phospho-kinome of PCa cells

To further investigate how the conditioned media regulates LNCaP cells proliferation, expression levels of cell cycle regulators, the AR, and the phospho-kinome were analyzed in conditioned media-treated LNCaP cells. LNCaP cells were treated with Con. D, Con. R, Con. B, or Con. E for 6 days.

Surprisingly, no regulation at mRNA level was observed for the analyzed factors *MYC*, *CCND1*, *E2F1*, *PCNA*, and *CDKN2A* (Figure 11A). Also, the protein levels of two well-

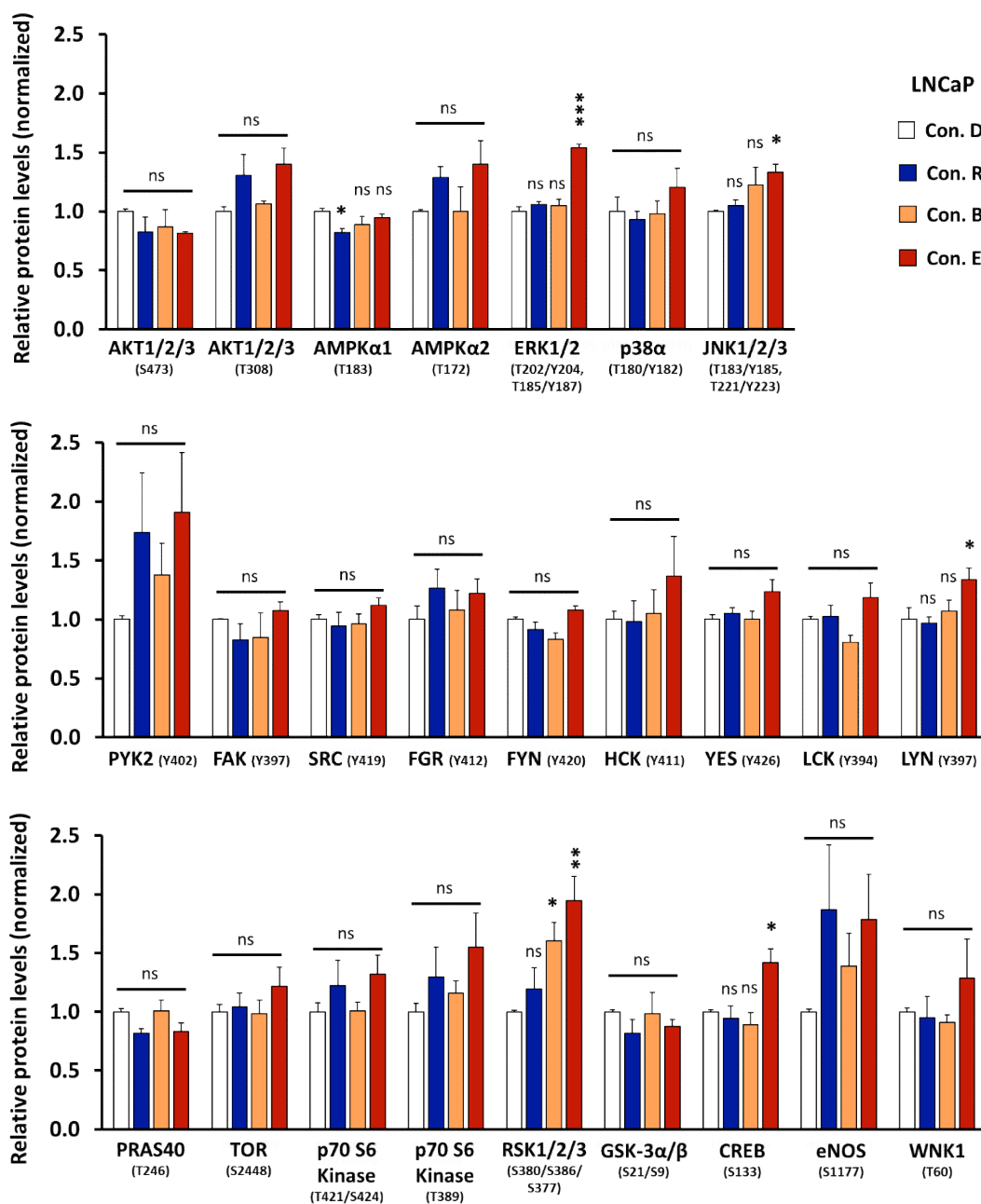
known senescence regulators  $p16^{\text{INK4a}}$  and  $p21^{\text{Cip1/Waf1}}$  were not clearly affected after treating with conditioned media (Figure 11B). This suggests that cellular senescence may not be the reason for Con. R-mediated growth suppression, unless other cellular senescence pathways were triggered. Additionally, no regulation of AR at protein level was observed (Figure 11B). Hence, the data show that expressions of analyzed cell proliferating key factors, senescence regulators, and AR are not associated with the conditioned media-regulated LNCaP cell proliferation.



**Figure 11. Conditioned media do not affect the expression of cell cycle regulators.** LNCaP cells were treated with Con. R, Con. B, Con. E, or Con. D as control for 6 days. **(A)** mRNA levels of *MYC*, *CCND1*, *E2F1*, *PCNA*, and *CDKN2A* were analyzed by qRT-PCR. Bar graphs are shown as mean + SEM from total of six technical replicates (n = 6) of two independent experiments.  $\beta$ -Actin and *TBP* served as housekeeping genes. Normalized mRNA levels of Con. D-treated cells were set arbitrarily as 1. Statistical analysis was performed by using one-way ANOVA followed by Dunnett's multiple comparisons test. ns, not significant. **(B)** Protein levels of AR,  $p16^{\text{INK4a}}$ , and  $p21^{\text{Cip1/Waf1}}$  were analyzed by Western blotting and normalized to  $\beta$ -Actin. Numbers indicate normalized band intensities relative to Con. D treatment.

The phospho-kinome of conditioned media-treated LNCaP cells was analyzed by loading cell lysates on human phospho-kinase arrays. Based on the observed effects of LNCaP cell proliferation by conditioned media, an opposite regulation of phospho-kinases was expected between Con. R-treated cells and Con. B- or Con. E-treated cells. Unfortunately, this expectation was not observed in any individual factor (Figure 12). However, the results show that treatment with Con. R reduced levels of phospho-AMPK $\alpha$ 1, phospho-CHK-2, and

$\beta$ -Catenin. No significant enhanced phosphorylation level was observed for other factors except EGFR, which was however significantly upregulated by Con. E as well. In contrast, treatment with Con. B or Con. E significantly enhanced levels of phospho-RSK1/2/3 and HSP60. Only Con. E significantly enhanced phosphorylation levels of ERK1/2, JNK1/2/3, LYN, CREB, HSP27, and MSK1/2. Notably, neither Con. B nor Con. E reduced phosphorylation level of any other analyzed factors. This specific regulation of multiple factors and not individual ones reflects the possibility of how conditioned media regulate LNCaP cell proliferation.



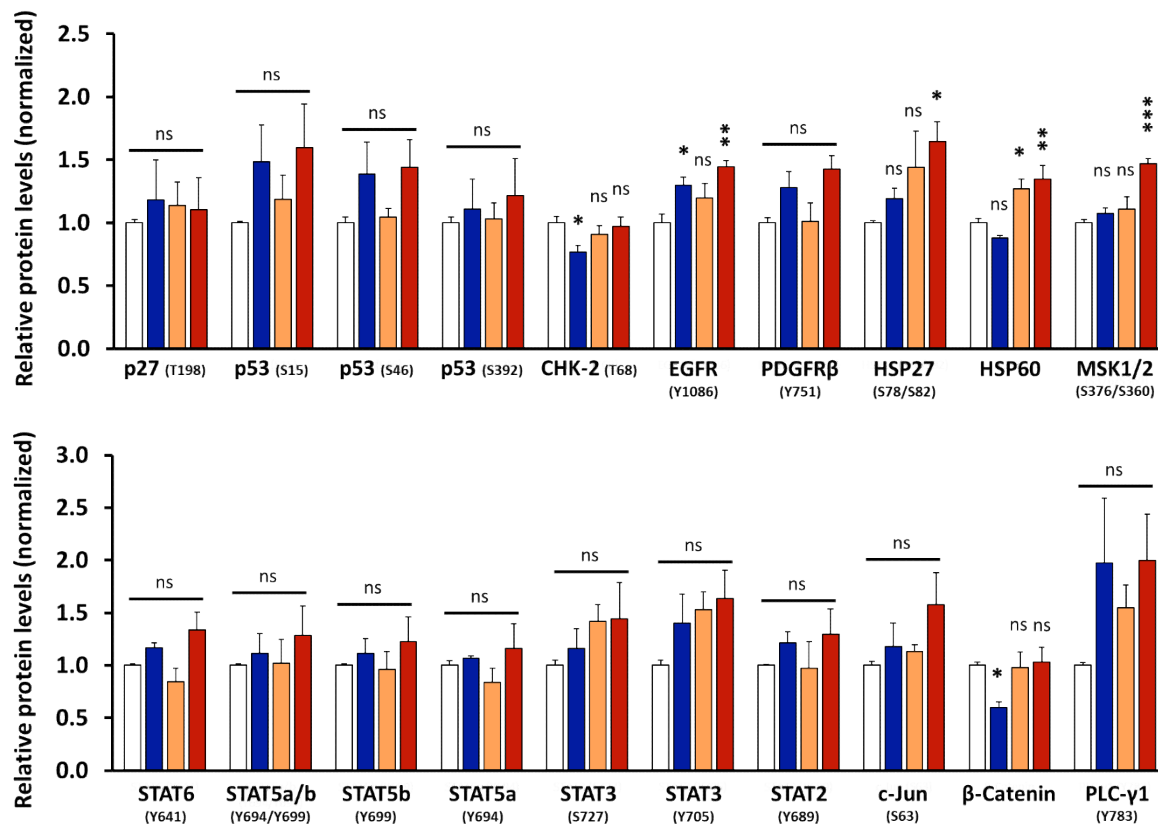


**Figure 12. Conditioned media regulate phospho-kinome of PCa cells.** Similar experiments were performed as described in Figure 11 with LNCaP cells. Protein extraction and analysis of phospho-kinase regulation were conducted using human phospho-kinase array kit. The antibody arrays recognize in total 43 kinase phosphorylation sites and 2 other proteins. Bar graphs are shown as mean + SEM from total of four technical replicates ( $n = 4$ ) of two independent experiments. Normalized protein levels of Con. D-treated cells were set arbitrarily as 1. Statistical analysis was performed by using one-way ANOVA followed by Dunnett's multiple comparisons test. \*,  $p \leq 0.05$ ; \*\*,  $p \leq 0.01$ ; \*\*\*,  $p \leq 0.001$ ; ns, not significant.

A bioinformatic ingenuity pathway analysis (IPA) was performed to analyze whether cytokines secreted by AR ligand-treated LNCaP cells may modulate the phospho-kinome of conditioned media-treated cells. Interestingly, IPA revealed that Adiponectin and IGF-1R can activate and lead to phosphorylation of AMPK $\alpha$ 1 (Supplemental Figure S4A). The secretion of these two factors from LNCaP cells was suppressed by SAL and not affected by ENZ (Figure 7D). Thus, this finding correlates to the significant reduced phospho-AMPK $\alpha$ 1 level in Con. R-treated cells. Furthermore, IPA indicated that the phospho-kinome of Con. E-treated cells can be regulated by secreted cytokines including Eotaxin-1, IL-17A, IL-4, NT-3, PIGF, TPO, TIMP-1, soluble TNF-R2, and VEGF-A (Supplemental Figure S4B). Secretion of these

cytokines from LNCaP cells was enhanced by ENZ and not affected by SAL (Figure 7D). IPA revealed that they can affect phosphorylation of ERK, whereas JNK and RSK phosphorylation can also be affected by IL-4 and VEGF-A (Supplemental Figure S4B). Thus, an enhanced secretion of these cytokines in Con. E associates with induced phospho-ERK, -JNK, and -RSK levels in Con. E-treated cells.

Taken together, the data suggest that phospho-kinome of PCa cells can be modulated by secreted cytokines of AR ligand-treated LNCaP cells. This may partially explain the observed results of conditioned media-regulated LNCaP cell proliferation.

#### **4.6 AR ligands and conditioned medium containing SASP of AR agonist-treated PCa cells regulate the expression of stemness markers**

Among other possibilities, it has been suggested that PCa stem/progenitor cells survive therapeutic intervention including AR antagonists and contribute to re-growth of PCa (Wen *et al.* 2016, Klarmann *et al.* 2009, Li and Tang 2011). It has also been reported that chemotherapy-induced senescence could change stem-cell-related properties of malignant cells and promotes cancer stemness (Milanovic *et al.* 2018). Therefore, the hypothesis was that AR ligands and/or AR ligand-induced SASP can regulate stemness and stemness markers. To examine this hypothesis, LNCaP cells were treated with conditioned media or AR ligands. After that, the expression of stemness markers including OCT4, NANOG, SCF, MET, SOX2, MYC, and ALDH1A1 were analyzed.

Interestingly, treatment with Con. R significantly downregulated stemness markers *POU5F1* (OCT4), *NANOG*, *KITLG* (SCF), and *MET* mRNA levels (Figure 13A). No upregulation at mRNA level of analyzed stemness markers was observed by either Con. B or Con. E. Surprisingly, no clear reduction of OCT4, SOX2, and MYC protein levels by Con. R was detected (Figure 13B). Also, none of analyzed stemness markers was clearly affected at protein level by Con. B or Con. E. However, among the analyzed stemness markers, ALDH1A1 protein was slightly downregulated by Con. R. These data suggest that some stemness markers can be regulated by conditioned medium of SAL-treated LNCaP cells.

SAL-treated LNCaP cells exhibited significant downregulation of *POU5F1*, *NANOG*, *KITLG*, and *MET* mRNA levels (Figure 13C). The protein levels of OCT4, SOX2, MYC, and

ALDH1A1 were also reduced by SAL treatment (Figure 13B). In contrast to SAL, AR antagonists significantly upregulated *NANOG* and *MET* mRNA levels (Figure 13C). Antagonist-induced OCT4, SOX2, and ALDH1A1 were also observed (Figure 13B). Thus, the data suggest that both mRNA and protein levels of analyzed stemness markers are AR ligand-controlled. This supports the hypothesis that stemness can be regulated by AR ligands.

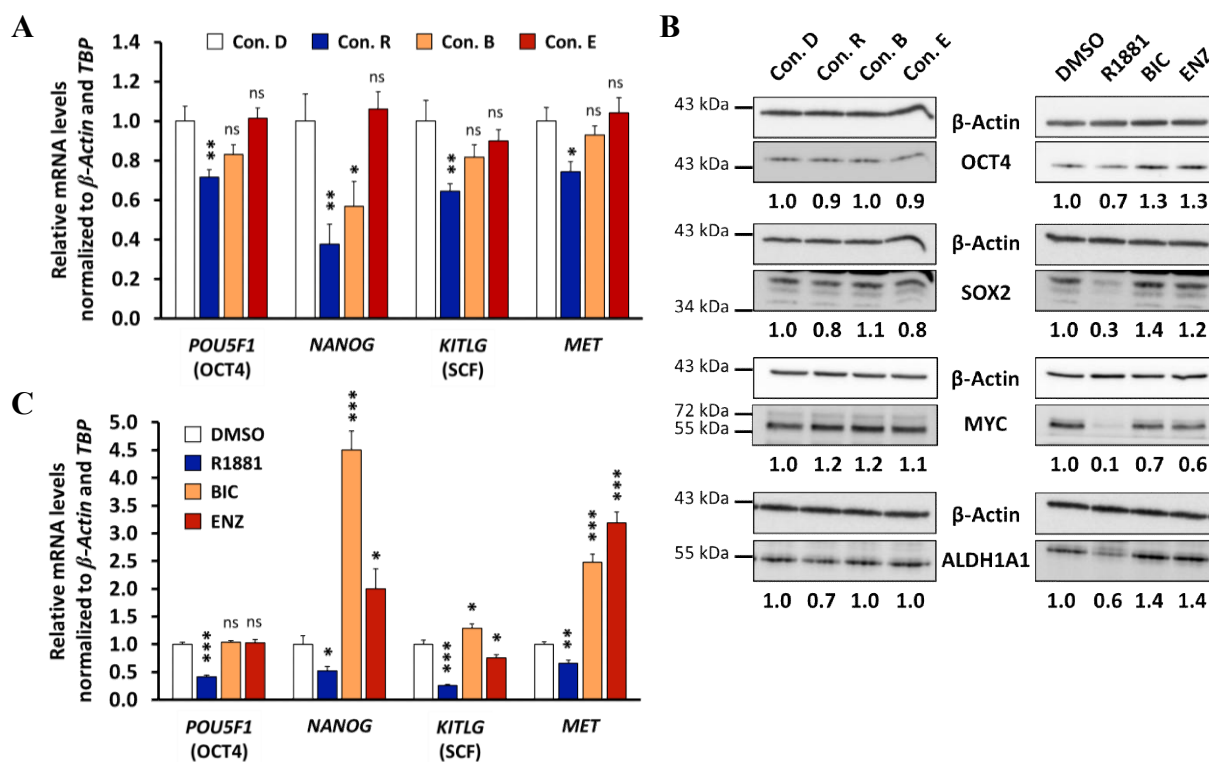


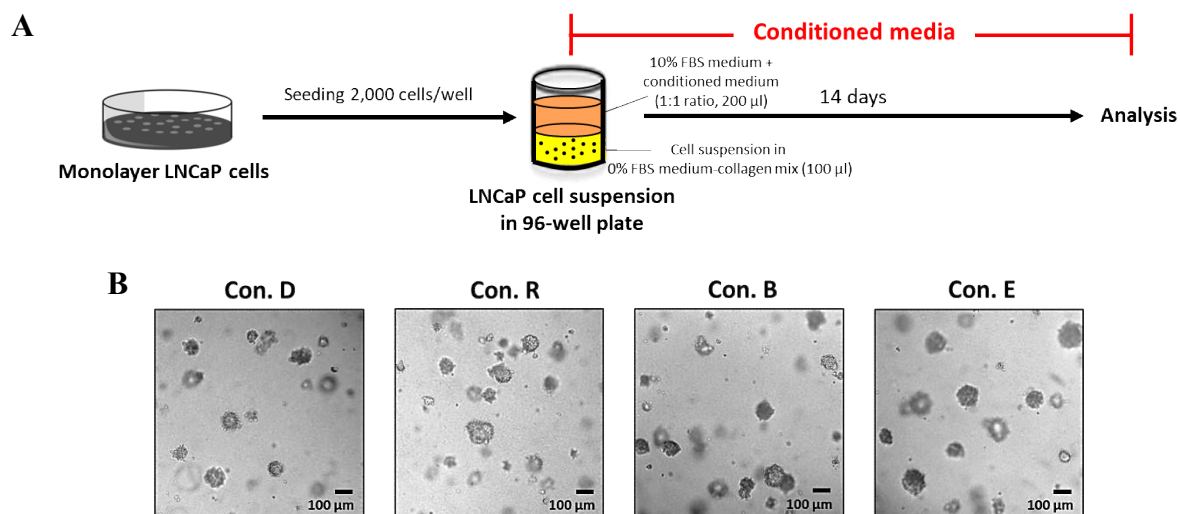
**Figure 13. Con. R and AR ligands regulate the expression of stemness markers.** LNCaP cells were treated with conditioned media or AR ligands for 6 days. **(A)** mRNA levels of *POU5F1*, *NANOG*, *KITLG*, and *MET* were analyzed by qRT-PCR after treating with indicated conditioned media. Bar graphs are shown as mean + SEM from total of six technical replicates ( $n = 6$ ) of two independent experiments.  $\beta$ -Actin and *TBP* served as housekeeping genes. One-way ANOVA followed by Dunnett's multiple comparisons test was performed for statistical analysis. **(B)** Protein levels of OCT4, SOX2, MYC, and ALDH1A1 were analyzed by Western blotting and normalized to  $\beta$ -Actin. Numbers indicate normalized band intensities relative to Con. D (for conditioned media) and to DMSO (for AR ligands) treatments. **(C)** Normalized mRNA levels of indicated stemness markers were analyzed by qRT-PCR after treating with indicated ligands. Bar graphs are shown as mean + SEM from total of six technical replicates ( $n = 6$ ) of two independent experiments. Normalized mRNA levels of control-treated cells in (A) and (C) were set arbitrarily as 1. Statistical analysis was performed by using two-tailed unpaired t-test comparing each treatment to DMSO treatment. \*,  $p \leq 0.05$ ; \*\*,  $p \leq 0.01$ ; \*\*\*,  $p \leq 0.001$ ; ns, not significant.



#### 4.7 SASP does not affect 3D colony formation of PCa cells

3D colony formation assay is an *in vitro* method that commonly used to identify and study properties of cancer stem cells (Bahmad *et al.* 2018, Beaver *et al.* 2014). Single cells can grow and form 3 types of colonies termed as holoclone, meroclone, and paraclone. The definition of each clonal type is based on morphology and proliferation/renewal capacity. An increased number of holoclone and meroclone formation has been suggested as an indicative for enrichment of PCa stemness (Beaver *et al.* 2014). Since Con. R and AR ligands regulate the expression of stemness markers, the hypothesis was that they also affect holoclone and meroclone formation efficiency as well as the size of colonies.

Here, the effect of conditioned media on holoclone and meroclone formation was analyzed by 3D colony formation assays as illustrated in Figure 14A. The suspension of single cells was treated for 14 days with Con. D, Con. R, Con. B, or Con. E. The medium-collagen mix technique adapted from Bahmad *et al.* (2018) allowed each single cell to grow freely in 3D at a fixed position, making it easy to analyze how many percent of seeded single cell formed holoclone and meroclone. Representative pictures show that the morphology of generated colonies is similar between treatments (Figure 14B). Also, the colony formation efficiency and the size of colonies were not affected (Figure 14B-D). Thus, the data suggest that conditioned media derived from AR ligand-induced cellular senescent PCa cells including Con. R may not have an impact on colony formation and colony growth, being in line with slightly changed protein level of stemness markers.



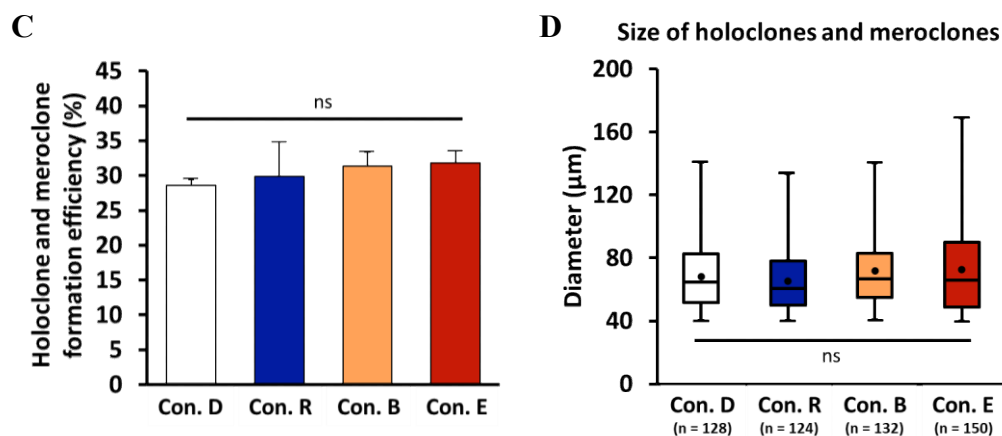
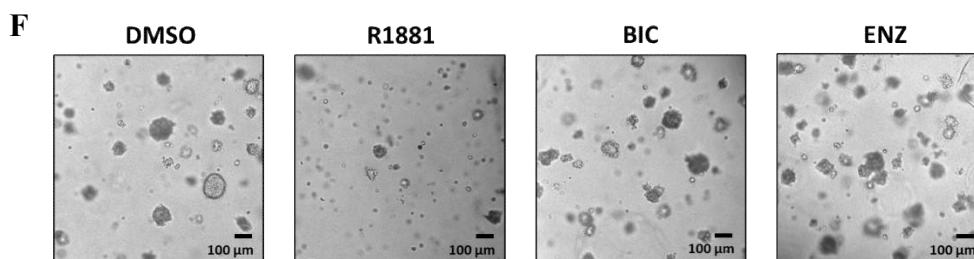
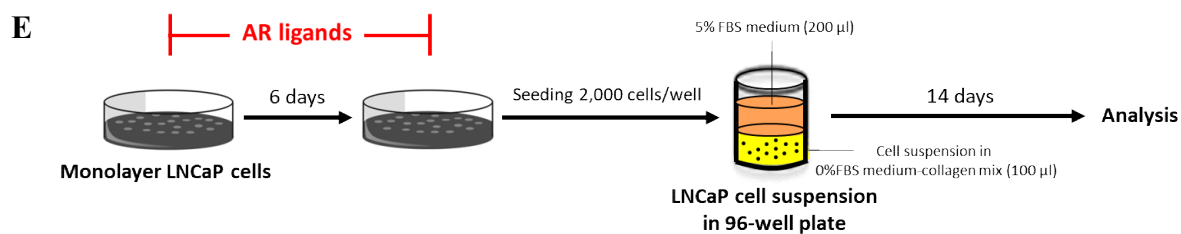
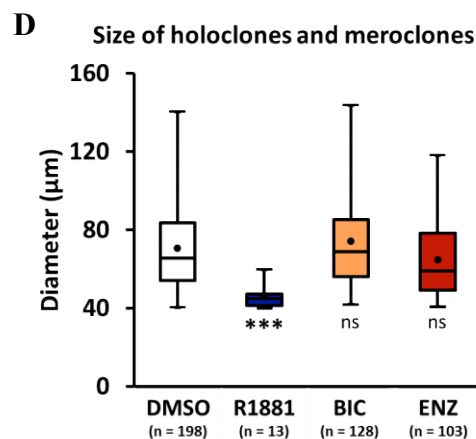
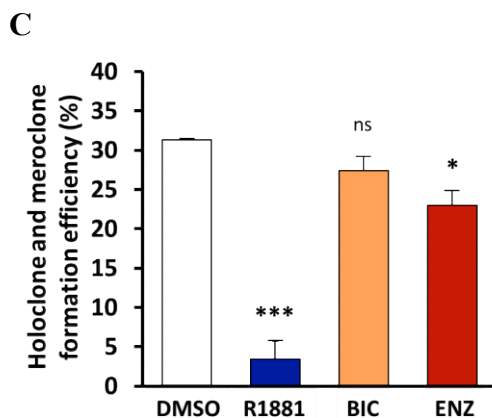
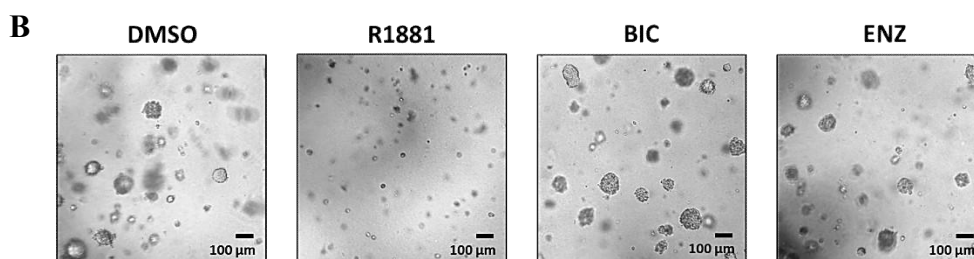
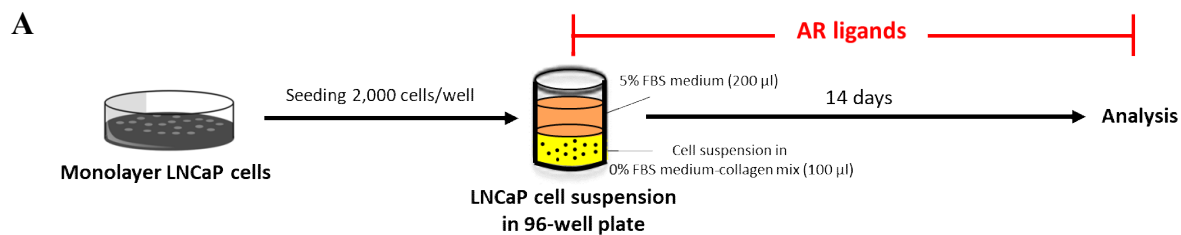


**Figure 14. Conditioned media do not affect LNCaP 3D colony formation.** (A) Illustration of experimental setup for (B-D). LNCaP cells were seeded in 0% FBS medium-collagen mix for 3D colony formation assays. The single cell suspension was treated for 14 days with Con. D as control, Con. R, Con. B, or Con. E. (B) Representative pictures after 14 days of colony formation. (C) Holoclone and meroclone formation efficiency (%) indicates the percentage of single cells from the seeding day that formed a colony with a diameter larger than 40  $\mu\text{m}$  at day 14. Bar graphs are shown as mean + SEM from four technical replicates ( $n = 4$ ) of two independent experiments. (D) Box and whisker plots compare the size of colonies larger than 40  $\mu\text{m}$  in diameter from both independent experiments. Box plots represent 50 percentiles, lines between box plot represent the median diameter, dots represent the mean diameter, and the end of each whisker line represents maximum and minimum diameter. Statistical analyses in (C) and (D) were performed by using one-way ANOVA followed by Dunnett's multiple comparisons test. ns, not significant.

#### 4.8 AR agonist suppresses 3D colony formation and reduces colony size

To examine the effect of AR ligands on holoclone and meroclone formation, 3D colony formation assays were conducted as illustrated in Figure 15A. The suspension of single cells was treated for 14 days with AR ligands. The results show that R1881 at SAL and ENZ suppressed colony formation efficiency (Figure 15B and C). Moreover, colonies derived from R1881 treatment exhibited significantly smaller size than the control (Figure 15D). Next, another experimental setup was performed as illustrated in Figure 15E. LNCaP monolayer was treated for 6 days with AR ligands. Thereafter, cells were seeded and cultured without ligand for 14 days. Interestingly, significant suppression of colony formation was observed only in R1881-pretreated condition (Figure 15F and G), but the size of generated colonies was similar to other treatments (Figure 15H). Notably, similar results to R1881 treatment were also observed in both experimental setups when using DHT at SAL (data not shown).

Taken together, both experimental setups reveal consistent results that SAL suppresses PCa holoclone and meroclone formation efficiency. Thus, it indicates that SAL reduces stemness, which is consistent with reduced expression of all analyzed stemness markers by SAL.



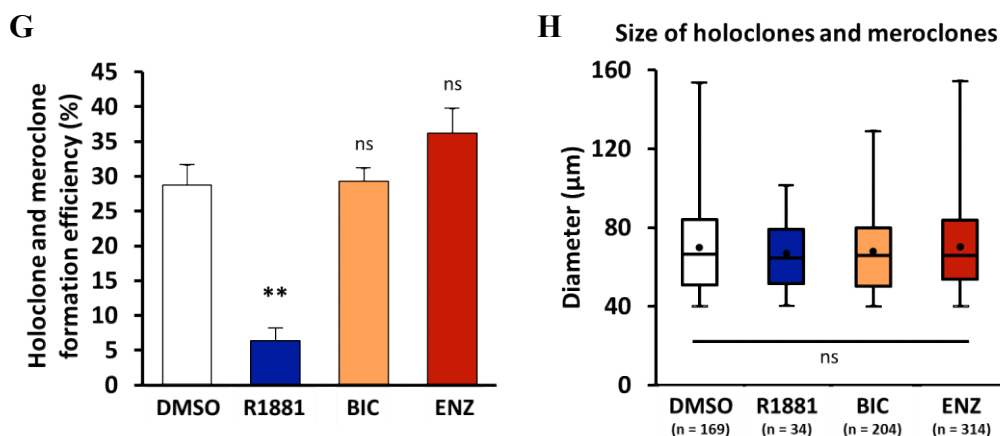
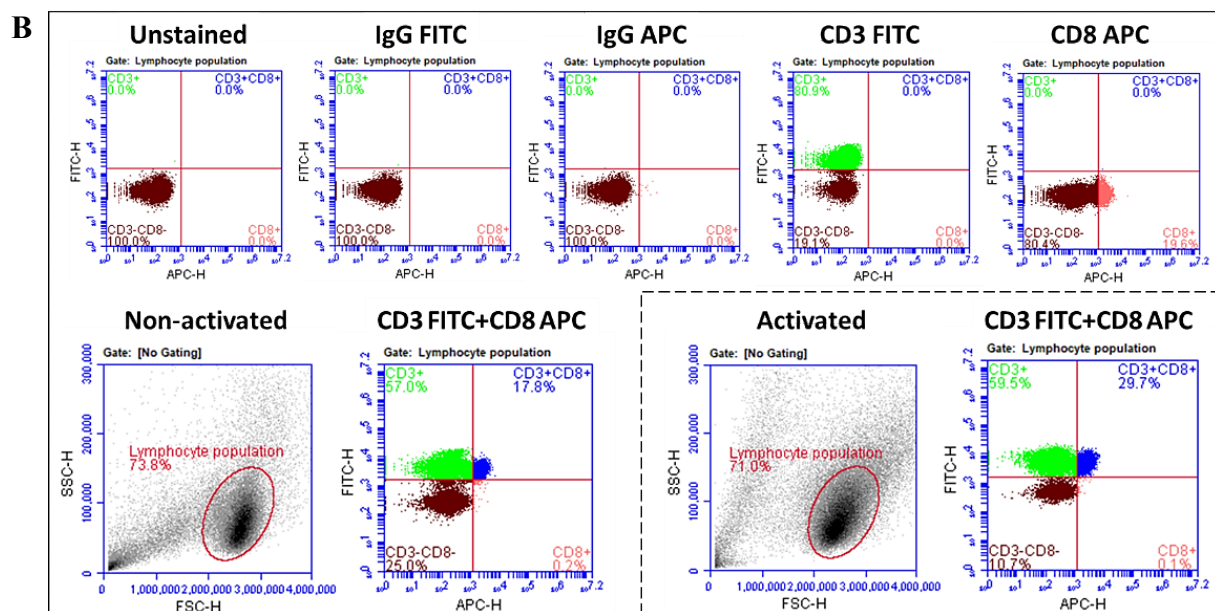
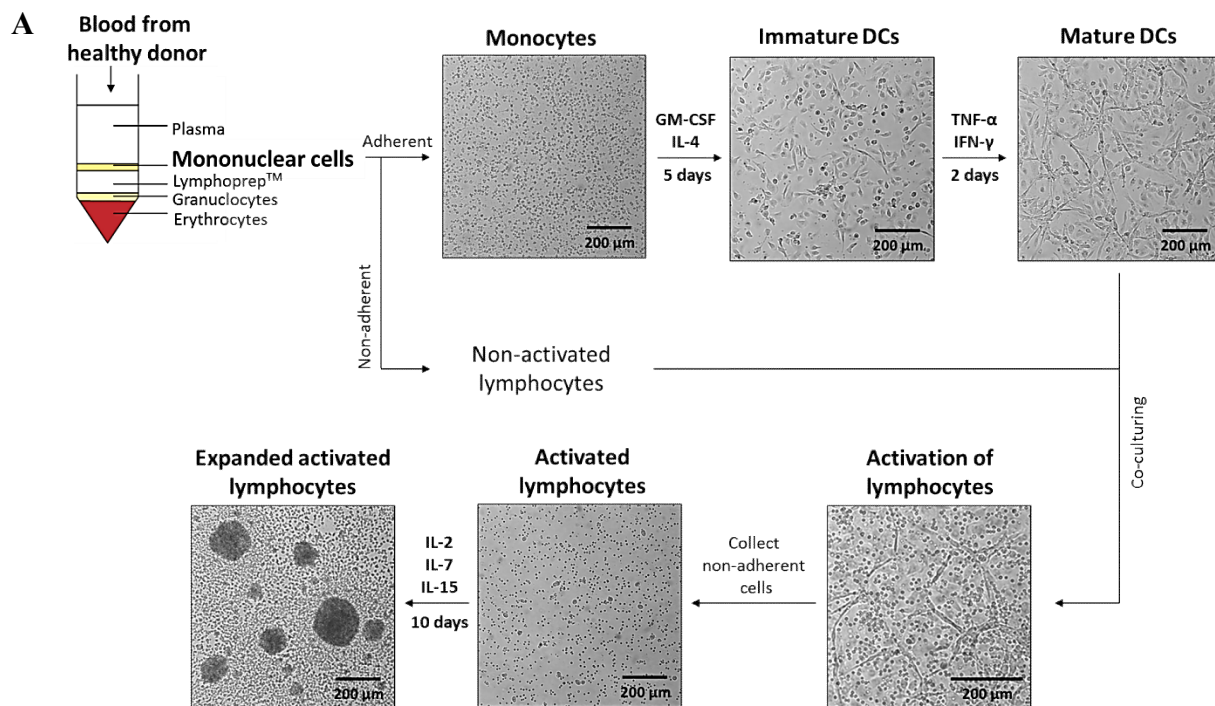


**Figure 15. SAL treatment suppresses LNCaP 3D colony formation.** (A) Illustration of experimental setup for (B-D). Similar experiments were performed as Figure 14 except that the single cell suspension was treated for 14 days with 0.1% DMSO as solvent control, 1 nM R1881, 1  $\mu$ M BIC, or 1  $\mu$ M ENZ. (B) Representative pictures after 14 days of treatment. (C) Holoclone and meroclone formation efficiency (%) indicates the percentage of single cells from the seeding day that formed a colony with a diameter larger than 40  $\mu$ m at day 14. Bar graphs are shown as mean + SEM from three independent experiments (N = 3). Statistical analysis was performed by using two-tailed unpaired t-test comparing holoclone and meroclone formation efficiency of each treatment to DMSO treatment. \*,  $p \leq 0.05$ ; \*\*,  $p \leq 0.01$ ; \*\*\*,  $p \leq 0.001$ ; ns, not significant. (D) Box and whisker plots compare the size of colonies larger than 40  $\mu$ m in diameter from all three independent experiments. Statistical analysis was performed by using one-way ANOVA followed by Dunnett's multiple comparisons test. \*\*\*,  $p \leq 0.001$ ; ns, not significant. (E) Illustration of experimental setup for (F-H). LNCaP monolayer was treated for 6 days with the same treatments and concentrations as (A-D). Thereafter, the cells were seeded and cultured for 14 days without AR ligands. (F) Representative pictures after 14 days of colony formation. (G) Holoclone and meroclone formation efficiency (%) and statistical analysis were calculated as in (C). (H) Box and whisker plots as well as statistical analysis were performed as in (D).

#### 4.9 SASP does not affect lymphocyte-mediated apoptosis

The secretome from AR ligand-treated cells revealed significant enriched GO terms for regulation of immunity (Table 4). It indicates that the induced SASP can influence immune system. Immune cell attraction leading to tumor cell clearance is probably the main tumor suppressive role of SASP (Rao and Jackson 2016, Saleh *et al.* 2018, Kang *et al.* 2011). Through immune cell surface receptors, immune cells can recognize SASP factors in the tumor microenvironment as well as cell surface antigens of tumor cells. Thus, the response of immune cells depends as well on the balance between immune-attractant and -suppressive SASP factors. This led to the hypothesis that distinct secretomes induced by AR ligands differentially influence immune cell response. In this study, the effect of lymphocyte-mediated cytotoxicity was analyzed with conditioned media-treated PCa cells. For that purpose, human

lymphocytes were isolated from blood samples of a healthy donor, activated, and clonal expanded *ex vivo* prior co-culturing with treated PCa cells (Figure 16A).





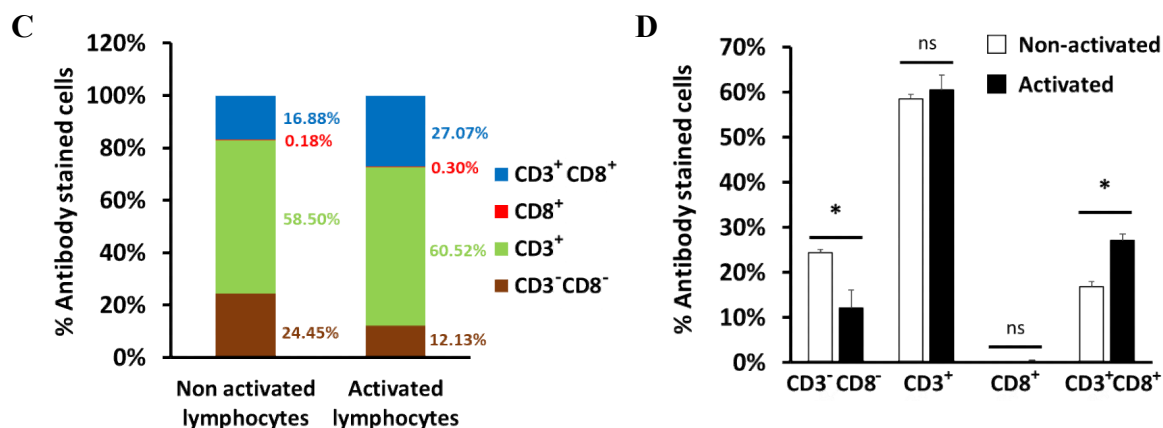


**Figure 16. Culturing and activation of human immune cells.** (A) Illustration of experimental setup for culturing and activation of immune cells adapted from Junking *et al.* (2017). Isolation of peripheral blood mononuclear cells (PBMCs) was performed with Lymphoprep™ solution. Adherent cells were cultured as monocytes and differentiated into mature dendritic cells (DCs) by treating with GM-CSF (50 ng/ml), IL-4 (25 ng/ml), TNF- $\alpha$  (50 ng/ml), and IFN- $\gamma$  (50 ng/ml). Non-adherent cells (non-activated lymphocytes) were activated by co-culturing with mature DCs. Activated lymphocytes were collected and further cultured (expanded) with IL-2 (20 ng/ml), IL-7 (10 ng/ml), and IL-15 (20 ng/ml) for 10 days. (B) Detection of CD3<sup>+</sup> and CD8<sup>+</sup> lymphocyte populations by flow cytometry. Detection intensity threshold was set according to unstained, IgG FITC, IgG APC, CD3 FITC, and CD8 APC stained populations. Green = CD3<sup>+</sup>; red = CD8<sup>+</sup>; blue = CD3<sup>+</sup>CD8<sup>+</sup>; brown = CD3<sup>-</sup>CD8<sup>-</sup>. (C) Percentage of CD3<sup>+</sup> and CD8<sup>+</sup> antibodies stained cells analyzed from flow cytometry data. Numbers indicates the mean percentage of 4 different populations within non-activated or activated lymphocytes populations. The mean percentage was calculated from three independent experiments (N = 3). (D) Separated histogram data from (C) as mean + SEM. Statistical analysis was performed by using two-tailed unpaired t-test comparing activated population to non-activated population. \*, p $\leq$ 0.05; ns, not significant.

Mononuclear cells were successfully isolated as monocytes (adherent cells) and non-activated lymphocytes (non-adherent cells) (Figure 16A). Differentiation of antigen presenting cells or mature dendritic cells (DCs) from monocytes was confirmed by morphological changes from spherical to a dendritic shape. These cells were used for activating lymphocytes by co-culturing. After that, activated lymphocytes were further cultured for clonal expansion, which was indicated by colony formation of lymphocytes (Figure 16A). Successful activation and clonal expansion were further confirmed by a significant increased proportion of CD3<sup>+</sup>CD8<sup>+</sup> cytotoxic T cells in the activated lymphocyte population (Figure 16B-D).

Next, lymphocyte-mediated killing assays of PCa cells were conducted by co-culturing conditioned media-treated LNCaP cells with activated lymphocytes. The ratio between lymphocytes and PCa cells as well as the incubation time were optimized based on

preliminary experiments (Supplemental Figure S5). Intracellular protein of PCa cells was extracted after co-culturing for 1.5 h with lymphocytes. c-PARP was successfully detected as an indication for lymphocyte-mediated apoptosis (Figure 17A). No c-PARP was detected when cells were not co-cultured with lymphocytes. This suggests that conditioned media alone do not trigger apoptosis in LNCaP cells. Surprisingly, no clear difference of c-PARP level was observed between Con. D-, Con. R-, and Con. E-treated LNCaP cells that were co-cultured with lymphocytes (Figure 17A). This suggests that conditioned media do not affect lymphocyte-mediated apoptosis. Furthermore, to analyze the LNCaP cell viability, crystal violet staining was performed after co-culturing for 6 h with lymphocytes (Figure 17B). The percentage of cell survival was calculated from crystal violet absorbance (Figure 17C). Consistent with detected c-PARP levels, similar crystal violet staining or percentage of cell survival was detected after co-culturing with lymphocytes. Thus, the results suggest that conditioned media do not affect lymphocyte-mediated killing of LNCaP cells.

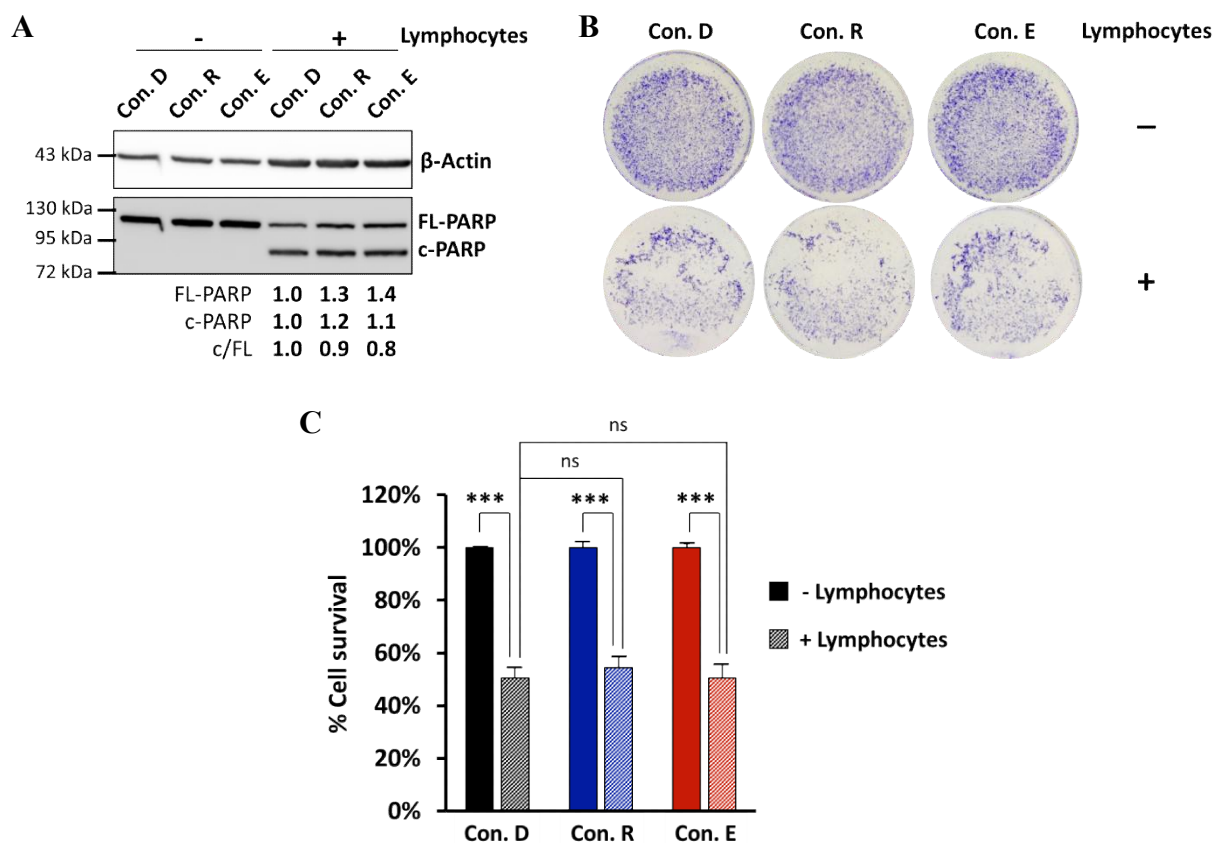


**Figure 17. Conditioned media do not affect lymphocyte-mediated apoptosis.** LNCaP cells were treated for 4 days with Con. D as control, Con. R, or Con. E. Thereafter, PCa cells were co-cultured

with or without activated lymphocytes in a ratio of 1:5 (PCa cells: lymphocytes). **(A)** Protein extraction was performed after co-culturing for 1.5 h. Detection of full length PARP (FL-PARP) and cleaved PARP (c-PARP) was conducted by Western blotting and normalized to  $\beta$ -Actin. Upper and middle numbers indicate normalized FL-PARP and c-PARP band intensities relative to Con. D+lymphocytes. Lower numbers indicate the ratios of c-PARP *versus* FL-PARP levels. **(B)** Representative pictures of crystal violet staining after co-culturing for 6 h. **(C)** Percentage of cell survival calculated from crystal violet absorbance (OD 590 nm). Cell survival without lymphocyte co-culture was set arbitrarily as 100%. Bar graphs are shown as mean + SEM from total of four technical replicates (n = 4) of two independent experiments. Statistical analysis was performed by using one-way ANOVA followed by Bonferroni's multiple comparisons test. \*\*\*,  $p \leq 0.001$ ; ns, not significant.

#### 4.10 SASP suppresses lymphocyte proliferation

The results from GO analysis also suggest that the induced SASP of AR ligand-treated PCa cells regulate lymphocyte proliferation (Table 4). Moreover, this particular GO term was significantly enriched by all sets of secreted cytokines from treated LNCaP, but not by all sets of C4-2 cells. Hence, the hypothesis was that the SASP of AR ligand-treated LNCaP cells may have more impact to the lymphocyte proliferation than the SASP of C4-2 cells. To verify this hypothesis, lymphocytes were treated with conditioned media during activation and clonal expansion. Similar experiments were conducted as described in Figure 16A except that Con. D, Con. R, and Con. E were used. Moreover, during clonal expansion with conditioned media, lymphocytes were also treated with or without IL-2, -7, and -15. Note that, addition of these three cytokines is recommended during lymphocyte clonal expansion in the original protocol (Figure 16A; Junking *et al.* 2017), since they promote proliferation, survival and differentiation of lymphocytes (Rochman *et al.* 2009).

A clear difference was observed during clonal expansion between with and without IL-2, -7, and -15 (Figure 18A; Supplemental Figure S6A). Lymphocytes formed colonies as an indication of clonal expansion/proliferation due to addition of these three cytokines as expected. No colony formation was observed without addition of these cytokines even the cells were treated with conditioned media. This indicates that IL-2, -7, and -15 are sufficient for lymphocyte clonal expansion/proliferation.

Focusing on lymphocytes that were co-treated with the three cytokines and conditioned media, lymphocyte colonies cultured in either LNCaP Con. R or Con. E had significantly smaller size than Con. D (Figure 18A and B). The effect was observed after 6 days of clonal expansion.



Similar results were observed in another independent experiment (Supplemental Figure S6A and B). These data suggest that conditioned medium collected from either R1881- or ENZ-treated LNCaP cells suppresses lymphocyte proliferation. Notably, neither colony formation nor colony size was affected by conditioned media of C4-2 cells (Figure 18A and C). Therefore, it supports the notion that SASP of AR ligand-treated LNCaP cells have more impact on the lymphocyte proliferation than SASP of C4-2 cells.

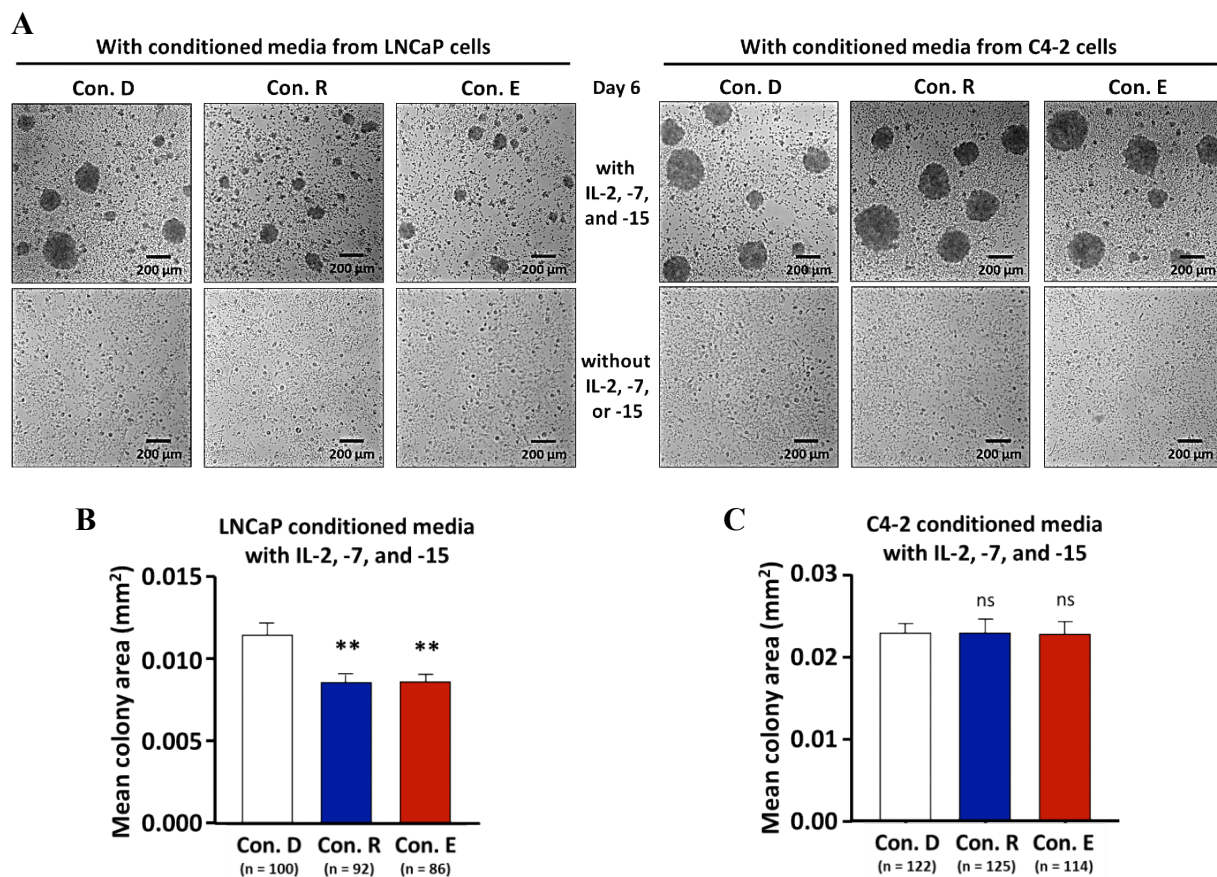


**Figure 18. Con. R and Con. E of LNCaP cells suppress lymphocyte clonal expansion.** Activation and clonal expansion of lymphocytes were performed as illustrated in Figure 16A except that Con. D as control, Con. R, and Con. E were used. Furthermore, during clonal expansion, activated lymphocytes were treated with or without IL-2, -7, and -15. **(A)** Representative pictures of lymphocyte colonies after 6 days of conditioned media with or without IL-2, -7, and -15 co-treatment. **(B and C)** Mean area of lymphocyte colonies after 6 days of clonal expansion with **(B)** LNCaP's conditioned media or **(C)** C4-2's conditioned media with IL-2, -7, and -15 treatment. Measured values from conditions without IL-2, -7, and -15 treatments were used for setting the threshold and therefore, area below 0.005 mm<sup>2</sup> was considered as background (data not shown). Bar graphs show mean area + SEM calculated from colonies that exhibited an area equal to or above 0.005 mm<sup>2</sup> with indicated number of colonies (n). Statistical analyses in **(B)** and **(C)** were performed by using one-way ANOVA followed by Dunnett's multiple comparisons test. \*\*, p<0.01; ns, not significant.

The results of GO analysis were further analyzed to identify possible cytokines associated with the observed effect of lymphocyte proliferation. Since lymphocyte proliferation was suppressed by either Con. R or Con. E of LNCaP cells, it may be explained by an overlapping SASP secretome of agonist- and antagonist-treated LNCaP cells. Hence, cytokines that the secretion was oppositely altered by agonist and antagonist are excluded. According to the list of secreted cytokines that enriched in the GO term “regulation of lymphocyte proliferation” (Supplemental Table S1), 6 candidates may be involved. This includes gp130, IGF-1, Leptin, RANTES, TGF  $\beta$ 1, and IGFBP-2. The secretion of the first five cytokines was enhanced by R1881 and ENZ, whereas the secretion of IGFBP-2 was suppressed (Supplemental Table S1). The data suggest that suppression of lymphocyte proliferation by conditioned media might be mediated by but not limited to these secreted cytokines. Secreted cytokines which were affected by R1881 or ENZ alone should not be excluded.

Taken together, the results indicate that conditioned media from AR ligand-treated LNCaP cells suppress lymphocyte proliferation. These data suggest immunosuppressive consequence from AR ligand-induced cellular senescence.

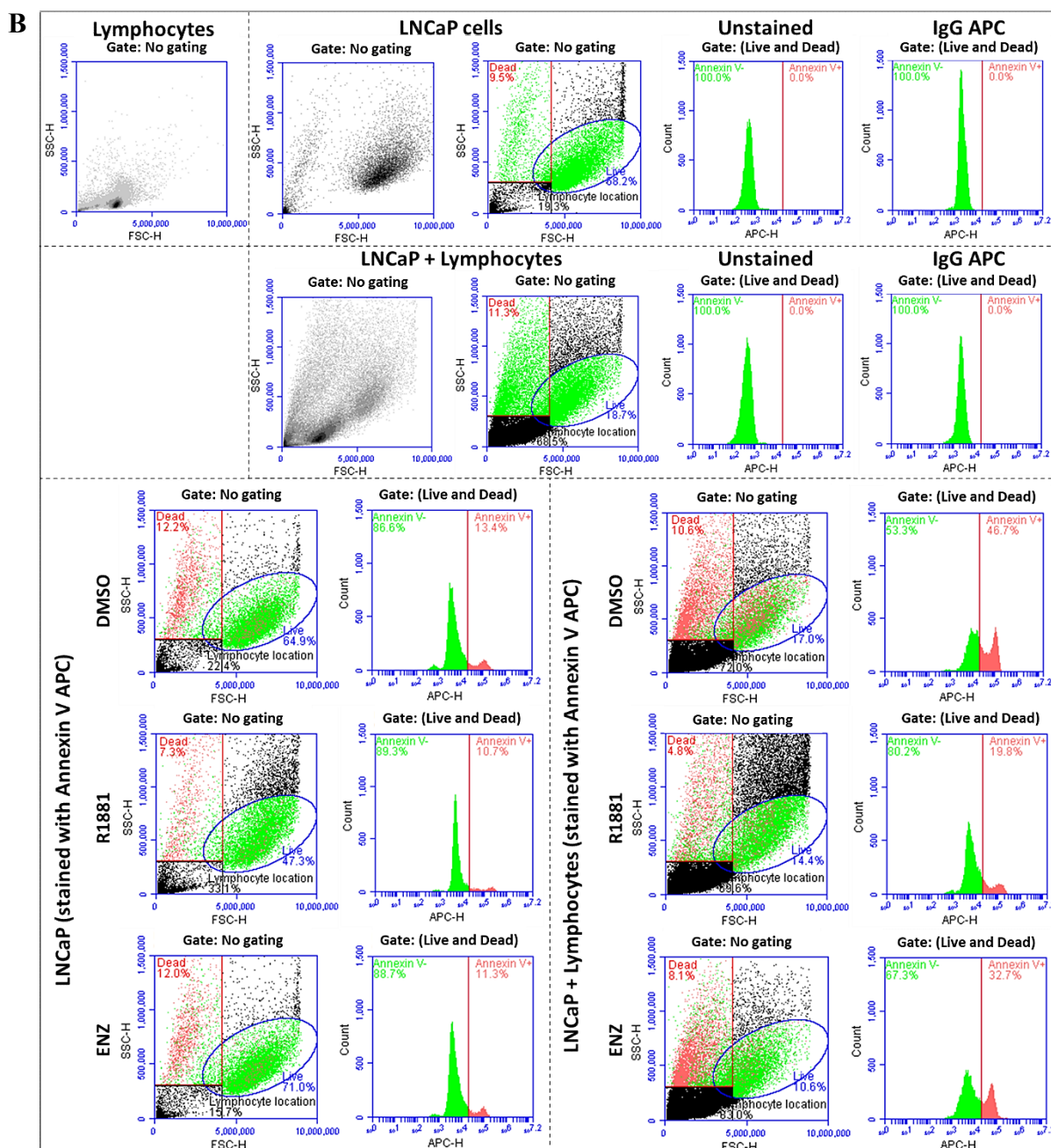
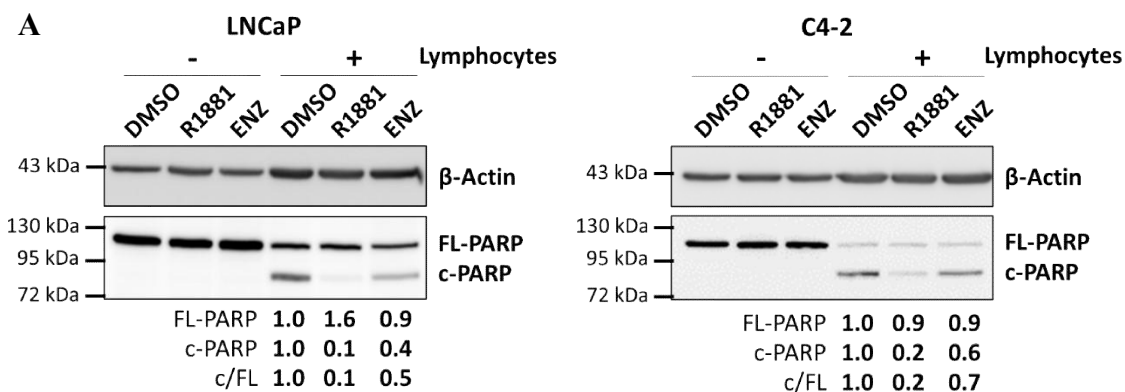
#### **4.11 Treatment with AR ligands renders PCa cells resistant to lymphocyte-mediated apoptosis**

Immunotherapy has become more popular in the clinic-oriented research field as option for fighting against cancer. However, it seems that PCa exhibits some mechanisms of immunosuppression to limit the effectiveness of therapy (Boettcher *et al.* 2019, Kwon *et al.* 2014). This thesis showed that lymphocyte proliferation can be suppressed by conditioned media derived from AR ligand-induced cellular senescent cells. Interestingly, it has been suggested that senescent cells activate pro-survival/anti-apoptotic signaling, leading to apoptotic resistance (Wong *et al.* 2018, Salminen *et al.* 2011). This led to the hypothesis that AR ligand-induced cellular senescent PCa cells are also resistant to lymphocyte-mediated cytotoxicity. To examine this, lymphocyte-mediated killing assays of PCa cells were conducted by co-culturing AR ligand-pretreated cells with activated lymphocytes.

Expression of c-PARP was successfully detected in both LNCaP and C4-2 cells as an indication for apoptosis mediated by activated lymphocytes after 1.5 h of co-culturing (Figure 19A). c-PARP was not detected in AR ligand-treated cells that were not co-cultured with lymphocytes. This confirms earlier data that AR ligand itself does not induce apoptosis. Interestingly, AR ligand-treated cells that were co-cultured with lymphocytes exhibited less c-PARP level than the DMSO-treated cells (Figure 19A). Thus, the data indicate that AR ligand-treated PCa cells are resistant to lymphocyte-mediated apoptosis.

This finding was also confirmed by results obtained from flow cytometry, where Annexin V stained LNCaP cells were detected after co-culture with lymphocytes for 3 h (Figure 19B and C). Without lymphocytes, a low percentage of Annexin V stained cells was detected at similar level between treatments. This possibly represents a basal apoptotic level. However, it was significantly increased by the presence of lymphocytes (Figure 19B and C). Importantly, both R1881- and ENZ-treated population had significantly less Annexin V stained cells than DMSO-treated population after co-culture. Thus, the data support the notion that AR ligand-treated PCa cells are resistant to lymphocyte-mediated apoptosis.

Resistance of apoptosis might result in better survival. To analyze PCa cell viability after co-culturing with lymphocytes, crystal violet staining was performed after co-culture for 6 h (Figure 19D). The percentage of cell survival was calculated from crystal violet absorbance (Figure 19E). Cell survival of LNCaP populations without lymphocyte co-culture was considered as 100%. As expected, the percentage of LNCaP cell survival was reduced after lymphocyte co-culture. This reflects that the LNCaP cells were killed by lymphocytes. Consistent with detected c-PARP and Annexin V, SAL-treated LNCaP cells showed a higher percentage of cell survival than control-treated cells (Figure 19E). Similar outcome was also observed in C4-2 cells (data not shown). Thus, the data confirm that SAL-treated PCa cells are resistant to lymphocyte-mediated apoptosis. Surprisingly, cell survival of ENZ-treated cells was similar to control-treated cells (Figure 19E). This result indicates that the earlier observed apoptotic resistance in ENZ-treated cells could not sustain 6 h of co-culturing with lymphocytes. Therefore, it also demonstrates that the resistance of ENZ-treated cells does not last as long as SAL-treated cells.



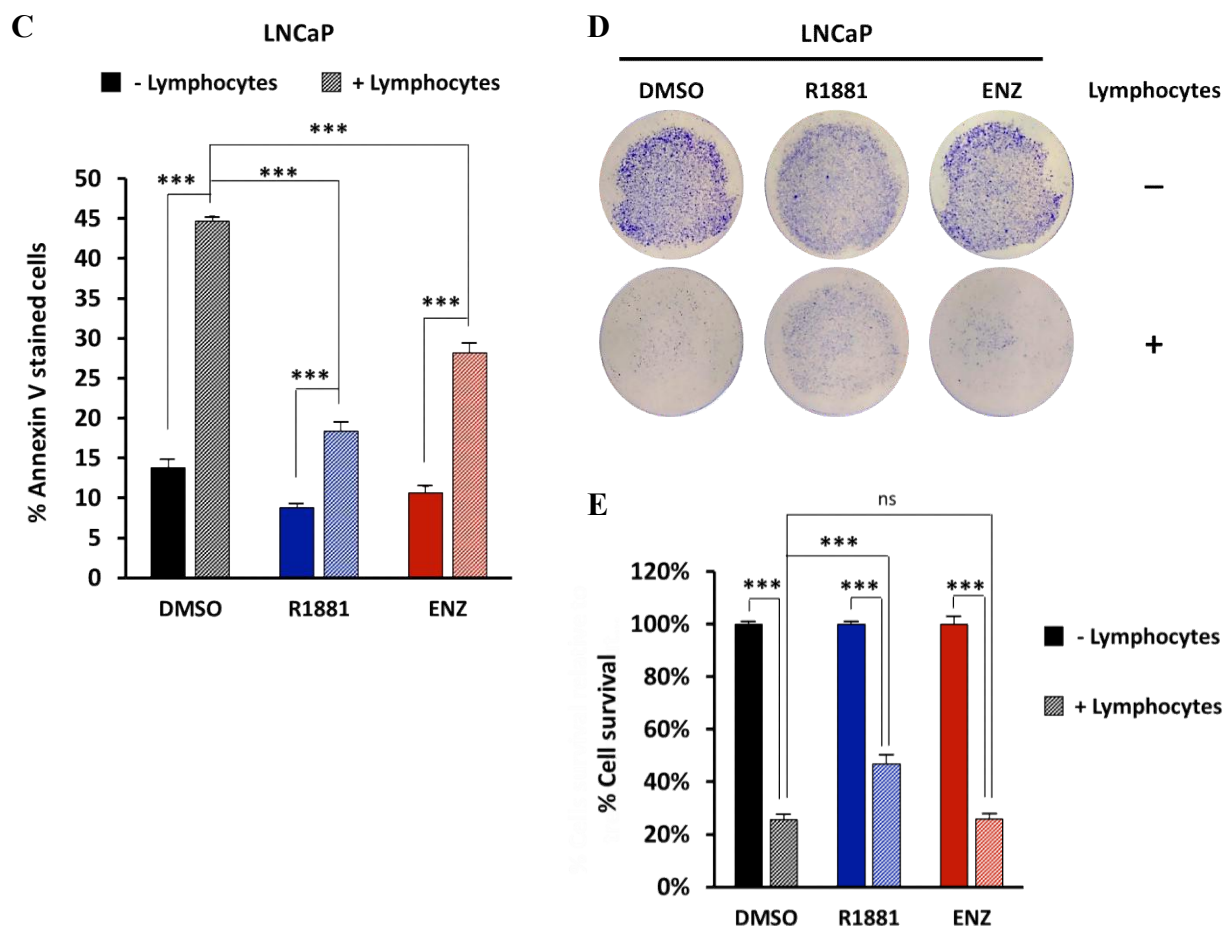


**Figure 19. AR ligand-induced cellular senescent PCa cells are resistant to lymphocyte-mediated apoptosis.** LNCaP and C4-2 cells were treated for 72 h with 1 nM R1881, 1  $\mu$ M ENZ, or 0.1% DMSO as solvent control. Thereafter, PCa cells were co-cultured with or without activated lymphocytes in a ratio of 1:5 (PCa cells: lymphocytes). **(A)** Protein extraction was performed after co-cultured for 1.5 h. Detection of full length PARP (FL-PARP) and cleaved PARP (c-PARP) was conducted by Western blotting and normalized to  $\beta$ -Actin. Upper and middle numbers indicate normalized FL-PARP and c-PARP band intensities relative to DMSO+lymphocytes. Lower numbers indicate the ratios of c-PARP versus FL-PARP levels. **(B)** Detection of Annexin V stained LNCaP cells was performed by flow cytometry after co-cultured for 3 h. LNCaP and lymphocytes populations were first identified for correct gating. Detection intensity threshold was set according to unstained and IgG APC stained populations (green = Annexin V negative; red = Annexin V positive). **(C)** Percentage of Annexin V stained LNCaP cells analyzed from the data of flow cytometry. Bar graphs are shown as mean + SEM from six technical replicates ( $n = 6$ ) of two independent experiments. **(D)** Representative pictures of crystal violet staining after co-cultured for 6 h. **(E)** Percentage of cell survival calculated from crystal violet absorbance (OD 590 nm). Cell survival without lymphocyte co-culture was set arbitrarily as 100%. Bar graphs are shown as mean + SEM from total of six technical replicates ( $n = 6$ ) of three independent experiments. Statistical analyses in (C) and (E) were performed by using one-way ANOVA followed by Bonferroni's multiple comparisons test. \*\*\*,  $p \leq 0.001$ ; ns, not significant.

#### 4.12 Induction of cellular senescence by AR ligands is associated with enhanced phosphorylation level of the pro-survival/anti-apoptotic factor AKT

This thesis reveals that treatment with AR ligands induces cellular senescence and also renders PCa cells resistant to lymphocyte-mediated apoptosis. Interestingly, an apoptotic resistance is one of the hallmark features of senescent cells (Salminen *et al.* 2011). The capability of senescent cells to resist cell death is due to activation or upregulation of pro-survival/anti-apoptotic pathways. Our group has previously reported that AKT, a pro-survival/anti-apoptotic factor, is activated in SAL-induced cellular senescent PCa cells (Roediger *et al.* 2014). This led to the hypothesis that AKT is also activated by ENZ.

To address this, LNCaP cells on one hand were treated for 72 h with SAL and ENZ as senescence-induced condition. On the other hand, cells were treated with low androgen level (LAL) and DMSO as control. Intracellular protein level of phospho-AKT (p-AKT) was analyzed by Western blotting. Note that phosphorylation of AKT is an indication for AKT activation (Balasuriya *et al.* 2020). The results show that p-AKT level and p-AKT/AKT ratio were induced by SAL but not LAL (Figure 20). This confirms the data of Roediger *et al.* (2014) and indicates that an activation of AKT is specific to androgen treatment at SAL. Interestingly, induced p-AKT level and the p-AKT/AKT ratio were also detected in ENZ-treated cells (Figure 20; Supplemental Figure S7). Thus, the data indicate that both SAL and ENZ activate AKT, which may serve as a common pro-survival/anti-apoptotic factor in AR ligand-induced cellular senescent PCa cells.

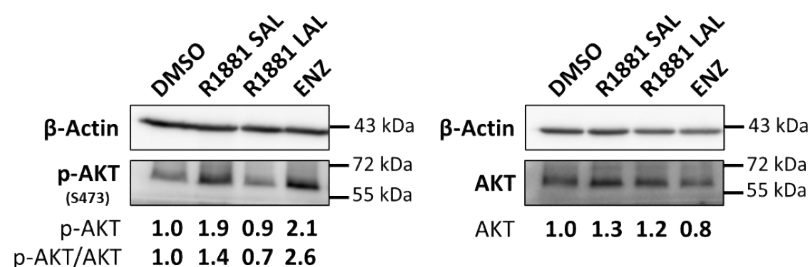


**Figure 20. AR ligands induce the phosphorylation level of the pro-survival/anti-apoptotic factor AKT.** LNCaP cells were treated for 72 h with 1 nM R1881 (SAL), 1 pM R1881 (LAL), 10  $\mu$ M ENZ, or 0.1% DMSO as solvent control. Protein extraction and Western blotting were performed to analyze protein levels of AKT and phosphorylated AKT (p-AKT) at serine 473 (S473).  $\beta$ -Actin served as loading control. Numbers indicate normalized pan-Akt or Akt band intensities relative to DMSO control. Ratio of p-AKT versus AKT levels was also calculated.



#### **4.13 AR antagonist- and agonist-treated PCa cells are preferentially sensitive to apoptosis induction by AKT and HSP90 inhibitors: Analysis of potential senolytic compounds**

So far, this study shows that although AR ligands induce cellular senescence in PCa cells, the treatment of these ligands alone might not be beneficial, because both AR ligands and the induced SASP can mediate immunosuppressive effects. Moreover, SASP of antagonist-treated cells can promote PCa cell proliferation. Therefore, this study also aimed to analyze some inhibitors of pro-survival/anti-apoptotic factor as potential senolytic compounds for eliminating AR ligand-induced cellular senescent cells.

Since the pro-survival/anti-apoptotic factor AKT is activated in AR ligand-treated PCa cells, it was hypothesized that inhibitors of AKT can serve as a senolytic compound. To examine this, LNCaP cells were first treated with AR ligands to induce cellular senescence and subsequently treated with the AKT inhibitor MK2206 (MK). AR is required for androgen-sensitive PCa cell survival (Yang *et al.* 2005) and it is known that both AR and AKT are stabilized by HSP90 (Centenera *et al.* 2015, Zhang *et al.* 2005). Thus, AR ligand-pretreated cells were also treated with HSP90 inhibitor Ganetespib (GT), a compound used in clinical trials for cancer therapy. HSP90 inhibitor GT has been suggested to induce apoptosis in senescent cells (Fuhrmann-Stroissnigg *et al.* 2017, 2018). Hence, it was also hypothesized that GT can serve as a senolytic compound for AR ligand-induced cellular senescent PCa cells.

Preliminary data indicates that both compounds inhibited LNCaP cell proliferation (data not shown) through apoptosis in a concentration dependent manner (Supplemental Figure S8). An induction of c-PARP by MK was detected after 24 h and by GT after 48 h of treatment. Hence, these time points were used and the optimized concentration of these inhibitors (1  $\mu$ M for MK and 25 nM for GT) were applied to AR ligand-treated cells.

Focusing first on the effect of the HSP90 inhibitor, GT treatment significantly enhanced c-PARP level in the cells that were pretreated with SAL (Figure 21A and B). An enhanced detachment of cells and a significant reduced percentage of SA  $\beta$ -Gal positive cells were observed by GT in SAL-pretreated cells (Supplemental Figure S9). In case of ENZ-pretreated cells, slightly induced c-PARP was detected but not significantly pronounced compared to

control-pretreated cells (Figure 21A and B). These data indicate a senolytic activity of GT preferentially for SAL-treated cells.

MK is a highly selective allosteric AKT inhibitor and has never been identified as a senolytic agent before. Interestingly, MK-induced c-PARP in SAL-pretreated cells is significantly less pronounced than in control-pretreated cells (Figure 21A and B). This result suggests that SAL-treated cells are resistant to MK-induced apoptosis. In contrast, the c-PARP level in ENZ-pretreated cells is significantly higher than in control (Figure 21A and B). MK-enhanced cell detachment was also observed in ENZ-pretreated cells (Supplemental Figure S10A). These data suggest that the ENZ-treated cells are sensitive to MK-mediated apoptosis.

Surprisingly, no reduction of SA  $\beta$ -Gal positive cells by MK was observed in ENZ-pretreated condition (Supplemental Figure S10B and C). Note that an increased SA  $\beta$ -Gal level was also observed after MK treatment in solvent-pretreated cells, which suggests that MK can also induce cellular senescence. This indication is in line with a previous study conducted by Xie *et al.* (2018). The data altogether lead to the hypothesis that MK on one hand triggers apoptosis and detachment of ENZ-induced cellular senescent cells, while on the other hand it induces cellular senescence in the remaining adherent cells (Supplemental Figure S10D). Thus, these dual activities might explain a compensated level of SA  $\beta$ -Gal staining.

Taken together, these data suggest a novel role of the AKT-inhibitor MK as a senolytic agent for AR antagonist-treated LNCaP cells, whereas GT can be used for eliminating SAL-induced cellular senescent LNCaP cells.

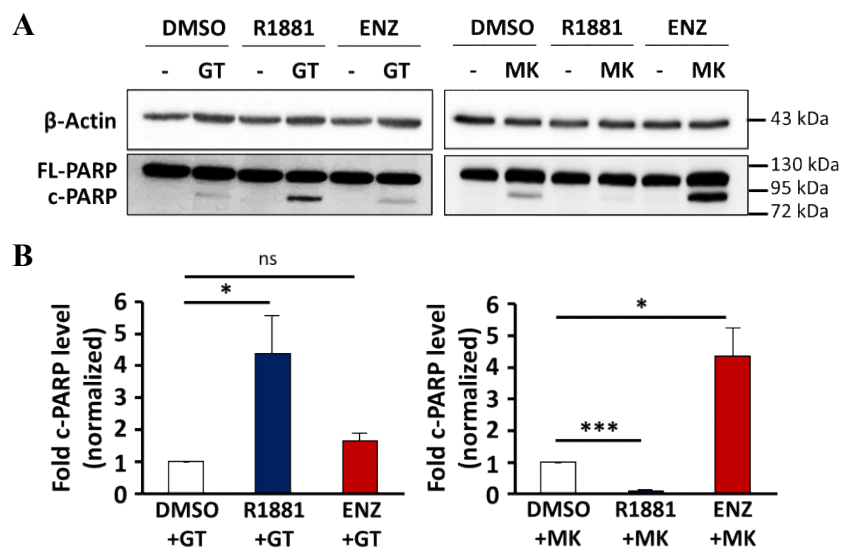




**Figure 21. Targeting senescent LNCaP cells with senolytic compounds.** LNCaP cells were treated for 72 h with 1 nM R1881, 10  $\mu$ M ENZ, or 0.1% DMSO as solvent control. After that, the AR ligands were removed, replaced by fresh medium with 25 nM Ganetespib (GT), 1  $\mu$ M MK2206 (MK), or 0.1% DMSO, and further incubated for additional 24 h for MK and 48 h for GT. **(A)** Protein extraction and Western blotting were performed to detect FL-PARP and c-PARP.  $\beta$ -Actin served as loading control. **(B)** Quantification of fold c-PARP levels normalized to  $\beta$ -Actin from Western blotting data. Values obtained from DMSO+GT and DMSO+MK were set arbitrarily as 1. Bar graphs are shown as mean + SEM from three independent experiments (N = 3). Statistical analysis was performed by using two-tailed unpaired t-test comparing each treatment to DMSO+inhibitor treatment. \*,  $p \leq 0.05$ ; \*\*\*,  $p \leq 0.001$ ; ns, not significant. These figures have been published by Pungsrinont *et al.* (2020).

#### **4.14 AR ligands differentially regulate phosphorylation of ribosomal S6 protein, a downstream target of the pro-survival/anti-apoptotic AKT signaling**

Despite an activation of AKT by SAL and ENZ, different senolytic effects by MK or GT were observed between SAL- and ENZ-treated cells. Thus, the hypothesis was that downstream signaling of AKT might be differentially regulated by AR ligands. To address this, protein levels of AR, p-AKT, AKT, downstream target of AKT signaling such as ribosomal S6 (S6) and its phosphorylated form (p-S6) were analyzed.

Interestingly, without treatment of MK or GT, the results show that both AR ligands upregulate p-AKT level but differentially regulate the downstream target of AKT signaling (Figure 22). On one hand, induction of p-S6 level was observed after SAL treatment. On the other hand, p-S6 level was not enhanced by ENZ. This suggests a distinction between AR agonist- and antagonist-induced cellular senescence. Importantly, it also implies that the AKT-S6 pathway is more active in SAL-treated cells.

Focusing on the effects of MK, it potently inhibited p-AKT level in all conditions (Figure 22). A strong reduction of p-S6 level by MK was observed in either ENZ- or solvent-pretreated cells, indicating that MK potently inhibited the AKT signaling in these cells. However, an inhibition of p-S6 level in ENZ-treated cells was not clearly distinct from control-treated cells. This suggests that other downstream targets of AKT might be involved in apoptotic sensitivity of ENZ-treated cells towards MK. Decreased p-S6 level by MK was also observed in SAL-pretreated cells when compared to without MK, but surprisingly, the p-S6 level still remained high (Figure 22). This remained p-S6 level suggests that activation of the AKT downstream target like p-S6 was not fully inhibited by MK. It also indicates that the p-S6 might be partly regulated by AR ligand independent of AKT phosphorylation. Interestingly, studies showed

that the p-S6 itself, besides AKT, may be a critical pro-survival/anti-apoptotic factor (Jeon *et al.* 2008, Wittenberg *et al.* 2016). This might explain how SAL-induced cellular senescent LNCaP exhibited resistance towards MK.

As expected, the protein level of AR as a HSP90 client was reduced by GT (Figure 22; Supplemental Figure S8). GT inhibited also AKT signaling. Downregulation of AKT, p-AKT, and p-S6 protein levels by GT were observed (Figure 22). Interestingly, a reduced p-AKT level by GT was not as potent as by MK, but the p-S6 level was strongly reduced by GT. This effect was observed even in SAL-pretreated cells. It shows that p-S6 was more effectively inhibited by GT than by MK. Assuming that the survival of SAL-treated cells depends on upregulated p-S6 levels, GT-inhibited p-S6 level will lead to potent apoptosis induction. This might explain the sensitivity of SAL-induced cellular senescent cells towards GT treatment.

Together, these results show that SAL and ENZ differentially regulate pro-survival/anti-apoptotic signaling, in which AKT-S6 pathway is more active in SAL-treated cells. The regulation of p-S6 level can explain the distinct observed situations between apoptosis induction by MK and GT in SAL-pretreated cells. Other downstream targets of AKT might be involved in apoptotic sensitivity of ENZ-treated cells towards MK.

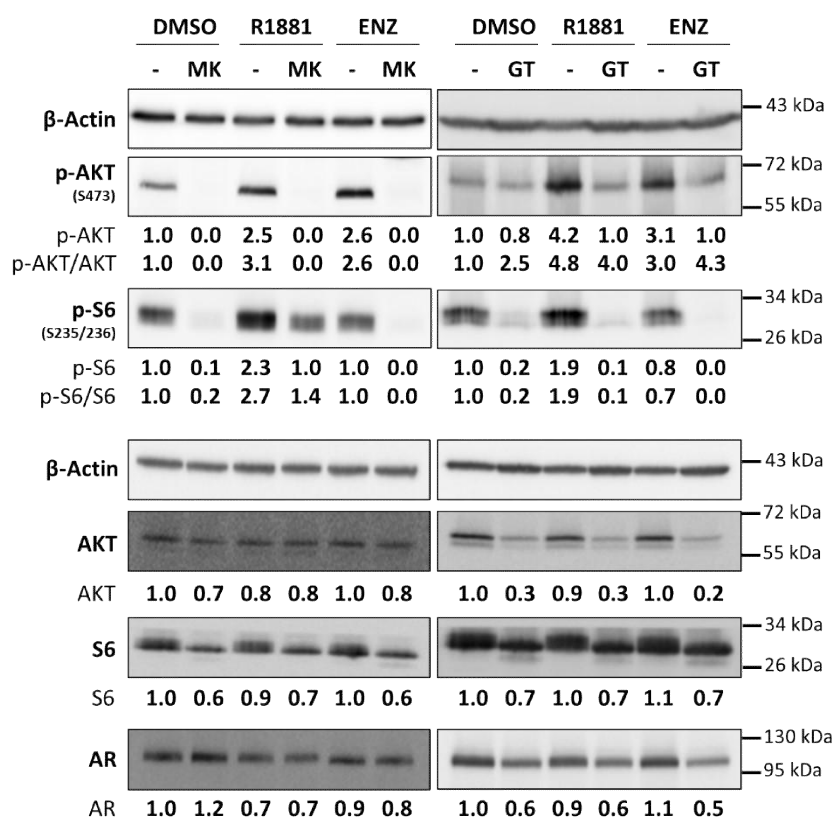


**Figure 22. AR agonist and antagonist differentially regulate pro-survival/anti-apoptotic signaling AKT-S6.** Similar experiments were performed as described in Figure 21. Detection of phospho-AKT (p-AKT), phospho-S6 (p-S6), AKT, S6, and AR was performed by Western blotting and normalized to  $\beta$ -Actin levels. For AR, AKT and S6, numbers indicate normalized band intensities relative to DMSO control. For p-AKT and p-S6, upper numbers indicate normalized band intensities relative to DMSO control and lower numbers indicate ratio of phosphorylated versus total protein levels. This figure has been published by Pungsrinont *et al.* (2020).

Taken all results together, this thesis shows that AR agonist at SAL and antagonists including the clinically used ENZ inhibit PCa cell proliferation via induction of cellular senescence. Interestingly, SAL- and ENZ-induced cellular senescent PCa cells possess distinct SASP secretomes. The data show that secreted levels of some SASP factors are associated with AR ligand-controlled transcription, while some are not and may be regulated at a non-genomic level by AR ligands. Bioinformatic analyses indicate that some AR ligand-induced SASP factors can regulate cell proliferation and immune responses. Initially, it seems that SAL may provide more advantages than antagonists, because the results show that the SASP of SAL-treated cells suppresses, but the SASP of antagonist-treated cells promotes LNCaP cell proliferation. Moreover, a reduced PCa stemness by SAL but not by antagonists was observed. However, further data suggest some immunosuppressive effects mediated by both AR ligands and the induced SASP. Unfortunately, both SAL- and ENZ-treated PCa cells are resistant to lymphocyte-mediated apoptosis, and the induced SASP can suppress lymphocyte proliferation. Thus, treatment of these ligands may provide long-term disadvantages in PCa therapy. Interestingly, this study suggests activated AKT as an underlying mechanism for apoptotic resistance of both SAL- and ENZ-treated cells, but through distinct AKT downstream signals. This different regulation preferentially sensitizes cells to a specific senolytic compound. ENZ-treated cells are sensitive to apoptosis induction by AKT inhibitor MK, and SAL-treated cells are sensitized by HSP90 inhibitor GT-induced apoptosis. Thus, the data suggest that it may be a useful strategy to combine AR ligand treatment with senolytic compounds. In line with this, AKT inhibitor with AR antagonist or HSP90 inhibitor with SAL treatment may be beneficial therapeutic options for PCa.

## 5 DISCUSSION

The AR represents a major drug target for PCa treatment. Our group has previously shown that AR agonist at SAL, 1<sup>st</sup> generation of AR antagonist BIC, and other AR antagonist-like compounds induce cellular senescence in PCa cells (Roediger *et al.* 2014, Esmaeili *et al.* 2016a, Hessenkemper *et al.* 2014, Roell *et al.* 2019, Fousteris *et al.* 2010). Cellular senescence is defined as an irreversible cell cycle arrest (Campisi 2001, Campisi and d'Adda di Fagagna 2007). Thus, AR ligand-induced cellular senescence seems to meet the main objective for suppressing PCa proliferation. However, senescent cells are metabolically active and known to exhibit SASP. It can mediate paracrine effects on neighboring cells and may act as either tumor promoter or suppressor (Gonzalez-Meljem *et al.* 2018, Lecot *et al.* 2016). Surprisingly, the SASP from AR ligand-mediated cellular senescence has not been studied. Therefore, the aims of this study were to analyze the composition of SASP secretome of AR ligand-treated PCa cells and to highlight functional effects of SASP on PCa and immune cells. Given the fact that SASP may act as tumor promoter, this study aimed also to analyze senolytic compounds in order to eliminate senescent cells by targeting pro-survival/anti-apoptotic pathways.

### 5.1 AR ligands induce cellular senescence leading to distinct SASP secretomes

This study confirms the previous studies that SAL and BIC induce cellular senescence in PCa cells. It is, however, the first study showing that cellular senescence is induced by the 2<sup>nd</sup> generation of AR antagonist ENZ (Pungsrinont *et al.* 2020), which is clinically used to treat PCa patients. An induction of SA  $\beta$ -Gal and a well-known senescence key regulator p16<sup>INK4a</sup> by ENZ were detected. Notably, SAL- and other antagonist-induced cellular senescence are also accompanied by an induction of p16<sup>INK4a</sup> level (Roediger *et al.* 2014, Hessenkemper *et al.* 2014, Esmaeili *et al.* 2016a, Gupta *et al.* 2020). Thus, it seems that p16<sup>INK4a</sup> is a central marker and regulator for AR ligand-mediated cellular senescence. Along with induction of SA  $\beta$ -Gal and p16<sup>INK4a</sup> expression, some cell cycle promoters were downregulated after AR ligand treatment, being in line with the observed inhibition of cell proliferation.

Interestingly, AR antagonists BIC and ENZ have been reported to trigger apoptosis in PCa cells (Wellington and Kearn 2006, Rodriguez-Vida *et al.* 2015). However, an induced c-PARP protein and an enhanced percentage of Annexin V positive cells were not detected after

treatment with either antagonist or SAL in the used cell lines. These data suggest that AR ligands do not induce apoptosis in these cells. Therefore, the data demonstrate that an inhibition of cell proliferation observed in this study is a consequence of AR ligand-induced cellular senescence.

It has been shown that secretory phenotypes can be altered when different senescence-inducing stimuli are used (Basisty *et al.* 2020, Coppé *et al.* 2010, Rao and Jackson 2016). In this thesis, the data of cytokine arrays show that SAL- and ENZ-induced cellular senescent PCa cells possess distinct SASP secretomes. Interestingly, AR is a nuclear transcription factor (Gelman 2002), in which some genes encoding SASP factors have been reported as AR responsive genes (Jin *et al.* 2013). This led to the hypothesis that the secreted level of some SASP factors of AR ligand-treated cells is a result of AR ligand-controlled transcription. Supporting this hypothesis, the data reveal that secreted levels of about 30% of the analyzed cytokines correlate with their transcription levels. In addition, this study analyzed TIMP-2 and ANG as representative SASP factors since their secreted levels were differentially altered among AR ligands. The results show that regulated mRNA levels of TIMP-2 in LNCaP cells and ANG in C4-2 cells corresponded to both intracellular protein and secreted levels. Thus, the data indicate that secretion of some SASP factors associate with AR ligand-controlled transcription. This can explain the distinction of SASP secretomes between SAL- and ENZ-treated cells.

Interestingly, it seems that secretion of some SASP factors is cell line dependent and can be controlled by an unknown mechanism. For example, *TIMP2* and *CCL25* (TECK) mRNA levels were upregulated by antagonists in both LNCaP and C4-2 cell lines. TIMP-2 and TECK secretion by LNCaP cells correlated with intracellular levels. However, the secreted levels of TIMP-2 and TECK from C4-2 cells inversely corresponded to intracellular levels. Therefore, these results suggest that the secretion of TIMP-2 and TECK from C4-2 cells was controlled by an unknown mechanism regardless of ligand-regulated mRNA level. Interestingly, AR interacts with multiple signaling cascades in the cytoplasm in a non-genomic manner (Saranyutanon *et al.* 2019, Gatson *et al.* 2006, Baron *et al.* 2004, Migliaccio *et al.* 2000). Those signaling pathways include but not limit to PI3K-AKT-mTOR and MAPK/ERK, which are also known to control and regulate SASP secretion (Bent *et al.* 2016, Anerillas *et al.* 2020, Watanabe *et al.* 2017). Thus, it is possible that secretion of some cytokines is regulated at a non-genomic level by AR ligands.

## **5.2 The SASP of AR ligand-treated PCa cells mediates paracrine effects on neighboring cells**

The paracrine effect mediated by SASP relies on the balance between secreted tumor-promoting and -suppressive factors (Coppé *et al.* 2010, Lecot *et al.* 2016). As earlier discussed, the transcription and the secretion of SASP factors are cell line specific and vary when cells are exposed to AR agonist or antagonist. This leads to controversial discussion whether AR ligand-induced SASP plays a role as tumor promoter or suppressor.

### **5.2.1 The SASP of AR ligand-treated cells modulates the phospho-kinome and regulates PCa cell proliferation**

This thesis shows that LNCaP cell proliferation was suppressed when cells were treated with Con. R, a conditioned medium containing SASP of SAL-treated LNCaP cells. In contrast, LNCaP cell proliferation was enhanced by Con. E, a conditioned medium containing SASP of ENZ-treated LNCaP cells. These data suggest that SAL-induced SASP may play a tumor suppressive role, whereas antagonist-induced SASP exerts the tumor promoting role.

The effect on cell proliferation by AR ligand-induced SASP may be explained by distinct SASP secretomes (Figure 23). SASP factors that are enriched in GO term “regulation of cell proliferation” and oppositely regulated by SAL and ENZ were hypothesized to be candidates. Secreted levels of SASP factors including ANG, BLC, GCP-2, soluble IL-6R, IL-2, GDNF, CXCL-11, IL-5, TIMP-2, and Lymphotoxin were oppositely affected by SAL and ENZ. Cytokine array data reveal that the secretion of the first six factors was enhanced by SAL and suppressed by ENZ, whereas the secretion of the other factors was suppressed by SAL and enhanced by ENZ. Thus, the data lead to the question whether it is possible that ANG, BLC, GCP-2, soluble IL-6R, IL-2, and GDNF may negatively regulate, whereas CXCL-11, TIMP-2, IL-5, and Lymphotoxin may positively regulate cell proliferation (Figure 23). Unfortunately, the negative role of ANG, BLC, and GCP-2 on cell proliferation is rarely reported. IL-6 signaling is generally known to promote progression of PCa (Nguyen *et al.* 2014, Culig *et al.* 2005). However, interaction between IL-6 and soluble IL-6R has been discussed for an anti-proliferative effect in PCa cells (Santer *et al.* 2010). IL-2 has been shown to inhibit cervical cancer cell proliferation (Valle-Mendiola *et al.* 2014). GDNF may suppress colorectal cancer cell proliferation through its alternative receptor, GAS1 (Fielder *et al.* 2018, Schueler-Furman

*et al.* 2006, Li *et al.* 2016). Thus, an enhanced secretion of soluble IL-6R, IL-2, and GDNF by SAL correlates with Con. R-suppressed cell proliferation. In contrast, the positive role on cell proliferation of CXCL-11 and TIMP-2 have been described in PCa and adenocarcinoma cells, respectively (Wang *et al.* 2018a, Kim *et al.* 2015). IL-5 is well-known as cell proliferating factor of some immune cells (Kouro and Takatsu 2009). Lymphotoxin enhances cell proliferation of epithelial ovarian carcinoma through its receptor (XCR1), which also expresses in PCa cells (Kim *et al.* 2012). Therefore, an enhanced secretion of CXCL-11, IL-5, TIMP-2, and Lymphotoxin by ENZ correlates as well with Con. E-enhanced LNCaP cell proliferation.

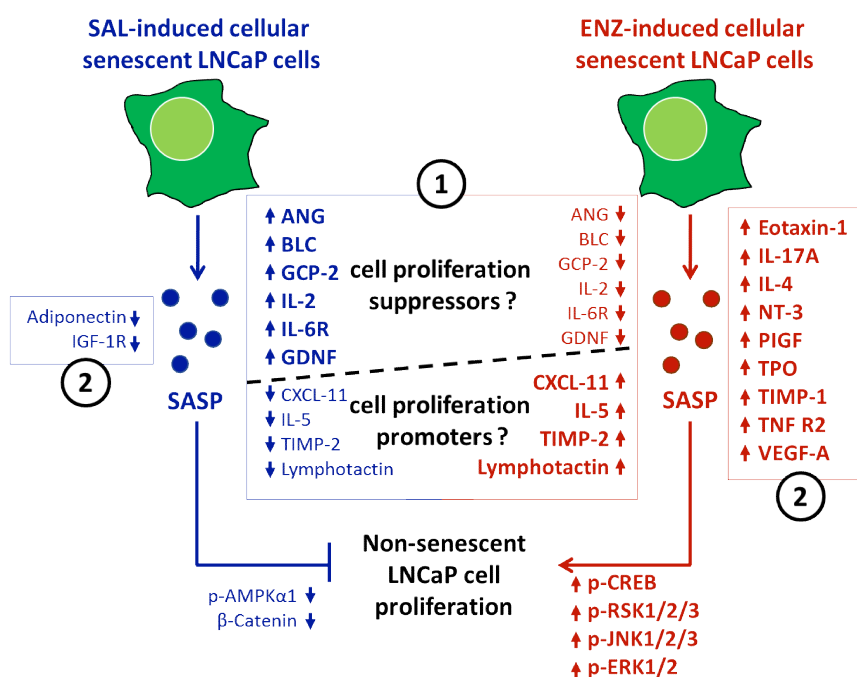


**Figure 23. The SASP of AR ligand-treated cells modulates phospho-kinome and regulates PCa cell proliferation.** SAL and ENZ-induced cellular senescent LNCaP cells possess distinct SASP secretomes. The secretion of some SASP factors is (1) oppositely regulated by SAL and ENZ, while the secretion of some factors is (2) either affected by SAL or ENZ. On one hand, conditioned medium containing SASP of SAL-treated cells suppresses LNCaP cell proliferation, AMPKα1 phosphorylation level, and β-Catenin protein level. On the other hand, conditioned medium containing SASP of ENZ-treated cells enhances LNCaP cell proliferation and phosphorylation levels of CREB, RSK1/2/3, JNK1/2/3, and ERK1/2. It is questioned whether ANG, BLC, GCP-2, IL-2, soluble IL-6R, and GDNF may act as inhibitor of cell proliferation, since their secreted levels are enhanced by SAL but suppressed by ENZ. *Vice versa*, the secretion of CXCL-11, IL-5, TIMP-2, and Lymphotoxin are suppressed by SAL but enhanced by ENZ. Thus, these factors are also questioned for their positive role on cell proliferation regulation. IPA suggests that SAL-suppressed secretion of Adiponectin and IGF-1R correlates with suppressed phospho-AMPKα1 level. In contrast, ENZ-enhanced secretion of Eotaxin-1, IL-17A, IL-4, NT-3, PIGF, TPO, TIMP-1, TNF R2, and VEGF-A correlates with induced phosphorylation levels of CREB, RSK1/2/3, JNK1/2/3, and ERK1/2.

The possibility of how SASP regulates LNCaP cell proliferation may also be explained by the regulation of phospho-kinome in conditioned media-treated cells.  $\beta$ -Catenin and phospho-AMPK $\alpha$ 1 levels were downregulated by Con. R and not affected by Con. E (Figure 23). Many studies have shown that the expression of  $\beta$ -Catenin is important for promoting PCa cell proliferation (Zhu *et al.* 2016, Wang *et al.* 2018b, Lu *et al.* 2009, Liang *et al.* 2018). AMPK-induced PCa cell progression and disease recurrence were also suggested (Li *et al.* 2017, Tennakoon *et al.* 2014). Thus, Con. R-reduced  $\beta$ -Catenin and phospho-AMPK $\alpha$ 1 levels correlate with reduced LNCaP cell proliferation. In contrast, phosphorylation levels of ERK, JNK, RSK, and CREB were induced by Con. E and not affected by Con. R (Figure 23). Both ERK and JNK are mitogen-activated protein kinases (MAPKs), and the activation of ERK or JNK is known to promote cell proliferation (Xu and Hu 2020, Mebratu and Tesfaigzi 2009). Interestingly, RSK can be phosphorylated by activated ERK. Both activated ERK and RSK translocate to the nucleus where they activate multiple transcription factors including CREB to promote cell survival and proliferation (Mebratu and Tesfaigzi 2009). Thus, increased phosphorylation of these kinases also correlates with Con. E-enhanced cell proliferation.

Interestingly, a bioinformatic IPA reveals that, on one hand, Adiponectin and IGF-1R may activate and lead to phosphorylation of AMPK $\alpha$ 1. The secretion of both factors was suppressed by SAL and not affected by ENZ (Figure 23). On the other hand, IPA shows that phosphorylation of JNK and RSK can be affected by IL-4 and VEGF-A, whereas ERK phosphorylation is affected by Eotaxin-1, IL-17A, IL-4, NT-3, PIGF, TPO, TIMP-1, TNF R2, and VEGF-A. Secreted levels of these factors were enhanced by ENZ and not affected by SAL (Figure 23). Thus, the secretion of these cytokines affected by either SAL or ENZ alone correlates with the modulated phospho-kinome, and therefore, their association on LNCaP cell proliferation should not be excluded.

Unlike LNCaP cells, the results surprisingly show that C4-2 cell proliferation was not affected by conditioned media collected from C4-2 cells. An insensitivity towards conditioned media of C4-2 cells might be due to many reasons including the concentration of the secreted cytokines as well as a castration-resistant stage of C4-2 cells. On one hand, the concentration of cytokines that regulate cell proliferation in conditioned media may not be sufficient to mediate detectable effect. On the other hand, it is known that the CRPCa cells exhibit some adaptive response to overcome androgen deprivation (Decker *et al.* 2012, Perner *et al.* 2015,



Lakshmana and Baniahmad 2019, Dutt and Gao 2009). This adaptive response can result in an enhanced basal activity of other signaling pathways, thus, the response towards cytokines in conditioned media may be reduced.

### 5.2.2 AR agonist, but not the agonist-induced SASP, suppresses PCa stemness

PCa stem/progenitor cells are hypothesized to be resistant to and survive therapeutic intervention (Maitland and Collins 2008, Tang *et al.* 2009, Li and Tang 2011). Thus, these cells may be a reason for tumor relapse. Interestingly, it has been reported that chemotherapy-induced senescence could change stem-cell-related properties of malignant cells and promotes cancer stemness (Milanovic *et al.* 2018). Therefore, it was hypothesized in this thesis that PCa stemness can also be regulated by SASP of AR ligand-treated PCa cells.

This study shows that some stemness markers especially at mRNA level can be regulated by conditioned medium containing SASP of SAL-treated LNCaP cells. However, it did not affect Yamanaka's factors at protein levels. Neither mRNA level nor protein level of analyzed stemness markers was affected by conditioned media containing SASP of antagonist-treated LNCaP cells. Importantly, the results show that conditioned media containing SASP of AR ligand-treated cells do not affect holoclone and meroclone formation of PCa cells. This is being in line with the analyzed protein level of stemness markers. Thus, it suggests that SASP of AR ligand-treated LNCaP cells do not have an impact on PCa stemness.

Interestingly, Wen *et al.* (2016) reported that the population of stem-like cells increased after AR antagonist treatment with either BIC or ENZ along with upregulation of stemness markers *POU5F1* (OCT4) and *NANOG*. This thesis shows that BIC and ENZ induce some stemness markers at both mRNA and protein levels including *NANOG*, *MET*, OCT4, SOX2, and ALDH1A1. Hence, the results are consistent with the study conducted by Wen *et al.* (2016). Notably, an increased stem-like cell population after ADT has also been reported (Tang *et al.* 2009). Thus, it seems that increased stem-like cell population correlates with reduced activity of AR signaling. Actually, the link between AR expression and PCa stemness has also been described. Srinivasan *et al.* (2018) showed that AR expression reduces PCa stemness characteristics by repressing stemness marker SOX2. *Vice versa*, loss of AR expression promotes PCa stem-like cell phenotype through STAT3 signaling and an increased SOX2 expression (Schroeder *et al.* 2014). Moreover, PCa stem/progenitor cells are often reported to

have low or undetectable AR level (Deng and Tang 2015, Leão *et al.* 2017). In fact, AR negative PCa cells are expected to be insensitive toward AR targeting therapies. This is in line with the hypothesis that PCa stem/progenitor cells are resistance and survive after certain therapies.

Unlike antagonists, the effect of SAL on PCa stem/progenitor cells is rarely reported. This study shows that SAL strikingly suppressed all analyzed stemness markers at both mRNA and protein levels. This is in line with an invert correlation between AR expression/activity and PCa stemness as earlier discussed. Furthermore, SAL potently inhibited holoclone and meroclone formation efficiency of LNCaP cells in both experimental setups of 3D colony formation assays. These data suggest that SAL-treated cell population possessed reduced stemness characteristics. Surprisingly, the colony size was affected when different experimental setups were used. Colonies formed during SAL treatment showed a reduced size, whereas the size of colonies formed from SAL-pretreated monolayer was unaffected. The latter is likely due to the absence of SAL during the 3D colony formation, suggesting that long-term SAL may be important for suppressing the self-renewal ability.

### **5.2.3 The SASP of AR ligand-treated cells suppresses lymphocyte proliferation**

It is known that SASP modulates tumor microenvironment as well as affects immune responses (Velarde *et al.* 2013, Rao and Jackson 2016, Toso *et al.* 2014). This includes regulation of lymphocyte proliferation and lymphocyte-mediated apoptosis of cancer cells. Interestingly, this study indicates that conditioned media containing SASP of AR ligand-treated LNCaP cells do not promote lymphocyte-mediated apoptosis, but suppress lymphocyte proliferation. Thus, this finding suggests an immune-suppressive role of AR ligand-induced SASP.

Since SASP of both SAL- and antagonist-treated cells show a similar effect by suppressing lymphocyte proliferation, it may be explained by an overlapping SASP secretome between agonist- and antagonist-treated LNCaP cells. This thesis focused on 6 cytokines, which were also significantly enriched in GO term “regulation of lymphocyte proliferation”. They are gp130, IGF-1, Leptin, RANTES, TGF  $\beta$ 1, and IGFBP-2. The secretion of the first five cytokines was enhanced by either SAL or ENZ, whereas the secretion of IGFBP-2 was suppressed by either SAL or ENZ. Interestingly, among these cytokines, Leptin and TGF  $\beta$ 1

have been described for their negative regulation of lymphocyte proliferation (Lord *et al.* 2002, Thomas and Massagué 2005, Kloss *et al.* 2018). In contrast, positive regulation of cell proliferation by IGFBP-2 in leukemia cells, PBMCs, and lymphocytes was also reported, whereas anti-IGFBP-2 showed anti-proliferative effect (Chen *et al.* 2013, Hettmer *et al.* 2005). These information support the notion that suppression of lymphocyte proliferation by conditioned media might be mediated by but not limited to suppressed secretion of IGFBP-2 and enhanced secretion of Leptin and TGF  $\beta$ 1. Indeed, secreted cytokines which were affected by SAL or ENZ alone should not be excluded.

Taken functional effects of SASP together, this study demonstrates for the first time possible paracrine effects mediated by SASP of AR ligand-treated PCa cells. The SASP of SAL-treated cells initially seems to play a role as tumor suppressor by inhibiting LNCaP cell proliferation, however, it also suppresses lymphocyte proliferation. Importantly, this study highlights the dark sides of AR antagonists. The SASP of antagonist-treated cells does not only suppress lymphocyte proliferation, but it also promotes LNCaP cell proliferation.

### **5.3 AR ligand-activated pro-survival/anti-apoptotic AKT signaling correlates with resistance of PCa cells against lymphocyte-mediated apoptosis**

Many immunotherapeutic strategies have been approved for various cancer types (Boettcher *et al.* 2019, Hodi *et al.* 2010, Tang *et al.* 2018, Kantoff *et al.* 2010). There are several ongoing clinical trials for PCa as well. However, since 2010, only Sipuleucel-T (cell-based vaccine) has so far been approved. It seems that PCa exhibits some mechanisms of immune-suppression to limit the effectiveness of immunotherapies (Pu *et al.* 2016, Kloss *et al.* 2018). Indeed, this may be due to an immune-suppressive tumor microenvironment modulated by SASP (as shown in this study). However, apart from SASP-suppressed lymphocyte proliferation, this study shows that AR ligand-treated PCa cells themselves exhibit an immune-tolerance feature. Either SAL- or ENZ-treated cells are resistance to lymphocyte-mediated apoptosis.

Lymphocyte-mediated apoptosis requires cell surface signal interaction of both lymphocytes and their target cells. While some antigens on cancer cells serve as targets for lymphocyte to recognize and kill cancer cells, some surface antigens can inhibit lymphocyte-mediated killing

(Morvan and Lanier 2016, Han *et al.* 2020). As example, one of cytolytic inhibitory signals is mediated through interaction of PD-L1 on cancer cells and the PD-1 receptor on cytotoxic T cells. Note that a negative correlation between AR and PD-L1 expressions has been reported (Jiang *et al.* 2020). In addition, it is possible that AR ligands alter the expression of other PCa cell surface factors, thus, hindering the immune cells to recognize and kill the target cells. However, further investigation on this point is required.

Besides changes of cell surface antigen expression, it is possible that some anti-apoptotic signals are activated in treated PCa cells. An apoptotic resistance is suggested to be one of the hallmark features of senescent cells (Salminen *et al.* 2011, Campisi and d'Adda di Fagagna 2007, Hampel *et al.* 2004). Senescent cells possess upregulated pro-survival/anti-apoptotic signaling pathways (Wong *et al.* 2018, Salminen *et al.* 2011). This study identifies that a pro-survival/anti-apoptotic AKT signaling is activated in AR ligand-induced cellular senescent PCa cells. However, the data reveal that the downstream signaling of AKT is differentially regulated between AR agonist- and antagonist-treated cells. The protein S6 is an example. SAL-treated cells exhibited increased p-S6 level, whereas the antagonist did not affect p-S6 level. This also implies that the pro-survival/anti-apoptotic AKT-S6 pathway is more active in SAL- than antagonist-treated cells. This distinct regulation of AKT-S6 pathway may also explain a resistance toward lymphocyte-mediated apoptosis. In line with this, the levels of c-PARP and Annexin V positive stained cells after co-culturing with lymphocytes were lower in SAL- than ENZ-treated cells. Moreover, higher cell viability after co-culture was observed in SAL-treated cells. Therefore, a more active AKT-S6 pathway may explain an apoptotic resistance of SAL-treated cells being more effective than ENZ-treated cells.

Taken together with the effects of SASP, these results reveal disadvantage issues of either SAL or AR antagonist treatment. Indeed, both ligands induce growth arrest by induction of cellular senescence, but the treated cells are resistance to lymphocyte-mediated apoptosis and exhibit a SASP that can suppress lymphocyte proliferation. This suggests that treatment with AR ligands alone may not be beneficial in long-term. Hence, new strategies are required to improve such disadvantages.

#### 5.4 An approach to a new therapeutic strategy: Targeting pro-survival/anti-apoptotic signaling with senolytic compounds after AR ligand-induced cellular senescence

This study proposes that induction of cellular senescence in PCa cells with AR ligands and elimination of those cells by senolytic compounds might be a very useful strategy. Senolytic compounds are small molecule compounds that selectively kill senescent cells by targeting activated pro-survival or anti-apoptotic pathways (Wong *et al.* 2018). However, as described earlier, a pro-survival/anti-apoptotic AKT signaling is differentially regulated by SAL and antagonist. This may lead to distinct senolytic sensitivity between SAL- and ENZ-pretreated cells.

This study analyzed senolytic activity of the AKT inhibitor (MK) and HSP90 inhibitor (GT) after AR ligand-induced cellular senescence. The data suggest that either MK or GT is capable of inhibiting AKT signaling. MK is a highly allosteric AKT inhibitor, and therefore directly inhibits AKT (Hirai *et al.* 2010). In contrast, GT indirectly inhibits AKT signaling because AKT is one of the clients of HSP90 (Zhang *et al.* 2005). In line with this, treatment with GT leads to reduced AKT protein level. Interestingly, the results show that SAL-induced cellular senescent LNCaP cells were sensitive to apoptosis induction by GT, but surprisingly exhibited resistance towards MK. In contrast, ENZ-induced cellular senescent LNCaP cells were preferentially sensitized by MK-mediated apoptosis. To our knowledge, this is the first study demonstrating a novel role of MK as senolytic compound for antagonist-pretreated PCa cells (Pungsrinont *et al.* 2020).

Interestingly, the above results can be explained by the regulation of AKT downstream targets mediated by AR ligands. In case of SAL-induced cellular senescence, it is hypothesized that the resistance to MK-mediated apoptosis is due to the remaining high p-S6 level after AKT inhibition. The high p-S6 level also demonstrates that SAL treatment phosphorylates directly or indirectly S6 independent of AKT phosphorylation. Indeed, it is possible that this process is mediated through non-genomic AR signaling. Interestingly, many studies showed that mouse embryonic fibroblasts (MEFs) expressing unphosphorylatable S6 (S6<sup>P-/-</sup>) are more sensitive to TRAIL-, etoposide-, and MG132-induced apoptosis than control MEFs (Meyuhas 2015, Jeon *et al.* 2008, Wittenberg *et al.* 2016). This suggests that p-S6 may be a critical pro-survival factor and supports the notion that p-S6 level is important for apoptotic resistance.

Moreover, p-S6 level may also explain the outcome that SAL-pretreated cells were sensitized by GT-mediated apoptosis. The data show that GT did not potently inhibit p-Akt level as strong as MK, but p-S6 level was however efficiently reduced by GT in SAL-pretreated cells. Assuming that the survival of SAL-treated LNCaP cells relies on the upregulated p-S6 level, the cells would be more sensitized to apoptosis if p-S6 level is reduced.

Unlike SAL-treated cells, although the level of p-AKT was clearly induced, the data reveal that the level of p-S6 was not elevated by ENZ. Thus, p-S6 levels is not the reason for ENZ-treated cells being sensitized by MK-induced apoptosis. This suggests that activated AKT signaling by ENZ does not go through S6, but rather activates other downstream pathways. Interestingly, Pilling and Hwang (2019) showed that ENZ induces phospho-BAD (p-BAD) level in 22Rv1 PCa cell line, leading to inactivation of BAD which is a pro-apoptotic factor and another downstream target of AKT. Moreover, p-BAD level was suppressed by co-treatment of MK and ENZ together, but was not suppressed when 22Rv1 cells were treated with MK alone. Importantly, an enhanced apoptosis by ENZ and MK co-treatment was also observed when compared to MK alone (Pilling and Hwang 2019). Notably, although Pilling and Hwang treated the cells with MK at the same time with ENZ, the outcome is similar to the result of this thesis, which MK was treated after ENZ-induced cellular senescence. Thus, AKT-BAD pathway might explain the AR antagonist-specific senolytic activity mediated by MK.

Taken together, the data show that treatment with senolytic compounds may be a beneficial therapeutic option along with AR ligands. However, the senolytic activity of a compound is limited when senescence is induced by different stimuli. Thus, the choice of a senolytic compound depends on the pro-survival/anti-apoptotic pathway activated by a particular senescence inducer.

## 6 CONCLUSIONS AND FUTURE PERSPECTIVES

This study highlights and summarizes for the first time overlapping and diverse features between SAL- and AR antagonist-induced cellular senescence (Figure 24). Apart from the fact that AR ligands induce cellular senescence leading to inhibition of PCa cell proliferation, the data show that SAL inhibits stemness characteristics. Moreover, the SASP of SAL-treated cells suppresses, but the SASP of antagonist-treated cells promotes LNCaP cell proliferation. This opposite effect on cell proliferation is due to a distinct composition of SASP secretome between SAL- and antagonist-treated cells, which can modulate the phospho-kinome of PCa cells. Thus, these data initially suggest that treatment with SAL may provide more advantages than antagonists. However, further evidences suggest that treatment with either SAL or antagonists alone may not be beneficial in long-term for PCa therapy. The results indicate immune-suppressive effects mediated by both AR ligands and the induced SASP. In line with this, AR ligand-treated PCa cells are resistant to lymphocyte-mediated apoptosis, and the SASP of ligand-treated LNCaP cells suppresses lymphocyte proliferation. This study identifies that activation of pro-survival/anti-apoptotic AKT signaling is one of the underlying mechanisms for apoptotic resistance of AR ligand-treated cells. However, the downstream target of AKT signaling is differentially regulated by AR ligands. It appears that one can take advantage of this different regulation. The data show that different regulation between antagonist- and SAL-treated cells leads to distinct apoptotic sensitivity towards specific senolytic compounds. Antagonist-treated cells are sensitive towards the AKT inhibitor, whereas SAL-treated cells are sensitive towards the HSP90 inhibitor. Taken together, the data suggest that induction of cellular senescence in PCa cells and elimination of these cells by senolytic compounds might be a very useful strategy for future therapeutic approach.

For future perspective, the data suggest that effective treatment could be achieved when a suitable senolytic compound for a particular AR ligand is used. Therefore, pro-survival/anti-apoptotic pathways should be identified and other inhibitors may be analyzed to find more candidates as senolytic compounds. Future approaches for PCa immunotherapy may also be drawn towards the usage of SASP inhibitors along with CAR-T cells. The expression profile of AR ligand-regulated cell surface antigens may be analyzed in order to generate potential CAR-T cells. This may improve the lymphocyte-mediated killing of AR ligand-treated PCa cells.

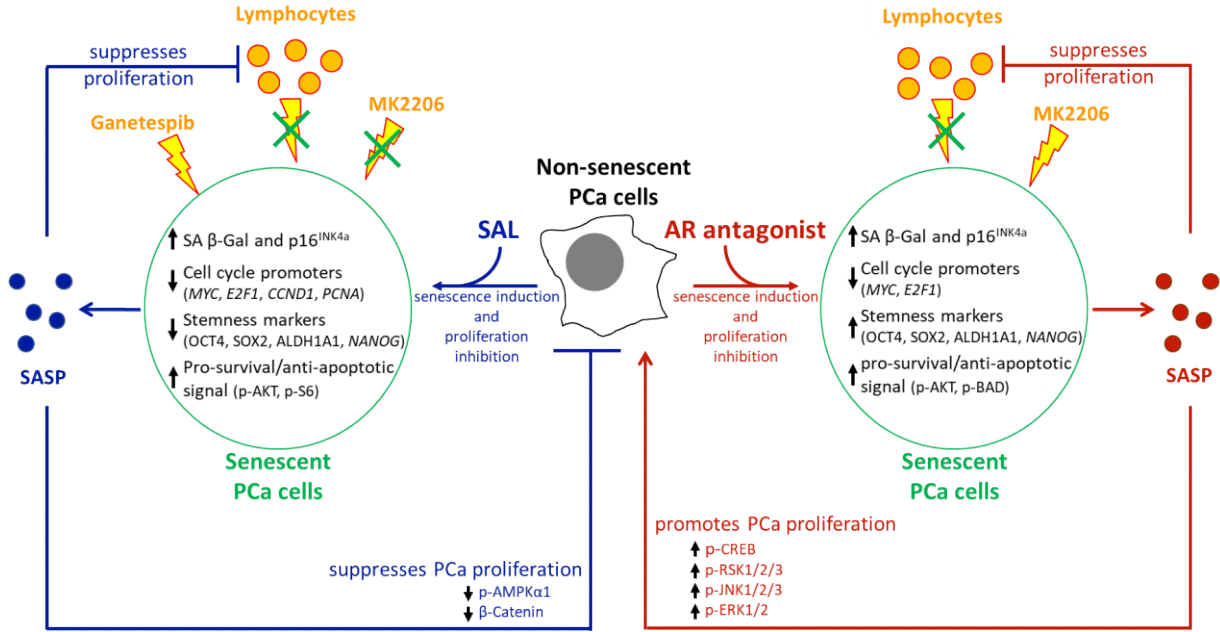


**Figure 24. Diverse effects between SAL- and AR antagonist-induced cellular senescence.** Either SAL (R1881) or AR antagonist (ENZ) treatment inhibits LNCaP cell proliferation by inducing cellular senescence and suppressing the expression of cell cycle promoters. SAL-treated cells exhibit reduced stemness characteristics, while AR antagonist induces expression of stemness markers. AR ligand-treated PCa cells are resistance towards lymphocyte-mediated apoptosis. Both ligands activate anti-apoptotic/pro-survival AKT signaling. However, downstream target of AKT signaling is differentially activated by SAL- and antagonist-treated cells. This leads to distinct response in apoptotic sensitivity towards senolytic compounds HSP90 inhibitor (Ganetespiib) and AKT inhibitor (MK2206). Interestingly, SASP secretomes between SAL- and antagonist-treated PCa cells differ from each other. Moreover, the paracrine effects mediated by SASP between those cells are also diverse. On the one hand, SASP of SAL-treated LNCaP cells suppresses both the proliferation of LNCaP cells and lymphocytes. On the other hand, SASP of antagonist-treated LNCaP cells promotes LNCaP cell proliferation, but suppresses lymphocyte proliferation. SASP-regulated LNCaP cell proliferation is partially explained by alteration of LNCaP phospho-kinome modulated by SASP.



---

**7 REFERENCES**

- Alessio N, Aprile D, Squillaro T, Di Bernardo G, Finicelli M, Melone MA, Peluso G, Galderisi U. 2019. The senescence-associated secretory phenotype (SASP) from mesenchymal stromal cells impairs growth of immortalized prostate cells but has no effect on metastatic prostatic cancer cells. *Aging*, 11(15):5817-5828.
- Andriole G, Bruchovsky N, Chung LW, Matsumoto AM, Rittmaster R, Roehrborn C, Russel D, Tindall D. 2004. Dihydrotestosterone and the prostate: the scientific rationale for 5 $\alpha$ -reductase inhibitors in the treatment of benign prostatic hyperplasia. *J Urol*, 172(4 Pt 1):1399-1403.
- Anerillas C, Abdelmohsen K, Gorospe M. 2020. Regulation of senescence traits by MAPKs. *Geroscience*, 42(2):397-408.
- Aoi T, Yae K, Nakagawa M, Ichisaka T, Okita K, Takahashi K, Chiba T, Yamanaka S. 2008. Generation of pluripotent stem cells from adult mouse liver and stomach cells. *Science*, 321(5889):699-702.
- Bahmad HF, Cheaito K, Chalhoub RM, Hadadeh O, Monzer A, Ballout F, El-Hajj A, Mukherji D, Liu YN, Daoud G, Abou-Kheir W. 2018. Sphere-formation assay: Three-dimensional *in vitro* culturing of prostate cancer stem/progenitor sphere-forming cells. *Front Oncol*, 8:347.
- Balasuriya N, Davey NE, Johnson JL, Liu H, Biggar KK, Cantley LC, Li SS, O'Donoghue P. 2020. Phosphorylation-dependent substrate selectivity of protein kinase B (AKT1). *J Biol Chem*, 295(24):8120-8134.
- Baron S, Manin M, Beaudoin C, Leotoing L, Communal Y, Veysièrè G, Morel L. 2004. Androgen receptor mediates non-genomic activation of phosphatidylinositol 3-OH kinase in androgen-sensitive epithelial cells. *J Biol Chem*, 279(15):14579-14586.
- Barrandon Y, Green H. 1987. Three clonal types of keratinocyte with different capacities for multiplication. *Proc Natl Acad Sci U S A*, 84(8):2302-2306.
- Basisty N, Kale A, Jeon OH, Kuehnemann C, Payne T, Rao C, Holtz A, Shah S, Sharma V, Ferrucci L, Campisi J, Schilling B. 2020. A proteomic atlas of senescence-associated secretomes for aging biomarker development. *PLoS Biol*, 18(1):e3000599.
- Bavik C, Coleman I, Dean JP, Knudsen B, Plymate S, Nelson PS. 2006. The gene expression program of prostate fibroblast senescence modulates neoplastic epithelial cell proliferation through paracrine mechanisms. *Cancer Res*, 66(2):794-803.
- Beaver CM, Ahmed A, Masters JR. 2014. Clonogenicity: holoclones and meroclones contain stem cells. *PLoS One*, 9(2):e89834.

- Bent EH, Gilbert LA, Hemann MT. 2016. A senescence secretory switch mediated by PI3K/AKT/mTOR activation controls chemoprotective endothelial secretory responses. *Genes Dev*, 30(16):1811-1821.
- Bernardini G, Benigni G, Antonangeli F, Ponzetta A, Santoni A. 2014. Multiple levels of chemokine receptor regulation in the control of mouse natural killer cell development. *Front Immunol*, 5:44.
- Bevan CL, Hoare S, Claessens F, Heery DM, Parker MG. 1999. The AF1 and AF2 domains of the androgen receptor interact with distinct regions of SRC1. *Mol Cell Biol*, 19(12):8383-8392.
- Boettcher AN, Usman A, Morgans A, VanderWeele DJ, Sosman J, Wu JD. 2019. Past, current, and future of immunotherapies for prostate cancer. *Front Oncol*, 9:884.
- Bohl CE, Gao W, Miller DD, Bell CE, Dalton JT. 2005. Structural basis for antagonism and resistance of bicalutamide in prostate cancer. *Proc Natl Acad Sci U S A*, 102(17):6201-6206.
- Bromley SK, Mempel TR, Luster AD. 2008. Orchestrating the orchestrators: chemokines in control of T cell traffic. *Nat Immunol*, 9(9):970-980.
- Brzozowska B, Gałeczki M, Tartas A, Ginter J, Kaźmierczak U, Lundholm L. 2019. Freeware tool for analysing numbers and sizes of cell colonies. *Radiat Environ Biophys*, 58(1):109-117.
- Burton DG, Giribaldi MG, Munoz A, Halvorsen K, Patel A, Jorda M, Perez-Stable C, Rai P. 2013. Androgen deprivation-induced senescence promotes outgrowth of androgen-refractory prostate cancer cells. *PLoS One*, 8(6):e68003.
- Cahu J, Bustany S, Sola B. 2012. Senescence-associated secretory phenotype favors the emergence of cancer stem-like cells. *Cell Death Dis*, 3(12):e446.
- Campisi J. 2001. Cellular senescence as a tumor-suppressor mechanism. *Trends Cell Biol*, 11(11):S27-31.
- Campisi J, d'Adda di Fagagna F. 2007. Cellular senescence: when bad things happen to good cells. *Nat Rev Mol Cell Biol*, 8(9):729-740.
- Centenera MM, Carter SL, Gillis JL, Marrocco-Tallarigo DL, Grose RH, Tilley WD, Butler LM. 2015. Co-targeting AR and HSP90 suppresses prostate cancer cell growth and prevents resistance mechanisms. *Endocr Relat Cancer*, 22(5):805-818.
- Chen X, Zheng J, Zou Y, Song C, Hu X, Zhang CC. 2013. IGF binding protein 2 is cell-autonomous factor supporting survival and migration of acute leukemia cells. *J Hematol Oncol*, 6(1):72.
- Choi N, Zhang B, Zhang L, Ittmann M, Xin L. 2012. Adult murine prostate basal and luminal cells are self-sustained lineages that can both serve as targets for prostate cancer initiation. *Cancer Cell*, 21(2):253-265.

- Claessens F, Verrijdt G, Schoenmakers E, Haelens A, Peeters B, Verhoeven G, Rombauts W. 2001. Selective DNA binding by the androgen receptor as a mechanism for hormone-specific gene regulation. *J Steroid Biochem Mol Biol*, 76(1-5):23-30.
- Collado M, Gil J, Efeyan A, Guerra C, Schuhmacher AJ, Barradas M, Benguría A, Zaballos A, Flores JM, Barbacid M, Beach D, Serrano M. 2005. Tumour biology: senescence in premalignant tumours. *Nature*, 436(7051):642.
- Collado M, Serrano M. 2006. The power and the promise of oncogene-induced senescence markers. *Nat Rev Cancer*, 6(6):472-476.
- Coppé JP, Patil CK, Rodier F, Sun Y, Muñoz DP, Goldstein J, Nelson PS, Desprez PY, Campisi J. 2008. Senescence-associated secretory phenotypes reveal cell-nonautonomous functions of oncogenic RAS and the p53 tumor suppressor. *PLoS Biol*, 6(12):2853-2868.
- Coppé JP, Desprez PY, Krtolica A, Campisi J. 2010. The senescence-associated secretory phenotype: the dark side of tumor suppression. *Annu Rev Pathol*, 5:99-118.
- Culig Z, Hoffmann J, Erdel M, Eder IE, Hobisch A, Hittmair A, Bartsch G, Utermann G, Schneider MR, Parczyk K, Klocker H. 1999. Switch from antagonist to agonist of the androgen receptor bicalutamide is associated with prostate tumour progression in a new model system. *Br J Cancer*, 81(2):242-251.
- Culig Z, Steiner H, Bartsch G, Hobisch A. 2005. Interleukin-6 regulation of prostate cancer cell growth. *J Cell Biochem*, 95(3):497-505.
- Cutress ML, Whitaker HC, Mills IG, Stewart M, Neal DE. 2008. Structural basis for the nuclear import of the human androgen receptor. *J Cell Sci*, 121(Pt7):957-968.
- Decker KF, Zheng D, He Y, Bowman T, Edwards JR, Jia L. 2012. Persistent androgen receptor-mediated transcription in castration-resistant prostate cancer under androgen-deprived conditions. *Nucleic Acids Res*, 40(21):10765-10779.
- Deng Q, Tang DG. 2015. Androgen receptor and prostate cancer stem cells: biological mechanisms and clinical implications. *Endocr Relat Cancer*, 22(6):T209-220.
- Denmeade SR. 2018. Bipolar androgen therapy in the treatment of prostate cancer. *Clin Adv Hematol Oncol*, 16(6):408-411.
- Di Mitri D, Toso A, Chen JJ, Sarti M, Pinton S, Jost TR, D'Antuono R, Montani E, Garcia-Escudero R, Guccini I, Da Silva-Alvarez S, Collado M, Eisenberger M, Zhang Z, Catapano C, Grassi F, Alimonti A. 2014. Tumour-infiltrating Gr-1+ myeloid cells antagonize senescence in cancer. *Nature*, 515(7525):134-137.
- Di X, Bright AT, Bellott R, Gaskins E, Robert J, Holt S, Gewirtz D, Elmore L. 2008. A chemotherapy-associated senescence bystander effect in breast cancer cells. *Cancer Bio Ther*, 7(6):864-872.

- Dimri GP, Lee X, Basile G, Acosta M, Scott G, Roskelley C, Medrano EE, Linskens M, Rubelj I, Pereira-Smith O, Peacocke M, Campisi J. 1995. A biomarker that identifies senescent human cells in culture and in aging skin *in vivo*. *Proc Natl Acad Sci U S A*, 92:9363-9367.
- Dutt SS, Gao AC. 2009. Molecular mechanisms of castration-resistant prostate cancer progression. *Future Oncol*, 5(9):1403-1413.
- Edline MP, Hsieh AC. 2014. PI3K-AKT-mTOR signaling in prostate cancer progression and androgen deprivation therapy resistance. *Asian J Androl*, 16(3):378-386.
- Ertingshausen MC. 2018. Analyse von zwei senolytischen Substanzen in seneszenten Prostatakrebszellen [Bachelor thesis, Baniahmad's group]. Jena: Friedrich Schiller University.
- Esmaeili M, Jennek S, Ludwig S, Klitzsch A, Kraft F, Melle C, Baniahmad A. 2016a. The tumor suppressor ING1b is a novel corepressor for the androgen receptor and induces cellular senescence in prostate cancer cells. *J Mol Cell Biol*, 8(3):207-220.
- Esmaeili M, Pungsrinont T, Schaefer A, Baniahmad A. 2016b. A novel crosstalk between the tumor suppressors ING1 and ING2 regulates androgen receptor signaling. *J Mol Med*, 94(10):1167-1179.
- Fielder GC, Yang TWS, Razdan M, Li Y, Lu J, Perry JK, Lobie PE, Liu DX. 2018. The GDNF family: A role in cancer?. *Neoplasia*, 20(1):99-117.
- Fousteris MA, Schubert U, Roell D, Roediger J, Bailis N, Nikolaropoulos SS, Baniahmad A, Giannis A. 2010. 20-Aminosteroids as a novel class of selective and complete androgen receptor antagonists and inhibitors of prostate cancer cell growth. *Bioorg Med Chem*, 18(19):6960-6969.
- Fuhrmann-Stroissnigg H, Ling YY, Zhao J, McGowan SJ, Zhu Y, Brooks RW, Grassi D, Gregg SQ, Stripay JL, Dorransoro A, Corbo L, Tang P, Bukata C, Ring N, Giacca M, Li X, Tchkonja T, Kirkland JL, Niedernhofer LJ, Robbins PD. 2017. Identification of HSP90 inhibitors as a novel class of senolytics. *Nat Commun*, 8(1):422.
- Fuhrmann-Stroissnigg H, Niedernhofer LJ, Robbins PD. 2018. Hsp90 inhibitors as senolytic drugs to extend healthy aging. *Cell Cycle*, 17(9):1048-1055.
- Gatson JW, Kaur P, Singh M. 2006. Dihydrotestosterone differentially modulates the mitogen-activated protein kinase and the phosphoinositide 3-kinase/Akt pathways through the nuclear and novel membrane androgen receptor in C6 cells. *Endocrinology*, 147(4):2028-2034.
- Gelmann EP. 2002. Molecular biology of the androgen receptor. *J Clin Oncol*, 20(13):3001-3015.
- Gonzalez-Meljem JM, Apps JR, Fraser HC, Martinez-Barbera JP. 2018. Paracrine roles of cellular senescence in promoting tumorigenesis. *Br J Cancer*, 118(10):1283-1288.

- Gupta S, Pungsrinont T, Ženata O, Neubert L, Vrzal R, Baniahmad A. 2020. Interleukin-23 represses the level of cell senescence induced by androgen receptor antagonists enzalutamide and darolutamide in castration-resistant prostate cancer cells. *Horm Cancer*, 11(3-4):182-190.
- Hampel B, Malisan F, Niederegger H, Testi R, Jansen-Dürr P. 2004. Differential regulation of apoptotic cell death in senescent human cells. *Exp Gerontol*, 39(11-12):1713-1721.
- Han Y, Liu D, Li L. 2020. PD-1/PD-L1 pathway: current researches in cancer. *Am J Cancer Res*, 10(3):727-742.
- Harris WP, Mostaghel EA, Nelson PS, Montgomery B. 2009. Androgen deprivation therapy: progress in understanding mechanisms of resistance and optimizing androgen depletion. *Nat Clin Pract Urol*, 6(2):76-85.
- He S, Zhang C, Shafi AA, Squeira M, Acquaviva J, Friedland JC, Sang J, Smith DJ, Weigel NL, Wada Y, Proia DA. 2013. Potent activity of the Hsp90 inhibitor ganetespib in prostate cells irrespective of androgen receptor status or variant receptor expression. *Int J Oncol*, 42(1):35-43.
- Heery DM, Kalkhoven E, Hoare S, Parker MG. 1997. A signature motif in transcriptional co-activators mediates binding to nuclear receptors. *Nature*, 387(6634):733-736.
- Hernandez-Segura A, de Jong TV, Melov S, Guryev V, Campisi J, Demaria M. 2017. Unmasking transcriptional heterogeneity in senescent cells. *Curr Biol*, 27(17):2652-2660.
- Hessenkemper W, Baniahmad A. 2012. Chaperones for proper androgen action – a plethora of assistance to androgen receptor function. *Horm Mol Biol Clin Investig*, 11(1):321-328.
- Hessenkemper W, Roediger J, Bartsch S, Houtsmuller AB, van Royen ME, Petersen I, Grimm MO, Baniahmad A. 2014. A natural androgen receptor antagonist induces cellular senescence in prostate cancer cells. *Mol Endocrinol*, 28(11):1831-1840.
- Hettmer S, Dannecker L, Foell J, Elmlinger MW, Dannecker GE. 2005. Effects of insulin-like growth factors and insulin-like growth factor binding protein-2 on the in vitro proliferation of peripheral blood mononuclear cells. *Hum Immunol*, 66(2):95-103.
- Hirai H, Sootome H, Nakatsuru Y, Miyama K, Taguchi S, Tsujioka K, Ueno Y, Hatch H, Majumder PK, Pan BS, Kotani H. 2010. MK-2206, an allosteric Akt inhibitor, enhances antitumor efficacy by standard chemotherapeutic agents or molecular targeted drugs in vitro and in vivo. *Mol Cancer Ther*, 9(7):1956-1967.
- Hodi FS, O'Day SJ, McDermott DF, Weber RW, Sosman JA, Haanen JB, Gonzalez R, Robert C, Schadendorf D, Hassel JC, Akerley W, van den Eertwegh AJ, Lutzky J, Lorigan P, Vaubel JM, Linette GP, Hogg D, Ottensmeier CH, Lebbé C, Peschel C, Quirt I, Clark JI, Wolchok JD,

- Weber JS, Tian J, Yellin MJ, Nichol GM, Hoos A, Urba WJ. 2010. Improved survival with ipilimumab in patients with metastatic melanoma. *N Engl J Med*, 363(8):711-723.
- Huangfu D, Osafune K, Maehr R, Guo W, Eijkelenboom A, Chen S, Muhlestein W, Melton DA. 2008. Induction of pluripotent stem cells from primary human fibroblasts with only Oct4 and Sox2. *Nat Biotechnol*, 26(11):1269-1275.
- Huggins C, Hodges CV. 1941. Studies on prostatic cancer: I. The effect of castration, of estrogen and of androgen injection on serum phosphatases in metastatic carcinoma of the prostate. *Cancer Res*, 1:293-297.
- Jemal A, Siegel R, Ward E, Murray T, Xu J, Thun MJ. 2007. Cancer statistics, 2007. *CA Cancer J Clin*, 57(1):43-66.
- Jeon YJ, Kim IK, Hong SH, Nan H, Kim HJ, Lee HJ, Masuda ES, Meyuhas O, Oh BH, Jung YK. 2008. Ribosomal protein S6 is a selective mediator of TRAIL-apoptotic signaling. *Oncogene*, 27(31):4344-4352.
- Jiang G, Shi L, Zheng X, Zhang X, Wu K, Liu B, Yan P, Liang X, Yu T, Wang Y, Cai X. 2020. Androgen receptor affects the response to immune checkpoint therapy by suppressing PD-L1 in hepatocellular carcinoma. *Aging*, 12(12):11466-11484.
- Jin HJ, Kim J, Yu J. 2013. Androgen receptor genomic regulation. *Transl Androl Urol*, 2(3):158-177.
- Junking M, Grainok J, Thepmalee C, Wongkham S, Yenchitsomanus PT. 2017. Enhanced cytotoxic activity of effector T-cells against cholangiocarcinoma by dendritic cells pulsed with pooled mRNA. *Tumour Biol*, 39(10):1010428317733367.
- Kalbasi A, Ribas A. 2020. Tumour-intrinsic resistance to immune checkpoint blockade. *Nat Rev Immunol*, 20(1):25-39.
- Kang TW, Yevsa T, Woller N, Hoenicke L, Wuestefeld T, Dauch D, Hohmeyer A, Gereke M, Rudalska R, Potapova A, Iken M, Vucur M, Weiss S, Heikenwalder M, Khan S, Gil J, Bruder D, Manns M, Schirmacher P, Tacke F, Ott M, Luedde T, Longerich T, Kubicka S, Zender L. 2011. Senescence surveillance of pre-malignant hepatocytes limits liver cancer development. *Nature*, 479(7374):547-551.
- Kantoff PW, Higano CS, Shore ND, Berger ER, Small EJ, Penson DF, Redfern CH, Ferrari AC, Dreicer R, Sims RB, Xu Y, Frohlich MW, Schellhammer PF, IMPACT Study Investigators. 2010. Sipuleucel-T immunotherapy for castration-resistant prostate cancer. *N Engl J Med*, 363(5):411-422.
- Kashyap V, Rezende NC, Scotland KB, Shaffer SM, Persson JL, Gudas LJ, Mongan NP. 2009. Regulation of stem cell pluripotency and differentiation involves a mutual regulatory circuit of

- the NANOG, OCT4, and SOX2 pluripotency transcription factors with polycomb repressive complexes and stem cell microRNAs. *Stem Cells Dev*, 18(7):1093-1108.
- Khan AQ, Ahmed EI, Elareer NR, Junejo K, Steinhoff M, Uddin S. 2019. Role of mRNA-regulated cancer stem cells in the pathogenesis of human malignancies. *Cells*, 8(8):840.
- Kim M, Rooper L, Xie J, Rayahin J, Burdette JE, Kajdacsy-Balla AA, Barbolina MV. 2012. The lymphotactin receptor is expressed in epithelial ovarian carcinoma and contributes to cell migration and proliferation. *Mol Cancer Res*, 10(11):1419-1429.
- Kim HI, Lee HS, Kim TH, Lee JS, Lee ST, Lee SJ. 2015. Growth-stimulatory activity of TIMP-2 is mediated through c-Src activation followed by activation of FAK, PI3-kinase/AKT, and ERK1/2 independent of MMP inhibition in lung adenocarcinoma cells. *Oncotarget*, 6(40):42905-42922.
- Klarmann GJ, Hurt EM, Mathews LA, Zhang X, Duhagon MA, Mistree T, Thomas SB, Farrar WL. 2009. Invasive prostate cancer cells are tumor initiating cells that have a stem cell-like genomic signature. *Clin Exp Metastasis*, 26(5):433-446.
- Kloss CC, Lee J, Zhang A, Chen F, Melenhorst JJ, Lacey SF, Maus MV, Fraietta JA, Zhao Y, June CH. 2018. Dominant-negative TGF- $\beta$  receptor enhances PSMA-targeted human CAR T cell proliferation and augments prostate cancer eradication. *Mol Ther*, 26(7):1855-1866.
- Kokal M, Mirzakhani K, Pungsrinont T, Baniahmad A. 2020. Mechanisms of androgen receptor agonist- and antagonist-mediated cellular senescence in prostate cancer. *Cancers*, 12(7):1833.
- Kotollosi R, Mirzakhani K, Ahlburg J, Kraft F, Pungsrinont T, Baniahmad A. 2020. Thyroid hormone induces cellular senescence in prostate cancer cells through induction of DEC1. *J Steroid Biochem Mol Biol*, 201:105689.
- Kouro T, Takatsu K. 2009. IL-5- and eosinophil-mediated inflammation: from discovery to therapy. *Int Immunol*, 21(12):1303-1309.
- Krishnamurthy J, Torrice C, Ramsey MR, Kovalev GI, Al-Regaiey K, Su L, Sharpless NE. 2004. Ink4a/Arf expression is a biomarker of aging. *J Clin Invest*, 114(9):1299-1307.
- Krtolica A, Parrinello S, Lockett S, Desprez P, Campisi J. 2001. Senescent fibroblasts promote epithelial cell growth and tumorigenesis: a link between cancer and aging. *Proc Natl Acad Sci U S A*, 98(21):12072-12077.
- Kwon ED, Drake CG, Scher HI, Fizazi K, Bossi A, van der Eertwegh AJ, Krainer M, Houede N, Santos R, Mahammedi H, Ng S, Maio M, Franke FA, Sundar S, Agarwal N, Bergman AM, Ciuleanu TE, Korbenfeld E, Sengeløv L, Hansen S, Logothetis C, Beer TM, McHenry MB, Gagnier P, Liu D, Gerritsen WR, CA184-043 Investigators. 2014. Ipilimumab versus placebo after radiotherapy in patients with metastatic castration-resistant prostate cancer that had

- progressed after docetaxel chemotherapy (CA184-043): a multicentre, randomised, double-blind, phase 3 trial. *Lancet Oncol*, 15(7):700-712.
- Lakshmana G, Baniahmad A. 2019. Interference with the androgen receptor protein stability in therapy-resistant prostate cancer. *Int J Cancer*, 144(8):1775-1779.
- Leão R, Domingos C, Figueiredo A, Hamilton R, Tabori U, Castelo-Branco P. 2017. Cancer stem cells in prostate cancer: Implications for targeted therapy. *Urol Int*, 99(2):125-136.
- Lecot P, Alimirah F, Desprez PY, Campisi J, Wiley C. 2016. Context-dependent effects of cellular senescence in cancer development. *Br J Cancer*, 114(11):1180-1184.
- Lee BY, Han JA, Im JS, Morrone A, Johung K, Goodwin EC, Kleijer WJ, DiMaio D, Hwang ES. 2006. Senescence-associated beta-galactosidase is lysosomal beta-galactosidase. *Aging Cell*, 5(2):187-195.
- Lehmann BD, Paine MS, Brooks AM, McCubrey JA, Renegar RH, Wang R, Terrian DM. 2008. Senescence-associated exosome release from human prostate cancer cells. *Cancer Res*, 68(19):7864-7871.
- Leung JK, Sadar MD. 2017. Non-genomic actions of the androgen receptor in prostate cancer. *Front Endocrinol*, 8:2.
- Levina V, Marrangoni A, Wang T, Parikh S, Su Y, Herberman R, Lokshin A, Gorelik E. 2010. Elimination of human lung cancer stem cells through targeting of the Stem Cell Factor-C-Kit autocrine signaling loop. *Cancer Res*, 70(1):338-346.
- Li H, Tang DG. 2011. Prostate cancer stem cells and their potential roles in metastasis. *J Surg Oncol*, 103(6):558-562.
- Li Q, Qin Y, Wei P, Lian P, Li Y, Xu Y, Li X, Li D, Cai S. 2016. Gas1 inhibits metastatic and metabolic phenotypes in colorectal carcinoma. *Mol Cancer Res*, 14(9):830-840.
- Li J, Zhong L, Wang F, Zhu H. 2017. Dissecting the role of AMP-activated protein kinase in human diseases. *Acta Pharm Sin B*, 7(3):249-259.
- Liang T, Ye X, Liu Y, Qiu X, Li Z, Tian B, Yan D. 2018. FAM46B inhibits cell proliferation and cell cycle progression in prostate cancer through ubiquitination of  $\beta$ -catenin. *Exp Mol Med*, 50(12):1-12.
- Liao J, Wu Z, Wang Y, Cheng L, Cui C, Gao Y, Chen T, Rao L, Chen S, Jia N, Dai H, Xin S, Kang J, Pei G, Xiao L. 2008. Enhanced efficiency of generating induced pluripotent stem (iPS) cells from human somatic cells by a combination of six transcription factors. *Cell Res*, 18(5):600-603.
- Liao RS, Ma S, Miao L, Li R, Yin Y, Raj GV. 2013. Androgen receptor-mediated non-genomic regulation of prostate cancer cell proliferation. *Transl Androl Urol*, 2(3):187-196.



- Liu D, Hornsby PJ. 2007. Senescent human fibroblasts increase the early growth of xenograft tumors via matrix metalloproteinase secretion. *Cancer Res*, 67(7):3117-3127.
- Lonergan PE, Tindall DJ. 2011. Androgen receptor signaling in prostate cancer development and progression. *J Carcinog*, 10:20.
- Lord GM, Matarese G, Howard JK, Bloom SR, Lechler RI. 2002. Leptin inhibits the anti-CD3-driven proliferation of peripheral blood T cells but enhances the production of proinflammatory cytokines. *J Leukoc Biol*, 72(2):330-338.
- Lu W, Tinsley HN, Keeton A, Qu Z, Piazza GA, Li Y. 2009. Suppression of Wnt/ $\beta$ -catenin signaling inhibits prostate cancer cell proliferation. *Eur J Pharmacol*, 602(1):8-14.
- Ma F, Chen D, Chen F, Chi Y, Han Z, Feng X, Li X, Han Z. 2015. Human umbilical cord mesenchymal stem cells promote breast cancer metastasis by interleukin-8- and interleukin-6-dependent induction of CD44(+)/CD24(-) cells. *Cell Transplant*, 24(12):2585-2599.
- Maitland NJ, Collins AT. 2008. Prostate cancer stem cells: a new target for therapy. *J Clin Oncol*, 26(17):2862-2870.
- Masiello D, Cheng S, Bublely GJ, Lu ML, Balk SP. 2002. Bicalutamide functions as an androgen receptor antagonist by assembly of a transcriptionally inactive receptor. *J Biol Chem*, 277(29):26321-26326.
- McEwan IJ. 2004. Molecular mechanisms of androgen receptor-mediated gene regulation: structure-function analysis of the AF-1 domain. *Endocr Relat Cancer*, 11(2):281-293.
- McHugh ML. 2011. Multiple comparison analysis testing in ANOVA. *Biochem Med*, 21(3):203-209.
- Mebratu Y, Tesfaigzi Y. 2009. How ERK1/2 activation controls cell proliferation and cell death: Is subcellular localization the answer?. *Cell Cycle*, 8(8):1168-1175.
- Meyuhas O. 2015. Ribosomal protein S6 phosphorylation: four decades of research. *Int Rev Cell Mol Biol*, 320:41-73.
- Migliaccio A, Castoria G, Di Domenico M, de Falco A, Bilancio A, Lombardi M, Barone MV, Ametrano D, Zannini MS, Abbondanza C, Auricchio F. 2000. Steroid-induced androgen receptor-oestradiol receptor beta-*Src* complex triggers prostate cancer cell proliferation. *EMBO J*, 19(20):5406-5417.
- Milanovic M, Fan DNY, Belenki D, Däbritz JHM, Zhao Z, Yu Y, Dörr JR, Dimitrova L, Lenze D, Monteiro Barbosa IA, Mendoza-Parra MA, Kanashova T, Metzner M, Pardon K, Reimann M, Trumpp A, Dörken B, Zuber J, Gronemeyer H, Hummel M, Dittmar G, Lee S, Schmitt CA. 2018. Senescence-associated reprogramming promotes cancer stemness. *Nature*, 533(7686):96-100.
- Mirochnik Y, Veliceasa D, Williams L, Maxwell K, Yemelyanov A, Budunova I, Volpert OV. 2012. Androgen receptor drives cellular senescence. *PLoS One*, 7(3):e31052.

- Mishra P, Singh U, Pandey CM, Mishra P, Pandey G. 2019. Application of student's *t*-test, analysis of variance, and covariance. *Ann Card Anaesth*, 22(4):407-411.
- Morvan MG, Lanier LL. 2016. NK cells and cancer: you can teach innate cells new tricks. *Nat Rev Cancer*, 16(1):7-19.
- Nakagawa M, Koyanagi M, Tanabe K, Takahashi K, Ichisaka T, Aoi T, Okita K, Mochiduki Y, Takizawa N, Yamanaka S. 2008. Generation of induced pluripotent stem cells without Myc from mouse and human fibroblasts. *Nat Biotechnol*, 26(1):101-106.
- Narita M, Núñez S, Heard E, Narita M, Lin AW, Hearn SA, Spector DL, Hannon GJ, Lowe SW. 2003. Rb-mediated heterochromatin formation and silencing of E2F target genes during cellular senescence. *Cell*, 113(6):703-716.
- Nelson PS. 2012. Molecular states underlying androgen receptor activation: a framework for therapeutics targeting androgen signaling in prostate cancer. *J Clin Oncol*, 30(6):644-646.
- Nguyen DP, Li J, Tewari AK. 2014. Inflammation and prostate cancer: the role of interleukin 6 (IL-6). *BJU Int*, 113(6):986-992.
- Ntais C, Polycarpou A, Tsatsoulis A. 2003. Molecular epidemiology of prostate cancer: androgens and polymorphisms in androgen-related genes. *Eur J Endocrinol*, 149(6):469-477.
- Özcan S, Alessio N, Acar MB, Mert E, Omerli F, Peluso G, Galderisi U. 2016. Unbiased analysis of senescence associated secretory phenotype (SASP) to identify common components following different genotoxic stresses. *Aging*, 8(7):1316-1329.
- Ohuchida K, Mizumoto K, Murakami M, Qian LW, Sato N, Nagai E, Matsumoto K, Nakamura T, Tanaka M. 2004. Radiation to stromal fibroblasts increases invasiveness of pancreatic cancer cells through tumor-stromal interactions. *Cancer Res*, 64(9):3215-3222.
- Osguthorpe DJ, Hagler AT. 2011. Mechanism of androgen receptor antagonism by bicalutamide in the treatment of prostate cancer. *Biochemistry*, 50(19):4105-4113.
- Perner S, Cronauer MV, Schrader AJ, Klocker H, Culig Z, Baniahmad A. 2015. Adaptive responses of androgen receptor signaling in castration-resistant prostate cancer. *Oncotarget*, 6(34):35542-35555.
- Pernicová Z, Slabáková E, Kharraishvili G, Bouchal J, Král M, Kunická Z, Machala M, Kozubík A, Souček K. 2011. Androgen depletion induces senescence in prostate cancer cells through down-regulation of Skp2. *Neoplasia*, 13(6):526-536.
- Peterziel H, Mink S, Schonert A, Becker M, Klocker H, Cato AC. 1999. Rapid signaling by androgen receptor in prostate cancer cells. *Oncogene*, 18(46):6322-6329.
- Pfaffl MW. 2001. A new mathematical model for relative quantification in real-time RT-PCR. *Nucleic Acids Res*, 29(9):e45.

- Pilling AB, Hwang C. 2019. Targeting prosurvival BCL2 signaling through Akt blockade sensitizes castration-resistant prostate cancer cells to enzalutamide. *Prostate*, 79(11):1347-1359.
- Protopopov AI, Li J, Winberg G, Gizatullin RZ, Kashuba VI, Klein G, Zabarovsky ER. 2002. Human cell lines engineered for tetracycline-regulated expression of tumor suppressor candidate genes from a frequently affected chromosomal region, 3p21. *J Gene Med*, 4(4):397-406.
- Pu Y, Xu M, Liang Y, Yang K, Guo Y, Yang X, Fu YX. 2016. Androgen receptor antagonists compromise T cell response against prostate cancer leading to early tumor relapse. *Sci Transl Med*, 8(333):333ra47.
- Puhr M, Hoefler J, Eigentler A, Ploner C, Handle F, Schaefer G, Kroon J, Leo A, Heidegger I, Eder I, Culig Z, Van der Pluijm G, Klocker H. 2018. The glucocorticoid receptor is a key player for prostate cancer cell survival and a target for improved antiandrogen therapy. *Clin Cancer Res*, 24(4):927-938.
- Pungsrinont T, Sutter MF, Ertingshausen M, Lakshmana G, Kokal M, Khan AS, Baniahmad A. 2020. Senolytic compounds control a distinct fate of androgen receptor agonist- and antagonist-induced cellular senescent LNCaP prostate cancer cells. *Cell Biosci*, 10:59.
- Rao SG, Jackson JG. 2016. SASP: Tumor suppressor or promoter? Yes! *Trends Cancer*, 2(11):676-687.
- Rochman Y, Spolski R, Leonard WJ. 2009. New insights into the regulation of T cells by  $\gamma_c$  family cytokines. *Nat Rev Immunol*, 9(7):480-490.
- Rodriguez-Vida A, Galazi M, Rudman S, Chowdhury S, Sternberg CN. 2015. Enzalutamide for the treatment of metastatic castration-resistant prostate cancer. *Drug Des Devel Ther*, 9:3325-3339.
- Roediger J, Hessenkemper W, Bartsch S, Manvelyan M, Huettner SS, Liehr T, Esmacili M, Foller S, Petersen I, Grimm MO, Baniahmad A. 2014. Supraphysiological androgen levels induce cellular senescence in human prostate cancer cells through the Src-Akt pathway. *Mol Cancer*, 13:214.
- Roell D, Rösler TW, Hessenkemper W, Kraft F, Hauschild M, Bartsch S, Abraham TE, Houtsmuller AB, Matusch R, van Royen ME, Baniahmad A. 2019. Halogen-substituted anthranilic acid derivatives provide a novel chemical platform for androgen receptor antagonists. *J Steroid Biochem Mol Biol*, 188:59-70.
- Saleh T, Tyutynuk-Massey L, Cudjoe EK Jr, Idowu MO, Landry JW, Gewirtz DA. 2018. Non-cell autonomous effects of the senescence-associated secretory phenotype in cancer therapy. *Front Oncol*, 8:164.

- Salminen A, Ojala J, Kaarniranta K. 2011. Apoptosis and aging: increased resistance to apoptosis enhances the aging process. *Cell Mol Life Sci*, 68(6):1021-1031.
- Santer FR, Malinowska K, Culig Z, Cavarretta IT. 2010. Interleukin-6 trans-signalling differentially regulates proliferation, migration, adhesion and maspin expression in human prostate cancer cells. *Endocr Relat Cancer*, 17(1):241-253.
- Saranyutanon S, Srivastava SK, Pai S, Singh S, Singh AP. 2019. Therapies targeted to androgen receptor signaling axis in prostate cancer: Progress, challenges, and hope. *Cancers*, 12(1):51.
- Schroeder A, Herrmann A, Cherryholmes G, Kowolik C, Buettner R, Pal S, Yu H, Müller-Newen G, Jove R. 2014. Loss of androgen receptor expression promotes a stem-like cell phenotype in prostate cancer through STAT3 signaling. *Cancer Res*, 74(4):1227-1237.
- Schueler-Furman O, Glick E, Segovia J, Linial M. 2006. Is GAS1 a co-receptor for the GDNF family of ligands?. *Trends Pharmacol Sci*, 27(2):72-77.
- Siegel RL, Miller KD, Jemal A. 2020. Cancer statistics, 2020. *CA Cancer J Clin*, 70(1):7-30.
- Simova J, Sapega O, Imrichova T, Stepanek I, Kyjacoova L, Mikyskova R, Indrova M, Bieblova J, Bubenik J, Bartek J, Hodny Z, Reinis M. 2016. Tumor growth accelerated by chemotherapy-induced senescent cells is suppressed by treatment with IL-12 producing cellular vaccines. *Oncotarget*, 7(34):54952-54964.
- Sin WC, Lim CL. 2017. Breast cancer stem cells-from origins to targeted therapy. *Stem Cell Investig*, 4:96.
- Sonnenschein C, Olea N, Pasanen ME, Soto AM. 1989. Negative controls of cell proliferation: human prostate cancer cells and androgens. *Cancer Res*, 49(13):3474-3481.
- Srinivasan D, Senbanjo L, Majumdar S, Franklin RB, Chellaiah MA. 2018. Androgen receptor expression reduces stemness characteristics of prostate cancer cells (PC3) by repression of CD44 and SOX2. *J Cell Biochem*, 120(2):2413-2428.
- Sutter M. 2018. Analysis of proliferation by co-targeting heat shock protein 90 and androgen receptor in prostate cancer cells [Bachelor thesis, Baniahmad's group]. Jena: Friedrich Schiller University.
- Takahashi K, Tanabe K, Ohnuki M, Narita M, Ichisaka T, Tomoda K, Yamanaka S. 2007. Induction of pluripotent stem cells from adult human fibroblasts by defined factors. *Cell*, 131(5):861-872.
- Takai H, Smogorzewska A, de Lange T. 2003. DNA damage foci at dysfunction telomeres. *Curr Biol*, 13(17):1549-1556.
- Tang Y, Hamburger AW, Wang L, Khan MA, Hussain A. 2009. Androgen deprivation and stem cell markers in prostate cancers. *Int J Clin Exp Pathol*, 3(2):128-138.

- Tang J, Yu JX, Hubbard-Lucey VM, Neftelinov ST, Hodge JP, Lin Y. 2018. Trial watch: The clinical trial landscape for PD1/PDL1 immune checkpoint inhibitors. *Nat Rev Drug Discov*, 17(12):854-855.
- Tennakoon JB, Shi Y, Han JJ, Tsouko E, White MA, Burns AR, Zhang A, Xia X, Ilkayeva OR, Xin L, Ittmann MM, Rick FG, Schally AV, Frigo DE. 2014. Androgens regulate prostate cancer cell growth via an AMPK-PGC-1 $\alpha$ -mediated metabolic switch. *Oncogene*, 33(45):5251-5261.
- Teply BA, Wang H, Lubber B, Sullivan R, Rifkind I, Bruns A, Spitz A, DeCarli M, Sinibaldi V, Pratz CF, Lu C, Silberstein JL, Luo J, Schweizer MT, Drake CG, Carducci MA, Paller CJ, Antonarakis ES, Eisenberger MA, Denmeade SR. 2018. Bipolar androgen therapy in men with metastatic castration-resistant prostate cancer after progression on enzalutamide: an open-label, phase 2, multicohort study. *Lancet Oncol*, 19(1):76-86.
- Thomas DA, Massagué J. 2005. TGF- $\beta$  directly targets cytotoxic T cell functions during tumor evasion of immune surveillance. *Cancer Cell*, 8(5):369-380.
- Thomson JA, Itskovitz-Elder J, Shapiro SS, Waknitz MA, Swiergiel JJ, Marshall VS, Jones JM. 1998. Embryonic stem cell lines derived from human blastocysts. *Science*, 282(5391):1145-1147.
- Toso A, Revandkar A, Di Mitri D, Guccini I, Proietti M, Sarti M, Pinton S, Zhang J, Kalathur M, Civenni G, Jarrossay D, Montani E, Marini C, Garcia-Escudero R, Scanziani E, Grassi F, Pandolfi PP, Catapano CV, Alimonti A. 2014. Enhancing chemotherapy efficacy in Pten-deficient prostate tumors by activating the senescence-associated antitumor immunity. *Cell Rep*, 9(1):75-89.
- Toste PA, Nguyen AH, Kadera BE, Doung M, Wu N, Gawlas I, Tran LM, Bikhchandani M, Li L, Patel SG, Dawson DW, Donahue TR. 2016. Chemotherapy-induced inflammatory gene signature and protumorigenic phenotype in pancreatic CAFs via stress-associated MAPK. *Mol Cancer Res*, 14(5):437-447.
- Traish AM, Morgentaler A. 2009. Epidermal growth factor receptor expression escapes androgen regulating in prostate cancer: a potential molecular switch for tumour growth. *Br J Cancer*, 101(12):1949-1956.
- Tran C, Ouk S, Clegg NJ, Chen Y, Watson PA, Arora V, Wongvipat J, Smith-Jones PM, Yoo D, Kwon A, Wasielewska T, Welsbie D, Chen CD, Higano CS, Beer TM, Hung DT, Scher HI, Jung ME, Sawyers CL. 2009. Development of a second-generation antiandrogen for treatment of advanced prostate cancer. *Science*, 324(5928):787-790.
- Ueda T, Bruchofsky N, Sadar MD. 2002. Activation of the androgen receptor N-terminal domain by interleukin-6 via MAPK and STAT3 signal transduction pathways. *J Biol Chem*, 277(9):7076-7085.

- Valle-Mendiola A, Weiss-Steider B, Rocha-Zavaleta L, Soto-Cruz I. 2014. IL-2 enhances cervical cancer cells proliferation and JAK3/STAT5 phosphorylation at low doses, while at high doses IL-2 has opposite effects. *Cancer Invest*, 32(4):115:125.
- Velarde MC, Demaria M, Campisi J. 2013. Senescent cells and their secretory phenotype as targets for cancer therapy. *Interdiscip Top Gerontol*, 38:17-27.
- Vjetrovic J, Shankaranarayanan P, Mendoza-Parra MA, Gronemeyer H. 2014. Senescence-secreted factors activate MYC and sensitize pretransformed cells to TRAIL-induced apoptosis. *Aging Cell*, 13(3):487-496.
- Vitkin N, Nersesian S, Siemens DR, Koti M. 2019. The tumor immune contexture of prostate cancer. *Front Immunol*, 20:603.
- Wang Y, Xu H, Si L, Li Q, Zhu X, Yu T, Gang X. 2018a. MiR-206 inhibits proliferation and migration of prostate cancer cells by targeting CXCL11. *Prostate*, 78(7):479-490.
- Wang D, Lu G, Shao Y, Xu D. 2018b. MiR-182 promotes prostate cancer progression through activation Wnt/ $\beta$ -catenin signal pathway. *Biomed Pharmacother*, 99:334-339.
- Watanabe S, Kawamoto S, Ohtani N, Hara E. 2017. Impact of senescence-associated secretory phenotype and its potential as a therapeutic target for senescence-associated diseases. *Cancer Sci*, 108(4):563-569.
- Wellington K, Keam SJ. 2006. Bicalutamide 150mg: a review of its use in the treatment of locally advanced prostate cancer. *Drugs*, 66(6):837-850.
- Wen S, Tian J, Niu Y, Li L, Yeh S, Chang C. 2016. ASC-J9<sup>®</sup>, and not Casodex or Enzalutamide, suppresses prostate cancer stem/progenitor cell invasion via altering the EZH2-STAT3 signals. *Cancer Lett*, 376(2):377-386.
- Wittenberg AD, Azar S, Klochendler A, Stolovich-Rain M, Avraham S, Birnbaum L, Binder Gallimidi A, Katz M, Dor Y, Meyuhas O. 2016. Phosphorylated ribosomal protein S6 is required for Akt-driven hyperplasia and malignant transformation, but not for hypertrophy, aneuploidy and hyperfunction of pancreatic  $\beta$ -cells. *PLoS ONE*, 11(2):e149995.
- Wong J, Qudrat A, Al Mosabbir A, Truong K. Advances in senotherapies. 2018. In: Rizvi SI, Çakatay U, editors. *Molecular Basis and Emerging Strategies for Anti-aging Interventions*. Singapore: Springer, 67-82.
- Wu HC, Hsieh JT, Gleave ME, Brown NM, Pathak S, Chung LW. 1994. Derivation of androgen-independent human LNCaP prostatic cancer cell sublines: role of bone stromal cells. *Int J Cancer*, 57(3):406-412.

- Xie J, Xu X, Yin P, Li Y, Guo H, Kujawa S, Chakravarti D, Bulun S, Kim JJ, Wei JJ. 2018. Application of ex vivo spheroid model system for the analysis of senescence and senolytic phenotypes in uterine leiomyoma. *Lab Invest*, 98(12):1575-1587.
- Xu R, Hu J. 2020. The role of JNK in prostate cancer progression and therapeutic strategies. *Biomed Pharmacother*, 121:109679.
- Xue W, Zender L, Miething C, Dickins RA, Hernando E, Krizhanovsky V, Cordon-Cardo C, Lowe SW. 2007. Senescence and tumour clearance is triggered by p53 restoration in murine liver carcinomas. *Nature*, 445(7128):656-660.
- Yang Q, Fung KM, Day WV, Kropp BP, Lin HK. 2005. Androgen receptor signaling is required for androgen-sensitive human prostate cancer cell proliferation and survival. *Cancer Cell Int*, 5(1):8.
- Yang S, Li WS, Dong F, Sun HM, Wu B, Tan J, Zou WJ, Zhou DS. 2014. KITLG is a novel target of miR-34c that is associated with the inhibition of growth and invasion in colorectal cancer cells. *J Cell Mol Med*, 18(10):2092-2102.
- Yu J, Vodyanik MA, Smuga-Otto K, Antosiewicz-Bourget J, Frane JL, Tian S, Nie J, Jonsdottir GA, Ruotti V, Stewart R, Slukvin II, Thomson JA. 2007. Induced pluripotent stem cell lines derived from human somatic cells. *Science*, 318(5858):1917-1920.
- Zhang R, Luo D, Miao R, Bai L, Ge Q, Sessa WC, Min W. 2005. Hsp90-Akt phosphorylates ASK1 and inhibits ASK1-mediated apoptosis. *Oncogene*, 24(24):3954-3963.
- Zhu Z, Zhang H, Lang F, Liu G, Gao D, Li B, Liu Y. 2016. Pin1 promotes prostate cancer cell proliferation and migration through activation of Wnt/ $\beta$ -catenin signaling. *Clin Transl Oncol*, 18(8):792-797.

## 8 APPENDIX

## 8.1 Recipe of cell culture media, self-prepared buffers, solutions, and reaction mixes

## 8.1.1 Cell culture media (stored at 4°C)

<u>0% FBS RPMI medium:</u> (500 ml)	477.5 ml 5 ml 5 ml 12.5 ml	RPMI medium 1640 100x Penicillin-Streptomycin 100 mM Sodium pyruvate 1 M HEPES buffer pH 7.5	(1x) (1 mM) (25 mM)
<u>0% FBS DMEM medium:</u> (500 ml)	382.5 ml  100 ml 5 ml 12.5 ml	DMEM medium with high D-Glucose L-Glutamine sodium pyruvate Ham's F-12 nutrient mix 100x Penicillin-Streptomycin 1 M HEPES buffer pH 7.5	(25 mM) (4 mM) (1 mM) (20% v/v) (1x) (25 mM)
<u>0.5% FBS RPMI medium:</u> (20 ml)	18 ml 2 ml	0% FBS RPMI medium 5% FBS RPMI medium	
<u>4% HS RPMI or DMEM: medium (50 ml)</u>	48 ml 2 ml	0% FBS RPMI or DMEM medium Human AB serum (HS)	(4% v/v)
<u>5% FBS RPMI or DMEM: medium (500 ml)</u>	475 ml 25 ml	0% FBS RPMI or DMEM medium FBS	(5% v/v)
<u>5% HS AIM-V medium:</u> (40 ml)	38 ml 2 ml	Serum free AIM-V medium Human AB serum (HS)	(5% v/v)
<u>10% FBS RPMI or DMEM: medium (50 ml)</u>	45 ml 5 ml	0% FBS RPMI or DMEM medium FBS	(10% v/v)
<u>10% HS RPMI or DMEM: medium (40 ml)</u>	36 ml 4 ml	0% FBS RPMI or DMEM medium Human AB serum (HS)	(10% v/v)

## 8.1.2 Cell culture buffers/solutions

<u>1 M HEPES buffer pH 7.5:</u> (1 L)	Dissolve 238.31 g of HEPES in Milli-Q H <sub>2</sub> O, adjust pH to 7.5, sterile filter with 0.2 µm filter, and store at room temperature		
<u>10x PBS buffer pH 7.4 (1 L):</u>	80 g 2 g 17.8 g 2.4 g	NaCl KCl Na <sub>2</sub> HPO <sub>4</sub> ·2H <sub>2</sub> O KH <sub>2</sub> PO <sub>4</sub>	(1.37 M) (27 mM) (100 mM) (18 mM)
	Dissolve in Milli-Q H <sub>2</sub> O, adjust pH to 7.4, sterile filter with 0.2 µm filter, and store at room temperature		
<u>1x PBS buffer:</u>	Dilute 10x PBS buffer with Milli-Q H <sub>2</sub> O, autoclave, and store at room temperature		
<u>10x Trypsin diluting buffer:</u> (500 ml)	1.98 g 0.3 g 40 g	KCl KH <sub>2</sub> PO <sub>4</sub> NaCl	(53 mM) (4.4 mM) (1.37 M)



	1.75 g	NaHCO <sub>3</sub>	(42 mM)
	0.3 g	Na <sub>2</sub> HPO <sub>4</sub> ·2H <sub>2</sub> O	(3.4 mM)
	5 g	D-Glucose	(56 mM)
	Dissolve in Milli-Q H <sub>2</sub> O, sterile filter with 0.2 µm filter and store at room temperature		
<u>1x Trypsin/EDTA solution:</u> <u>(1 L)</u>	100 ml	10x Trypsin/EDTA solution (Gibco)	
	100 ml	10x Trypsin diluting buffer	
	Dissolve in Milli Q H <sub>2</sub> O, sterile filtered with 0.2 µm filter and store at -20°C		
<u>2% FBS in 1x PBS buffer:</u> <u>(50 ml)</u>	49 ml	1x PBS buffer	
	1 ml	FBS	
	Store at 4°C		
<u>Lymphocyte freezing solution:</u> <u>(1 ml)</u>	0.9 ml	Human AB serum (HS)	
	0.1 ml	100% DMSO	
<u>Red blood cell lysis buffer:</u> <u>(1 L)</u>	8.3 g	NH <sub>4</sub> Cl	(155 mM)
	1.008 g	NaHCO <sub>3</sub>	(12 mM)
	200 µl	0.5 M EDTA pH 8.0	(0.1 mM)
	Dissolve in Milli-Q H <sub>2</sub> O, autoclave, and store at room temperature		

### 8.1.3 Buffers/solutions for fixing, SA β-Gal staining, and crystal violet staining

<u>1% Glutaraldehyde fixing:</u> <u>solution</u>	Freshly dilute 50% glutaraldehyde solution (Roth) with 1x PBS		
<u>SA β-Gal staining solution:</u> <u>(37 ml)</u>	22.866 ml	Milli-Q H <sub>2</sub> O	
	7.4 ml	0.2 M Citric acid/sodium phosphate buffer (pH 6.0)	(40 mM)
	1.85 ml	100 mM K <sub>3</sub> Fe(CN) <sub>6</sub> solution	(5 mM)
	1.85 ml	100 mM K <sub>4</sub> Fe(CN) <sub>6</sub> solution	(5 mM)
	1.11 ml	5 M NaCl	(150 mM)
	74 µl	1 M MgCl <sub>2</sub>	(2 mM)
	1.85 ml	20 mg/ml X-Gal solution	(1 mg/ml)
	Adjust pH to 6.0 with either 0.1 M citric acid or 0.2 M sodium phosphate solution and protect from light		
<u>0.2 M Citric acid/sodium:</u> <u>phosphate buffer (pH 6.0)</u>	36.85 ml	0.1 M Citric acid solution	
	63.15 ml	0.2 M Sodium phosphate solution	
	Adjust pH to 6.0 with either 0.1 M citric acid or 0.2 M sodium phosphate solution and store at -20°C		
<u>X-Gal solution (20 mg/ml):</u>	Dissolve X-Gal (Invitrogen) in dimethylformamide (DMF), protect from light, and store at -20°C		
<b>NOTE:</b> To prepare 0.1 M Citric acid, 0.2 M Sodium phosphate, 100 mM K <sub>3</sub> Fe(CN) <sub>6</sub> , and 100 mM K <sub>4</sub> Fe(CN) <sub>6</sub> solutions, C <sub>6</sub> H <sub>8</sub> O <sub>7</sub> , Na <sub>2</sub> HPO <sub>4</sub> , K <sub>3</sub> Fe(CN) <sub>6</sub> , and K <sub>4</sub> Fe(CN) <sub>6</sub> powders were dissolved in Milli-Q H <sub>2</sub> O respective.			
<u>1% Crystal violet solution:</u> <u>(50 ml)</u>	Dissolve 0.5 g of Crystal violet (Roth) in Milli-Q H <sub>2</sub> O and store at room temperature		
<u>0.1% Crystal violet solution:</u>	Freshly dilute 1% crystal violet solution with 1x PBS		

<u>Sørensen's solution (500 ml):</u>	4.5 g	Tri-sodium citrate	(35 mM)
	0.833 ml	37% HCl	(0.02 N)
	200 ml	EtOH (VWR)	(40% v/v)
	Dissolve in Milli-Q H <sub>2</sub> O and store at room temperature		

#### 8.1.4 Flow cytometry buffer/solution (stored at 4°C)

<u>1% PFA fixing solution (10 ml):</u>	7.5 ml	2% FBS in 1x PBS buffer
	2.5 ml	4% PFA solution

1x Annexin binding buffer: Dilute 10x Annexin binding buffer (MabTag) with Milli-Q H<sub>2</sub>O

#### 8.1.5 Buffers/solutions for protein extraction and Western blotting

<u>NETN buffer (100 ml):</u>	10 ml	1 M NaCl	(100 mM)
	2 ml	1 M Tris-HCl pH 8.0	(20 mM)
	200 µl	0.5 M EDTA	(1 mM)
	1.429 ml	70% NP-40 Tergitol <sup>®</sup> solution	(1% NP-40)
	Dissolve in Milli-Q H <sub>2</sub> O, sterile filter with 0.2 µm filter, and store at 4°C		

<u>Phosphatase inhibitors in: NETN buffer (800 µl)</u>	711.2 µl	NETN buffer	
	0.8 µl	100 mM Na <sub>3</sub> VO <sub>4</sub>	(100 µM)
	8 µl	1 M β-Glycerophosphate	(10 mM)
	80 µl	0.5 M NaF	(50 mM)

<u>5% Acrylamide stacking gel: (1 ml)</u>	0.68 ml	Milli-Q H <sub>2</sub> O
	0.17 ml	30% acrylamide mix
	0.13 ml	1 M Tris pH 6.8
	0.01 ml	10% SDS solution
	0.01 ml	10% ammonium persulfate (APS) solution
	0.001 ml	TEMED

<u>Resolving/separating gel (5 ml):</u>	(10% acrylamide)	(12% acrylamide)	(15% acrylamide)	
	Milli-Q H <sub>2</sub> O	1.9 ml	1.6 ml	1.1 ml
	30% acrylamide mix	1.7 ml	2.0 ml	2.5 ml
	1.5 M Tris pH 8.8	1.3 ml	1.3 ml	1.3 ml
	10% SDS solution	0.05 ml	0.05 ml	0.05 ml
	10% APS solution	0.05 ml	0.05 ml	0.05 ml
	TEMED	0.002 ml	0.002 ml	0.002 ml

<u>10x Electrophoresis running: buffer (1 L)</u>	30.3 g	Tris	(250 mM)
	144.1 g	Glycine	(1.92 M)
	100 ml	10% SDS solution	(1% SDS)
	Dissolve in Milli-Q H <sub>2</sub> O and store at room temperature		

<u>10x Blotting buffer (500 ml):</u>	15.15 g	Tris	(250 mM)
	72.05 g	Glycine	(1.92 M)
	5 ml	10% SDS solution	(0.1% SDS)
	Dissolve in Milli-Q H <sub>2</sub> O and store at 4°C		

<u>1x Blotting buffer (2 L):</u>	200 ml	10x blotting buffer	
	200 or 400 ml	Methanol	(10 or 20% v/v)
	Dissolve in Milli-Q H <sub>2</sub> O and store at 4°C		

10% Skim milk (500 ml): Dissolve 50 g of skim milk in 1x TBS-T buffer, mix until homogeneous,

centrifuge at 4,700 rpm (20 mins at room temperature), collect supernatant, and store at -20°C

<u>5x TBS-T buffer (2 L):</u>	60.57 g	Tris	(250 mM)
	87.66 g	NaCl	(750 mM)
	Dissolve in Milli-Q H <sub>2</sub> O and adjust pH to 7.5 with 37% HCl		
	10 ml	TWEEN® 20	(0.5%)
	Store at 4°C		

**NOTE:** 1x Electrophoresis running and 1x TBST-T buffers were diluted from 10x and 5x stocks respectively with Milli-Q H<sub>2</sub>O and stored at 4°C

### 8.1.6 Reaction mixes for cDNA synthesis and qRT-PCR

#### Reaction mix for cDNA synthesis (20 µl):

2 µl	10x Reverse transcriptase buffer
0.8 µl	25x dNTP mix
2 µl	10x random primers
1 µl	MultiScribe™ Reverse Transcriptase
10 µl	0.2 µg/µl RNA
4.2 µl	DEPC-treated H <sub>2</sub> O

#### qRT-PCR reaction mix (5 µl):

0.1 µl	10 µM forward primer
0.1 µl	10 µM reverse primer
2.5 µl	2x SYBR® Green Supermix
1 µl	cDNA
1.3 µl	DEPC-treated H <sub>2</sub> O

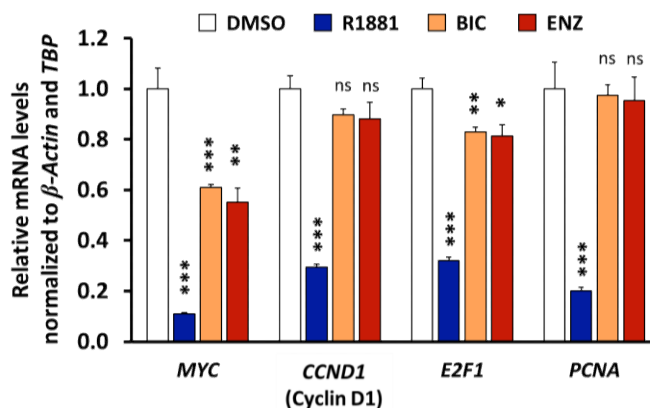
#### cDNA synthesis steps:

10 min	25°C	Initial step and primer attachment
120 min	37°C	cDNA synthesis
5 min	85°C	Inactivation of RT

#### qRT-PCR steps:

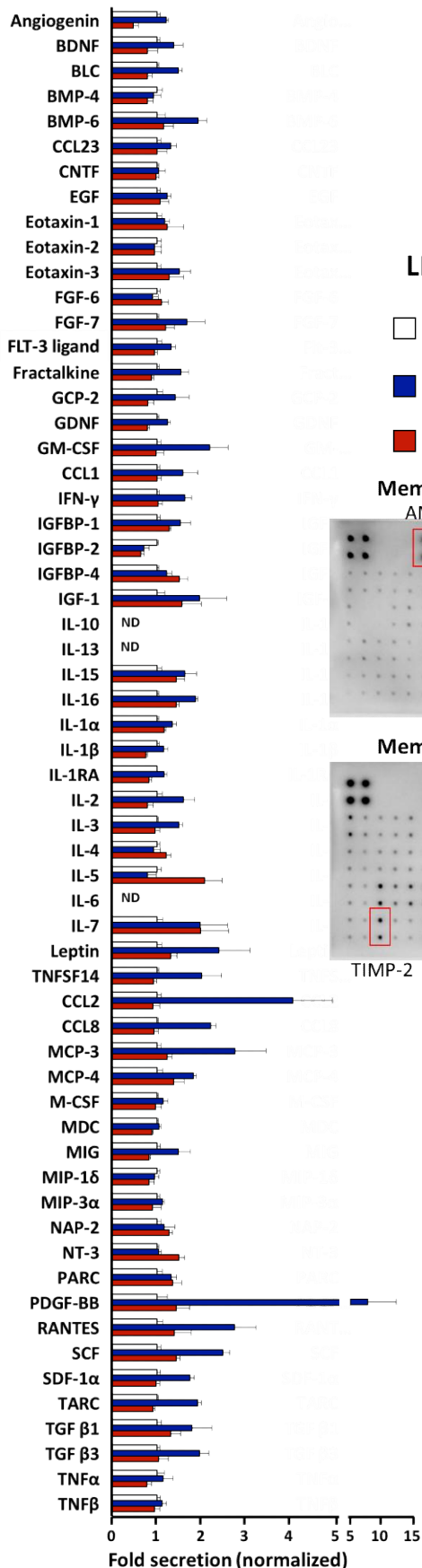
10 min	95°C	Denaturation	} 45 cycles
10 sec	95°C		
15 sec	Annealing Temperature		
30 sec	72°C		
30 sec	95°C	} Melting step	
5 sec	65°C		
increasing 0.5°C/sec until reached 95°C			

## 8.2 Supplemental results (Figures and Table)

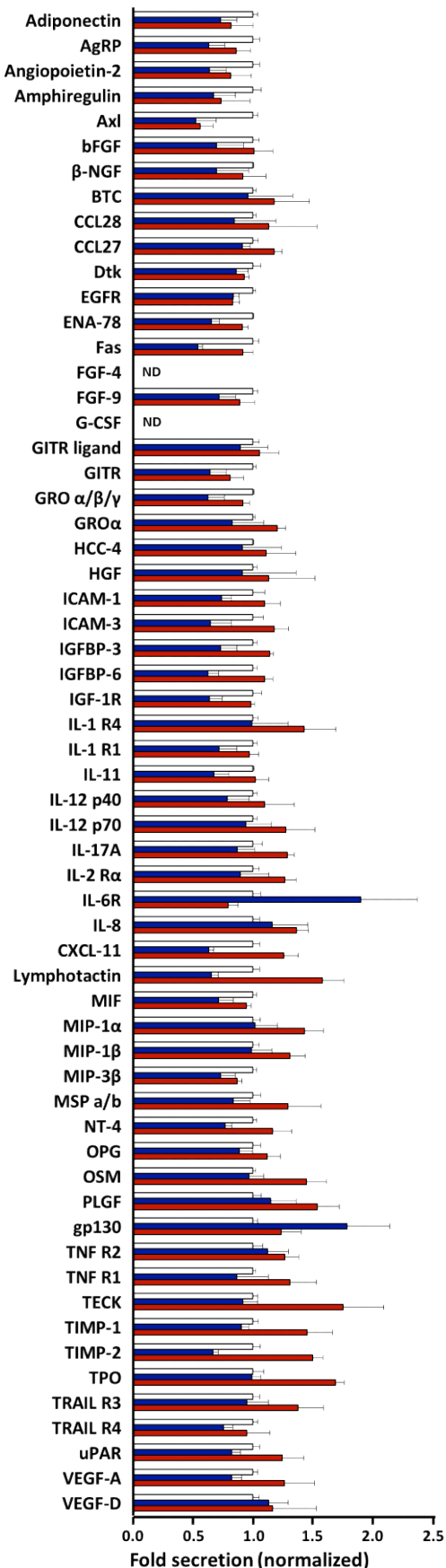


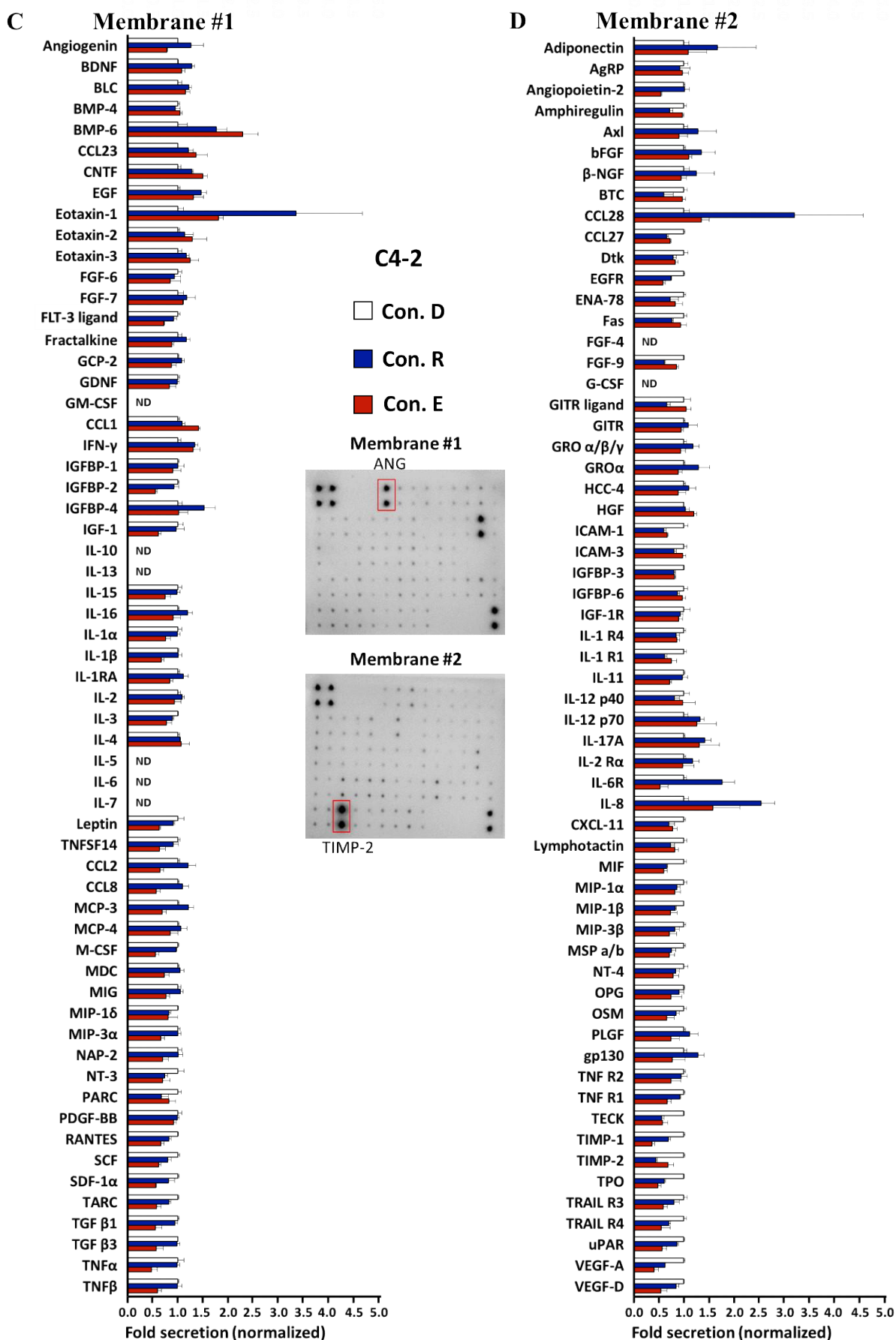
**Supplemental Figure S1. AR ligands suppress the expression of cell cycle regulators.** LNCaP cells were treated with R1881 (1 nM), BIC (1 µM), ENZ (1 µM), or DMSO (0.1%) as solvent control for 6 days. RNA extraction was performed and mRNA levels of *MYC*, *CCND1* (Cyclin D1), *E2F1*, and *PCNA*, were analyzed by qRT-PCR. Bar graphs are shown as mean + SEM from total of six technical replicates (n = 6) of two independent experiments. *β-Actin* and *TBP* served as housekeeping genes. Statistical analysis was performed by using two-tailed unpaired t-test comparing each treatment to DMSO treatment. \*, p<0.05; \*\*, p<0.01; \*\*\*, p<0.001; ns, not significant.

**A Membrane #1**

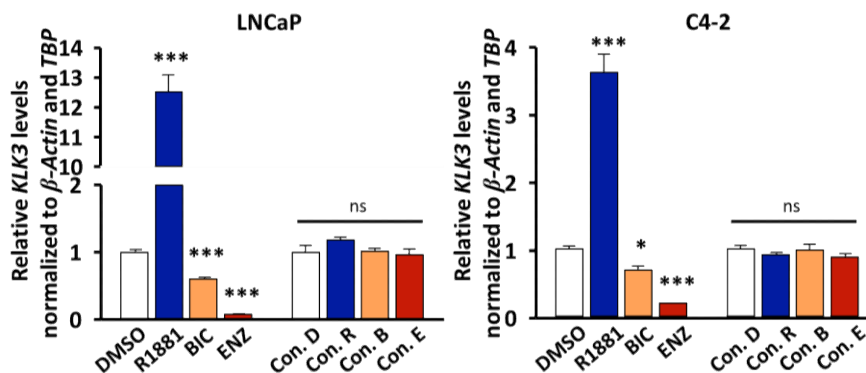


**B Membrane #2**



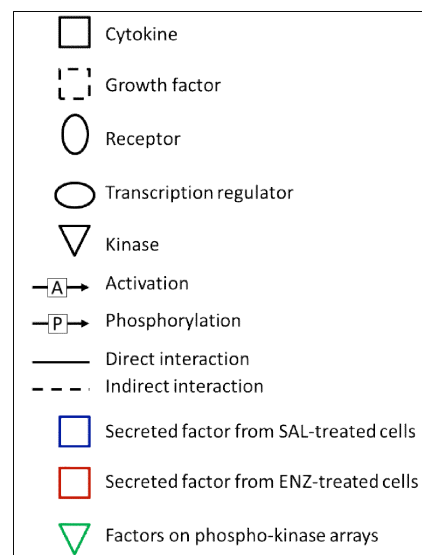
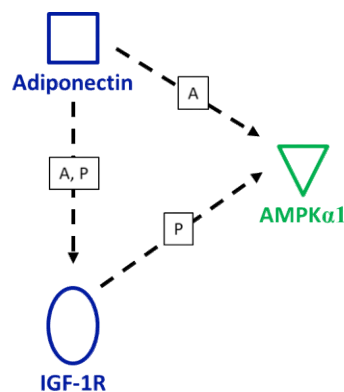


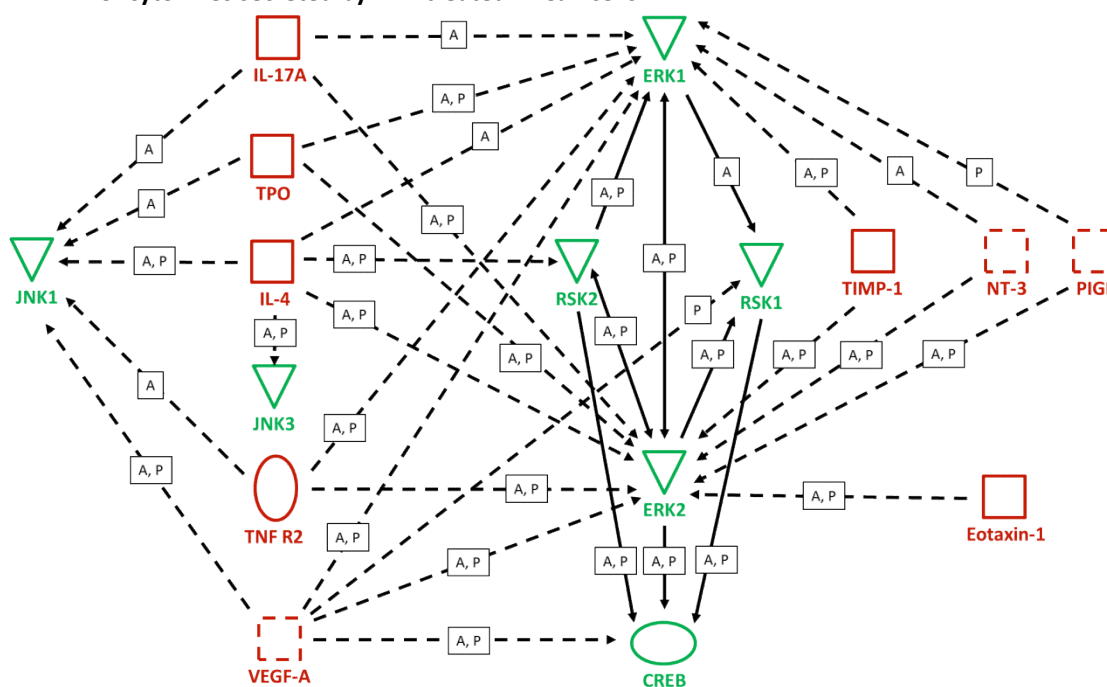
**Supplemental Figure S2. Cytokine secretion levels from AR ligand-induced cellular senescent PCa cells.** Experiments were performed as described in Figure 7. (A-D) Fold secretion of 120 cytokines analyzed from detected signals of human cytokine arrays. Arrays were incubated with conditioned medium collected from DMSO- (Con. D), R1881- (Con. R), or ENZ-treated (Con. E) LNCaP (A and B) or C4-2 (C and D) cells. Normalized fold secretion in Con. D was set arbitrarily as 1. Bar graphs are shown as mean + SEM from total of four technical replicates ( $n = 4$ ) of two independent experiments. ND, not detected or below detection level. Inserted figures are example of detected signals on human cytokine arrays incubated with Con. D of LNCaP or C4-2 cells. Red squares localize the detected signals of Angiogenin (ANG) on membrane #1 and TIMP-2 on membrane #2, which were selected as representative targets for confirming arrays results.



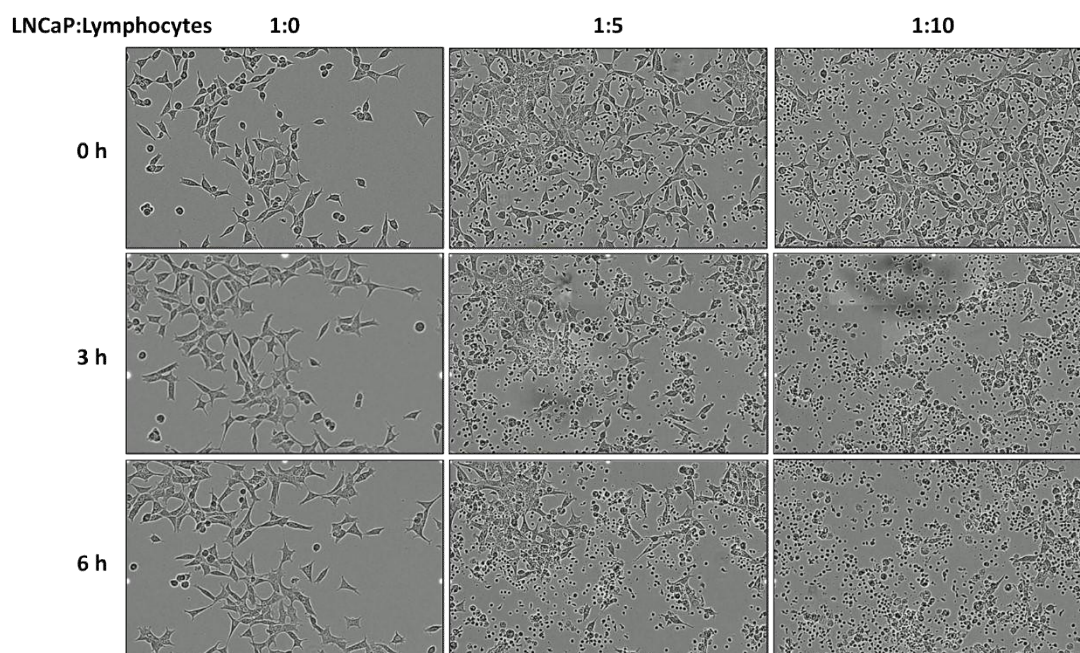
**Supplemental Figure S3. Conditioned media do not affect transcription levels of AR target gene *KLK3*.** Similar experiments with AR ligands were performed as described in Supplemental Figure S1 with LNCaP and C4-2 cells. In addition, other sets of cells were also treated for 6 days with conditioned medium derived from R1881- (Con. R), BIC- (Con. B), ENZ-induced cellular senescent PCa cells (Con. E), or DMSO-treated cells (Con. D) as control. RNA extraction was performed and mRNA level of AR target gene *KLK3*, a PSA encoding gene, was analyzed by qRT-PCR. Bar graphs are shown as mean + SEM from total of six technical replicates ( $n = 6$ ) of two independent experiments for LNCaP and three technical replicates ( $n = 3$ ) of single experiment for C4-2.  $\beta$ -Actin and *TBP* served as housekeeping genes. Normalized mRNA levels of control-treated cells were set arbitrarily as 1. For AR ligand treatment, statistical analysis was performed by using two-tailed unpaired t-test compared each treatment to DMSO treatment. For conditioned medium treatment, one-way ANOVA followed by Dunnett's multiple comparisons test was performed. \*,  $p \leq 0.05$ ; \*\*\*,  $p \leq 0.001$ ; ns, not significant.

**A IPA of cytokines secreted by R1881-treated LNCaP cells**



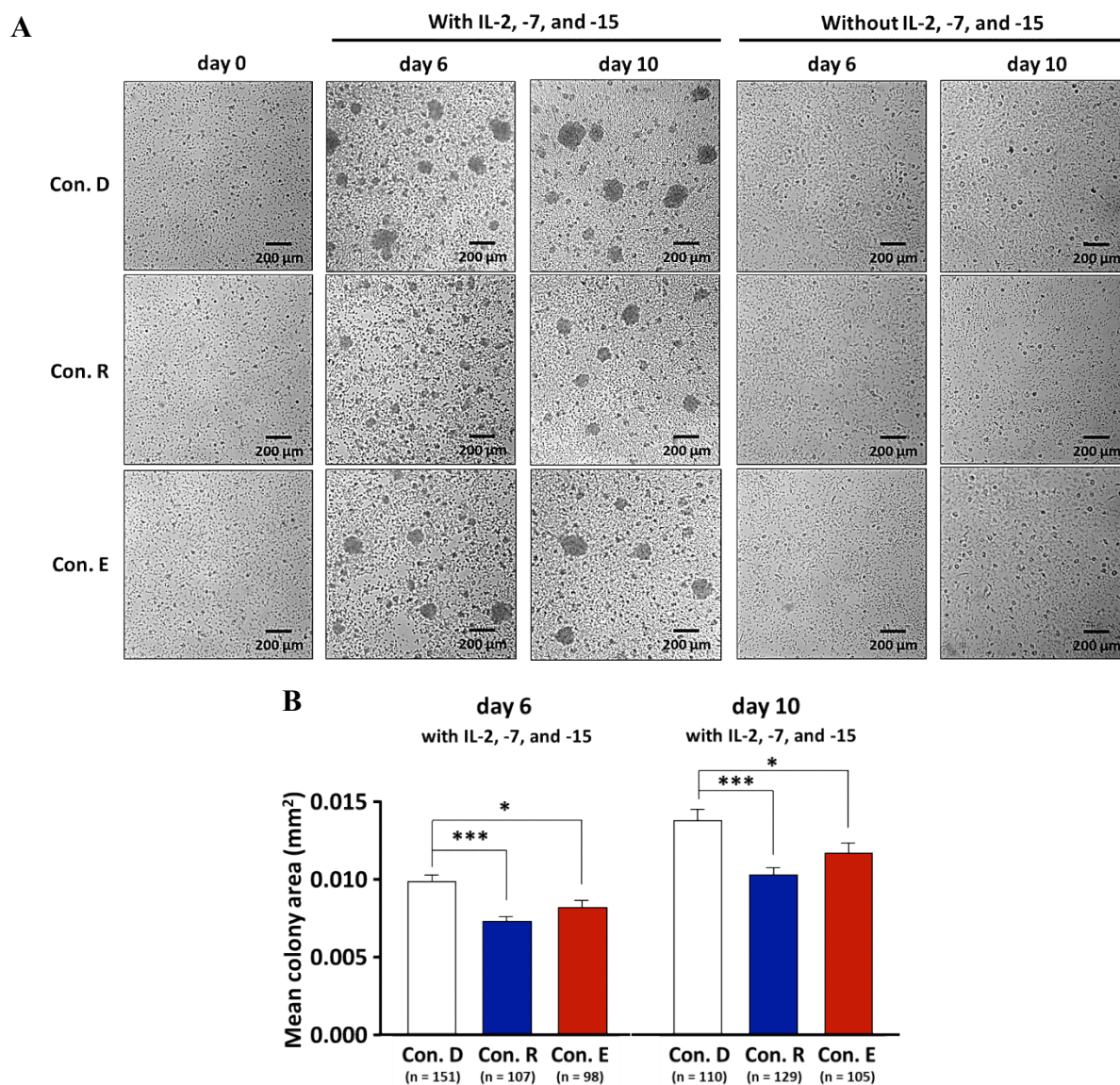
**B** IPA of cytokines secreted by ENZ-treated LNCaP cells

**Supplemental Figure S4. Some cytokines secreted by AR ligand-treated LNCaP cells can modulate the phospho-kinome.** IPA was performed to analyze kinases and protein targets of the phospho-kinase arrays along with secreted cytokines of AR ligand-treated LNCaP cells. IPA provides information based on database and publications for interactions (activation and/or phosphorylation) between these factors. (A) IPA of cytokines secreted by SAL-treated cells. (B) IPA of cytokines secreted by ENZ-treated cells. Note that, (A) and (B) show only interactions which are consistent with the results of phospho-kinase arrays in Figure 12. Secreted levels of Adiponectin and IGF-1R were suppressed by SAL. Con. R reduced phosphorylation level of AMPK $\alpha$ 1. Secreted levels of Eotaxin-1, IL-17A, IL-4, NT-3, PIGF, TPO, TIMP-1, TNF R2, and VEGF-A were enhanced by ENZ. Con. E induced phosphorylation levels of ERK1/2, JNK1/3, RSK1/2, and CREB.



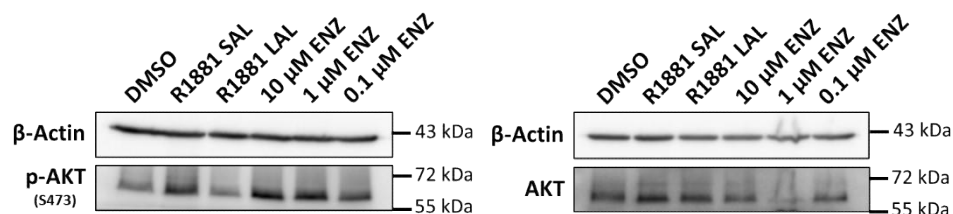


**Supplemental Figure S5. LNCaP cells were killed by activated lymphocytes.** LNCaP cells were co-cultured with activated lymphocytes with indicated ratios. Pictures were captured from live imaging microscope at 0, 3, and 6 h after co-culturing was started. The results suggest 1:5 ratio and 6 h to be the maximum co-culturing ratio and incubation time for analyzing the lymphocyte-mediated cytotoxicity on LNCaP cells.

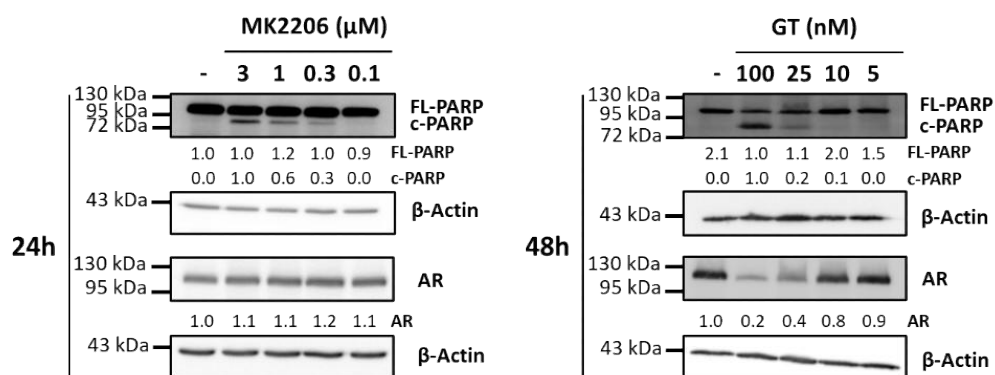


**Supplemental Figure S6. Conditioned media from AR ligand-induced cellular senescent LNCaP cells suppress lymphocyte clonal expansion.** Experiment was performed as described in Figure 18 with conditioned media of AR ligand-treated LNCaP cells. **(A)** Representative pictures at day 0, 6, and 10 of lymphocyte colonies after conditioned media with or without IL-2, -7, and -15 co-treatment. **(B)** Bar graphs show mean area + SEM calculated from colonies that exhibited an area equal to or above 0.005 mm<sup>2</sup> with indicated number of colonies (n). Statistical analysis was performed by using one-way ANOVA followed by Dunnett's multiple comparisons test. \*\*\*,  $p \leq 0.001$ ; \*,  $p \leq 0.05$ .

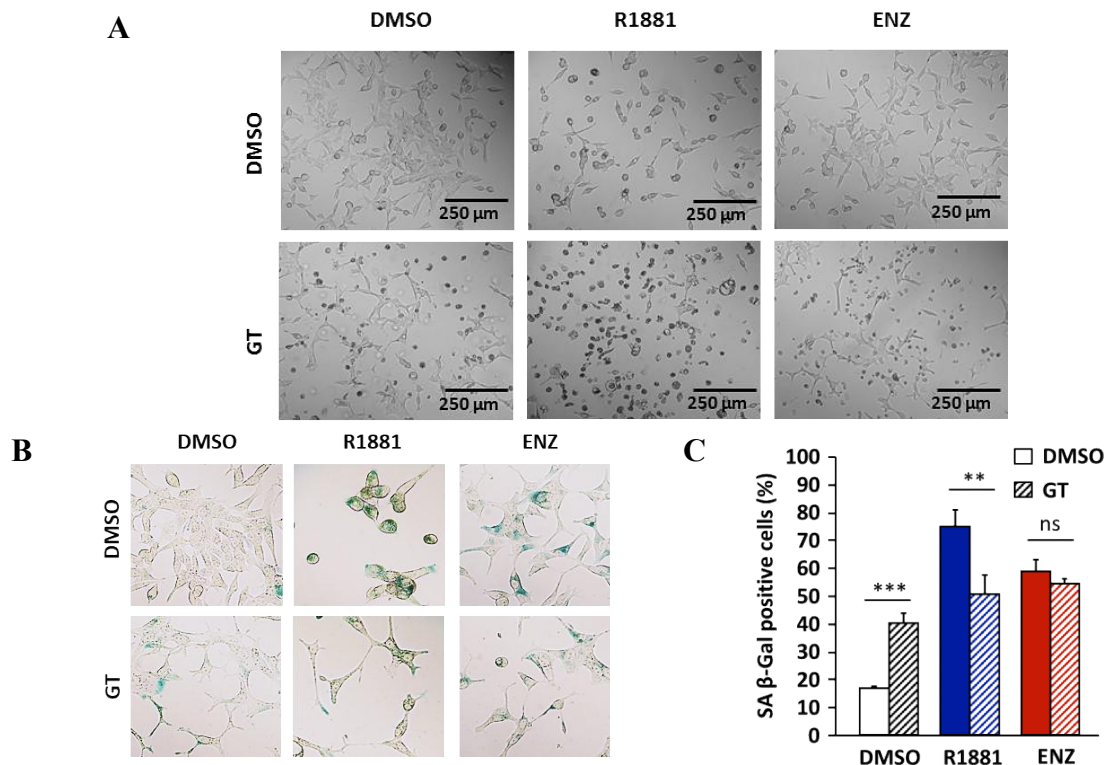




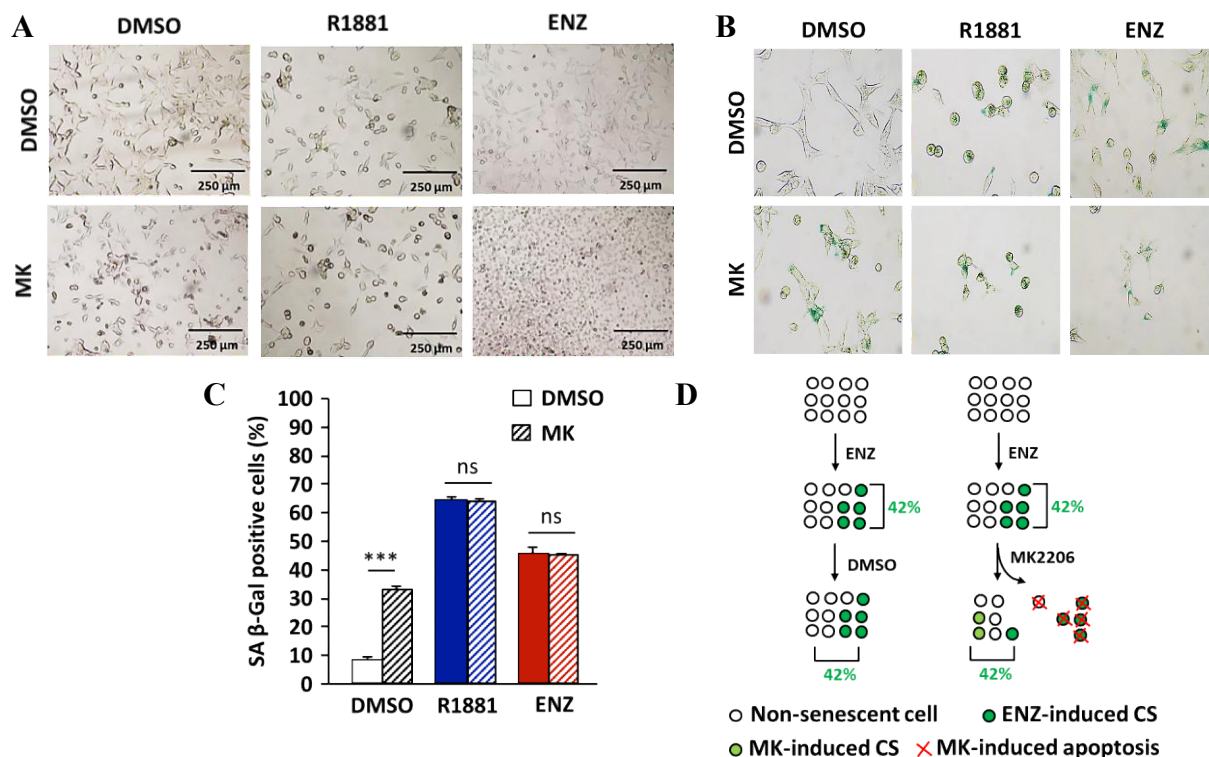
**Supplemental Figure S7. AR ligands induce phosphorylation level of AKT.** The same Western blot membranes shown in Figure 20 including the cropped out 1  $\mu$ M ENZ and 0.1  $\mu$ M ENZ treatments.



**Supplemental Figure S8. MK2206 and GT induce c-PARP levels in a concentration dependent manner.** LNCaP cells were treated with indicated concentration of MK2206 (left panel), GT (right panel), or 0.1% DMSO as solvent control. The protein was extracted and detection of FL-PARP, c-PARP, and AR was performed by Western blotting.  $\beta$ -Actin served as loading control. Inhibition of cell proliferation (data not shown) and induction of c-PARP were detected after 24 h treatment with MK2206 and after 48 h with GT. These figures have been published by Pungsrinont *et al.* (2020). The results with GT treatment are derived from Malika Sutter's Bachelor thesis (Baniahmad's group).



**Supplemental Figure S9. GT enhances detachment and reduces percentage of SA  $\beta$ -Gal positive cells after SAL-induced cellular senescence.** Similar experiments were performed as described in Figure 21. **(A)** Representative pictures of detaching cells under light microscope after indicated treatments. **(B)** Representative pictures of SA  $\beta$ -Gal staining under light microscope. **(C)** Percentage of SA  $\beta$ -Gal positive cells. Bar graphs are shown as mean + SD from three technical replicates ( $n = 3$ ) of a single experiment. Statistical analysis was performed by using two-tailed unpaired t-test comparing between with and without GT treatment within. \*\*,  $p \leq 0.01$ ; \*\*\*,  $p \leq 0.001$ ; ns, not significant. These figures have been published by Pungsrinont *et al.* (2020).



**Supplemental Figure S10. MK2206 induces LNCaP cell detachment but does not reduce the percentage of SA  $\beta$ -Gal positive cells.** LNCaP cells were treated for 72 h with 1 nM R1881, 10  $\mu$ M ENZ, or 0.1% DMSO as solvent control. After that, the AR ligands were removed. Fresh medium with 1  $\mu$ M MK2206 (MK) or 0.1% DMSO was added, and further incubated for additional 72 h. **(A)** Representative pictures of detaching cells under light microscope after indicated treatments. **(B)** Representative pictures of SA- $\beta$ -Gal staining under light microscope. **(C)** Percentage of SA  $\beta$ -Gal positive cells after 24 h of MK treatment. Bar graphs are shown as mean + SEM from three independent experiments ( $N = 3$ ). Statistical analysis was performed by using two-tailed unpaired t-test comparing between with and without MK. \*\*\*,  $p \leq 0.001$ ; ns, not significant. **(D)** A schematic figure illustrates an unchanged or compensated percentage level of SA  $\beta$ -Gal positive cells after MK in ENZ-pretreated cells. Numbers represent the calculated percentage of SA  $\beta$ -Gal positive cells. These data have been published by Pungsrinont *et al.* (2020). The results in A-C are derived from Maren Ertingshausen's Bachelor thesis (Baniahmad's group).

**Supplemental Table S1. List of cytokines secreted by treated LNCaP cells that enriched in regulation of cell proliferation, lymphocyte proliferation, and immune system process**

LNCaP		Regulation of cell proliferation	Regulation of lymphocyte proliferation	Regulation of immune system process	
R1881	Secreted cytokines				
<b>Enhanced secretion</b>	Angiogenin ( <i>ANG</i> )	■			
	BDNF	■			
	BLC ( <i>CXCL13</i> )	■		■	
	BMP-6	■			
	CCL1	■		■	
	CCL2	■			
	CCL23	■			
	CCL8	■		■	
	EGF	■			
	Eotaxin-3 ( <i>CCL26</i> )	■			
	FGF-7	■			
	FLT-3 ligand ( <i>FLT3LG</i> )	■	■	■	
	Fractalkine ( <i>CX3CL1</i> )	■	■	■	
	GCP-2 ( <i>CXCL6</i> )	■	■	■	
	GDNF	■			
	GM-CSF ( <i>CSF2</i> )	■	■	■	
	gp130 ( <i>IL6ST</i> )	■	■	■	
	IFN- $\gamma$ ( <i>IFNG</i> )	■	■		
	IGF-1	■			
	IGFBP-1	■			
	IGFBP-4	■			
	IL-15	■		■	
	IL-16	■			
	IL-1 $\alpha$ ( <i>IL1A</i> )	■	■	■	
	IL-2	■	■	■	
	IL-3	■			
	IL-6R	■	■	■	
	IL-7	■	■	■	
	Leptin ( <i>LEP</i> )	■	■	■	
	MCP-3 ( <i>CCL7</i> )	■			
	MCP-4 ( <i>CCL13</i> )	■			
	MIG ( <i>CXCL9</i> )	■		■	
	PARC ( <i>CCL18</i> )	■			
	PDGF-BB ( <i>PDGFB</i> )	■			
	RANTES ( <i>CCL5</i> )	■	■	■	
	SCF ( <i>KITLG</i> )	■	■	■	
	SDF-1 $\alpha$ ( <i>CXCL12</i> )	■			
	TARC ( <i>CCL17</i> )	■			
	TGF $\beta$ 1 ( <i>TGFB1</i> )	■	■	■	
	TGF $\beta$ 3 ( <i>TGFB3</i> )	■	■	■	
	TNFSF14	■			
	<b>Suppressed Secretion</b>	Adiponectin ( <i>ADIPOQ</i> )	■		
		AgRP	■		
		Amphiregulin ( <i>AREG</i> )	■		
		Angiopoietin-2 ( <i>ANGPT2</i> )	■		
Axl		■			
bFGF ( <i>FGF2</i> )		■			
CXCL-11		■		■	
ENA-78 ( <i>CXCL5</i> )		■			
Fas		■			
FGF-9		■			
GITR ( <i>TNFRSF18</i> )		■		■	
GRO $\alpha/\beta/\gamma$ ( <i>CXCL1/2/3</i> )		■			
ICAM-1		■			
ICAM-3		■			
IGF-1R		■			
IGFBP-2		■	■	■	
IGFBP-3		■			
IGFBP-6		■			
IL-1 R1		■		■	
IL-11		■			
IL-12 p40 ( <i>IL12B</i> )		■			
IL-5		■			
Lymphotactin ( <i>XL1</i> )		■			
MIF		■			
MIP-3 $\beta$ ( <i>CCL19</i> )		■			
NT-4 ( <i>NTF4</i> )		■			
TIMP-2		■			
TRAIL R4 ( <i>TNFRSF10D</i> )		■			
$\beta$ -NGF ( <i>NGF</i> )		■			

LNCaP		Regulation of cell proliferation	Regulation of lymphocyte proliferation	Regulation of immune system process
ENZ	Secreted cytokines			
<b>Enhanced secretion</b>	CXCL-11	■		
	Eotaxin-1 ( <i>CCL11</i> )	■		
	Eotaxin-3 ( <i>CCL26</i> )	■		
	gp130 ( <i>IL6ST</i> )	■	■	■
	GRO $\alpha$ ( <i>CXCL1</i> )	■		■
	IGF-1	■		
	IGFBP-1	■		
	IGFBP-4	■		
	IL-1 R4 ( <i>IL1RL1</i> )	■		■
	IL-12 p70 ( <i>IL12A</i> )	■		
	IL-15	■		■
	IL-16	■		
	IL-17A	■		■
	IL-2 R $\alpha$ ( <i>IL12RA</i> )	■		■
	IL-4	■		
	IL-5	■		
	IL-7	■		
	IL-8 ( <i>CXCL8</i> )	■		■
	Leptin ( <i>LEP</i> )	■		■
	Lymphotactin ( <i>XL1</i> )	■		■
	MCP-3 ( <i>CCL7</i> )	■		
	MCP-4 ( <i>CCL13</i> )	■		
	MIP-1 $\alpha$ ( <i>CCL3</i> )	■		■
	MIP-1 $\beta$ ( <i>CCL4</i> )	■		
	MSP ( <i>MST1</i> )	■		■
	NAP-2 ( <i>PPBP</i> )	■		
	NT-3 ( <i>NTF3</i> )	■		
	OSM	■		
	PARC ( <i>CCL18</i> )	■		
	PDGF-BB ( <i>PDGFB</i> )	■		
	PIGF ( <i>PGF</i> )	■		■
	RANTES ( <i>CCL5</i> )	■	■	■
	SCF ( <i>KITLG</i> )	■	■	■
	TECK ( <i>CCL25</i> )	■		
	TGF $\beta$ 1 ( <i>TGFB1</i> )	■	■	■
TIMP-1	■			
TIMP-2	■			
TNF R1 ( <i>TNFRSF1A</i> )	■			
TNF R2 ( <i>TNFRSF1B</i> )	■			
TPO ( <i>THPO</i> )	■		■	
TRAIL R3 ( <i>TNFRSF10C</i> )	■			
uPAR ( <i>PLAUR</i> )	■			
VEGF-A	■		■	
<b>Suppressed Secretion</b>	Amphiregulin ( <i>AREG</i> )	■		
	Angiogenin ( <i>ANG</i> )	■		
	Axl	■		
	BDNF	■		
	BLC ( <i>CXCL13</i> )	■		■
	BMP-4	■		
	GCP-2 ( <i>CXCL6</i> )	■		
	GDNF	■		
	IGFBP-2	■	■	■
	IL-1 $\beta$ ( <i>IL1B</i> )	■		
	IL-2	■		
	IL-6 R	■		
	TNF $\alpha$ ( <i>TNF</i> )	■		

\* Colours indicate enrichment of cytokines in particular GO term.

### 8.3 List of figures

<b>Figure 1.</b> Genomic and non-genomic signaling of AR control cell proliferation and survival .	2
<b>Figure 2.</b> Senescent cells are accompanied by SASP factors.....	6
<b>Figure 3.</b> Overview of the origin of the cancer stem cells .....	10
<b>Figure 4.</b> Illustration figures for 2D monolayer proliferation and 3D colony formation assays .....	18
<b>Figure 5.</b> AR ligands induce cellular senescence and not apoptosis.....	33
<b>Figure 6.</b> AR ligands suppress PCa cell proliferation.....	34
<b>Figure 7.</b> AR ligand-induced cellular senescent PCa cells possess distinct sets of secreted cytokines .....	36
<b>Figure 8.</b> Secreted level of some SASP factors by AR ligands is independent of transcription regulation .....	39
<b>Figure 9.</b> Cytokines secreted by AR ligand-treated PCa cells significantly enriched in GO terms regarding cell proliferation and immune system.....	42
<b>Figure 10.</b> Conditioned media from AR ligand-induced cellular senescence mediate paracrine effect on LNCaP cell proliferation .....	46
<b>Figure 11.</b> Conditioned media do not affect the expression of cell cycle regulators .....	48
<b>Figure 12.</b> Conditioned media regulate phospho-kinome of PCa cells.....	49
<b>Figure 13.</b> Con. R and AR ligands regulate the expression of stemness markers.....	52
<b>Figure 14.</b> Conditioned media do not affect LNCaP 3D colony formation .....	53
<b>Figure 15.</b> SAL treatment suppresses LNCaP 3D colony formation .....	55
<b>Figure 16.</b> Culturing and activation of human immune cells.....	57
<b>Figure 17.</b> Conditioned media do not affect lymphocyte-mediated apoptosis.....	59
<b>Figure 18.</b> Con. R and Con. E of LNCaP cells suppress lymphocyte clonal expansion.....	61
<b>Figure 19.</b> AR ligand-induced cellular senescent PCa cells are resistant to lymphocyte mediated apoptosis.....	64
<b>Figure 20.</b> AR ligands induce the phosphorylation level of the pro-survival/anti-apoptotic factor AKT .....	66
<b>Figure 21.</b> Targeting senescent LNCaP cells with senolytic compounds .....	68
<b>Figure 22.</b> AR agonist and antagonist differentially regulate pro-survival/anti-apoptotic signaling AKT-S6 .....	70

<b>Figure 23.</b> The SASP of AR ligand-treated cells modulates phospho-kinome and regulates PCa cell proliferation .....	75
<b>Figure 24.</b> Diverse effects between SAL- and AR antagonist-induced cellular senescence ...	84
<b>Supplemental Figure S1.</b> AR ligands suppress the expression of cell cycle regulators. ....	IV
<b>Supplemental Figure S2.</b> Cytokine secretion levels from AR ligand-induced cellular senescent PCa cells .....	V
<b>Supplemental Figure S3.</b> Conditioned media do not affect transcription levels of AR target gene <i>KLK3</i> .....	VII
<b>Supplemental Figure S4.</b> Some cytokines secreted by AR ligand-treated LNCaP cells can modulate the phospho-kinome .....	VII
<b>Supplemental Figure S5.</b> LNCaP cells were killed by activated lymphocytes .....	VIII
<b>Supplemental Figure S6.</b> Conditioned media from AR ligand-induced cellular senescent LNCaP cells suppress lymphocyte clonal expansion .....	IX
<b>Supplemental Figure S7.</b> AR ligands induce phosphorylation level of AKT .....	X
<b>Supplemental Figure S8.</b> MK2206 and GT induce c-PARP levels in a concentration dependent manner .....	X
<b>Supplemental Figure S9.</b> GT enhances detachment and reduces percentage of SA $\beta$ -Gal positive cells after SAL-induced cellular senescence .....	X
<b>Supplemental Figure S10.</b> MK2206 induces LNCaP cell detachment but does not reduce the percentage of SA $\beta$ -Gal positive cells .....	XI

#### 8.4 List of tables

<b>Table 1.</b> List of antibodies used for flow cytometry .....	24
<b>Table 2.</b> List of antibodies against human proteins used for Western blotting .....	27
<b>Table 3.</b> List of human primers used for qRT-PCR analysis .....	30
<b>Table 4.</b> Summary of significant enriched GO terms regarding cell proliferation and immune system by secreted cytokines of AR ligand-treated PCa cells .....	45
<b>Supplemental Table S1.</b> List of cytokines secreted by treated LNCaP cells that enriched in regulation of cell proliferation, lymphocyte proliferation, and immune system process .....	XII

## **8.5 Ehrenwörtliche Erklärung**

Hiermit erkläre ich, dass mir die Promotionsordnung der Medizinischen Fakultät der Friedrich-Schiller-Universität bekannt ist,

ich die Dissertation selbst angefertigt habe und alle von mir benutzten Hilfsmittel, persönlichen Mitteilungen und Quellen in meiner Arbeit angegeben sind,

mich folgende Personen bei der Auswahl und Auswertung des Materials sowie bei der Herstellung des Manuskripts unterstützt haben: Prof. Dr. rer. nat. Aria Baniahmad, Dr. rer. nat. Katrin Schindler, Dr. Mutita Junking, Miriam Kokal und Gopinath Lakshmana,

die Hilfe eines Promotionsberaters nicht in Anspruch genommen wurde und dass Dritte weder unmittelbar noch mittelbar geldwerte Leistungen von mir für Arbeiten erhalten haben, die im Zusammenhang mit dem Inhalt der vorgelegten Dissertation stehen,

dass ich die Dissertation noch nicht als Prüfungsarbeit für eine staatliche oder andere wissenschaftliche Prüfung eingereicht habe und

dass ich die gleiche, eine in wesentlichen Teilen ähnliche oder eine andere Abhandlung nicht bei einer anderen Hochschule als Dissertation eingereicht habe.

Jena, 08.12.2020

Thanakorn Pungsrinont

## 8.6 Acknowledgement

First of all, I would like to express deep gratitude to Prof. Dr. rer. nat. Aria Baniahmad, Institute of Human Genetics, Jena University Hospital, as my project supervisor, for his guidance, opportunity, and support throughout the entire project. Under his supervision, I have learned and earned a lot of experiences, which are necessary for my future career. Therefore, it is my great pleasure and respect to sincerely thank him once again.

I would like to express my appreciation to my co-supervisor PD Dr. rer. nat. habil. Jörg Müller, Institute for Molecular Cell Biology, Jena University Hospital, for his valuable time, guidance, and suggestions.

As a financial support in terms of a scholarship, I would like to thank DAAD and all the staffs, particularly Ms. Sonja Bärwinkel, Mr. Sebastian Grothus, and Ms. Natalie Bursinski.

Special appreciation goes to Dr. Mutita Junking, Dr. Chutamas Thepmalee, and Dr. Thaweesak Chieochansin, Division of Molecular Medicine, Department of Research and Development, Faculty of Medicine Siriraj Hospital, for their valuable time consulting about experiments with immune cells.

My sincere thanks go to my colleagues and friends for a friendly atmosphere in the Institute of Human Genetics. Thank you to Gabi, Dani, Katrin, Kimia, Marzieh, Miriam, Federico, Joana, Alex, Julia, Mirjam, Gopi, Maggie, Markus, Jan, Patricia, Hector, Awais, Maren, Malika, Laura, Sid, Aya, Faith, Anya, Anna, Tim, Corny, Divya, Neeraja, Astha, Toko, Shirin, Sogol, Somaya, Jessi, Roland, Louisa, Lukas, and Elmira.

Special thanks go to Miriam, Joana, Maren, Malika, Laura, Sid, Maggie, Anya, Louisa, and Lukas for your friendship, fun, tears, discussion, and help. You all improved my supervising experience. I am proud of you all and it was my honor to be able to help you more or less.

Lastly, I would like to share my success and happiness to my beloved family and fiancé. They are unforgettable factors which drive me to this point of my life and indeed further in the future. As a great source of power which always fulfills my strength and encourages me whenever I felt desperate, I deeply appreciate.

Best Regards,

Thanakorn Pungsrinont